Ultraviolet improved black holes

Master Thesis

SVEN KÖPPEL

November 2014

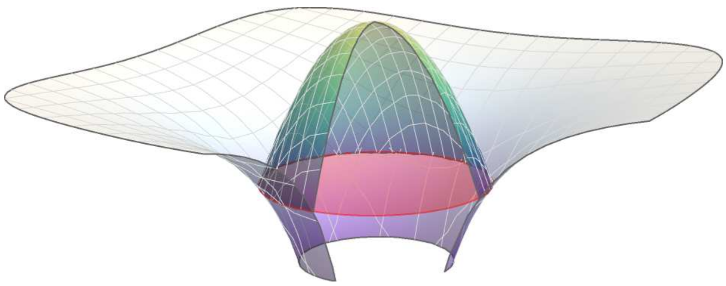

First Supervisor: PD DR. PIERO NICOLINI

Second Supervisor: PROF. DR. MARCUS BLEICHER

INSTITUTE FOR THEORETICAL PHYSICS &
FRANKFURT INSTITUTE FOR ADVANCED STUDIES

GOETHE UNIVERSITÄT FRANKFURT AM MAIN

Vorliegende Version ist vom **November 21, 2014, 08:24**

Abstract

In this thesis, black holes of Planck length extend are discussed. New families of black hole geometries is presented that exhibits a modified minimal length scale behaviour and implements gravity self-complete paradigm. These geometries are extended to the ADD large extra-dimensional scenario. This allows black hole remnant masses to reach the TeV scale. It is shown that the evaporation endpoint for this class of black holes is a cold stable remnant. One family of black holes considered in this thesis features a regular deSitter core that counters gravitational collapse with a quantum outward pressure. The other family of black holes turns out to fit nicely into the holographic information bound on black holes, leading to black hole area quantization and applications in the black hole entropic force. Thus, gravity can be derived as emergence phenomen from the fundamental thermodynamics.

The thesis contains an overview about recent quantum gravity black hole approaches and concludes with the derivation of nonlocal operators that modify the Einstein equations to ultraviolet complete field equations.

About the front picture

This picture shows an embedding diagram for the self-regular black hole in the outstanding case $\alpha \to \infty$.
By intention, there are no units as this is purely illustrative. The 3d picture can be constructed by rotating the graphs shown on the right around its y axis.

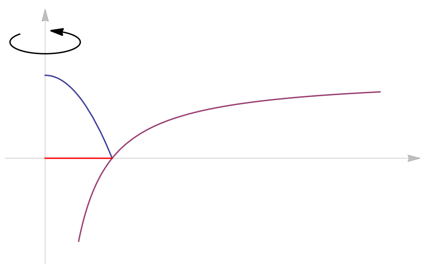

Contents

Todo list

Introduction

This work is about the quest of contemporary physics on the smallest scales and with the biggest energies. By historical evolution, in the 20th century two opposing theories developed: Quantum Physics, which is the physics at smallest scales and produced confusing paradoxa like Schrödinger's cat, and on the other hand (general) relativistic physics, which is the physics at the biggest scales and lead to General Relativity, the theory for space and time presented by Albert Einstein in 1915.

The combination of Quantum Mechanics and Special Relativity lead to Quantum Field Theory (QFT) and the formulation of the Standard Model of particle physics which is exceptionally and unexpectedly successful. From the viewpoint of an high-energy physicist, three of four fundamental interactions, namely the electromagnetic, weak nuclear and strong nuclear interactions can be joined in a unified theory, and gravity is simply the weakest and last interaction left as an "ordinary" field theory. A unification of the three Standard Model interactions is called grand unified theory (GUT). On the other hand, from the viewpoint of a relativist, General Relativity taught us that there is no background space where physics "takes place". This new principle lead to a bunch of new physics, where the most remarkable is perhaps the existence of black holes as regions of no escape in spacetime or even the existence of wormholes (Einstein-Rosen bridge). Certainly, General Relativity had the bigger impact on the science fiction genre.

Physics beyond the Standard Model is an uncomfortable job, because it still lacks experimental accessibility. One thing one can do as a theorist starting from QFT is curved space quantum field theory (QFTCS), that is, calculating quantum fields on a curved space background, but without space-matter interaction. In the *cube of physical theories*, as shown in figure 0.1, this is probably the half way to the "Theory of Everything". **PN:** QFTCS includes 1-loop graviton contractions

Actually, curved space QFT opened the door for the first quantum mechanical treatments of strong gravitational objects: black holes. In the 1970s, this lead to Hawking's groundbreaking prediction of thermal radiation of Schwarzschild black holes. In terms of "theories", Hawking radiation is really interdisciplinary:

$$T_{\mathrm{H}} = \frac{\hbar\, c^3}{8\pi\, G\, M k_{\mathrm{B}}}$$

There are "ingredients" from Quantum Mechanics (Planck constant $\hbar$), Special Relativity (speed of light c), Gravitation (Newton's constant G) and Thermodynamics (Boltzmann constant k_B).

But Hawking's temperature also contains the failure of General Relativity: The temperature increases with decreasing mass M, since it is written in the denominator. Since radiating black

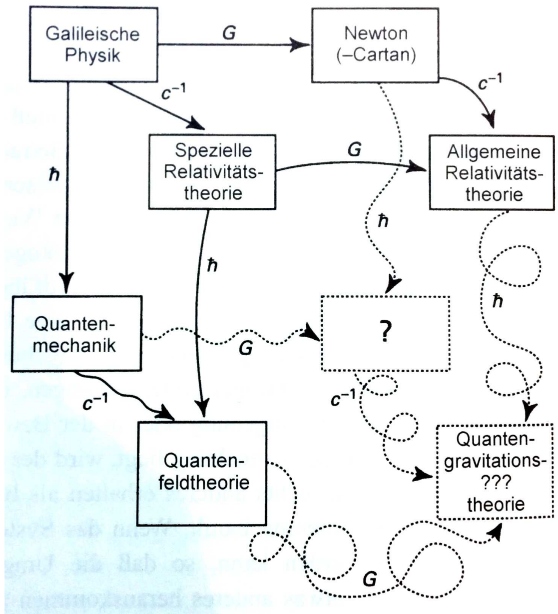

Figure 0.1: The *cube of physics*, a popular illustration about characteristic constants that describe the regime for physical phenomena. First appeared in a 1999 book from Penrose [62].

holes loose mass, they get hotter and hotter. If there are black holes (and there is a strong sense there are), the universe should be hot, but it is not.

In this thesis, I propose modifications to General Relativity dealing with this kind of *big mass* problem. As in physics, big mass correspond with high energy and low distance, we use the term *ultra-violet*, coming from the wavy nature of light, to describe an high energy regime. This thesis deals with ultra-violet corrections of the most simple black hole possible, the Schwarzschild black hole.

Outline

Adapt Outline for new thesis structure.

Section 1 is an introductory section about General Relativity. It will give an introduction to the formalism and shortly derive the Einstein equation. Then the first solutions on GR are shown and the different types of singularities and their origins are discussed. An outline about gravity in extra dimensions and the issue of observations of micro black holes is given.

Section **??** is devoted to the shortest scales of black holes. It deals with the breakdown of the Schwarzschild description in the Planck phase of black hole evaporation and presents various Quantum Gravity approaches to describe the Planck phase. In contrast, afterwards a short scale modification will be introduced that does not relies on a theory *beyond* General Relativity. To do so, Einstein Equations are solved for an ideal static isotropic "blurred" matter ball that shall describe a "quasi-classical" mass point. Two such profiles are presented unter the name *holographic* and the *self-regular* mass profile. They are extended to the large extradimensional scenario.

In section **??**, the geometry of the mass profiles is derived and discussed. The analogy to the Reissner-Nördstrom space-time becomes apparent. The appearance of a black hole *remnant* as smallest *self-encoding* building block of matter is described, it motivates to call General Relavity *self-complete* on minimal length scales. The regular DeSitter core of a black hole with its quantum interpretation is discussed.

Section **??** approaches the thermodynamical properties of this class of black holes. The associated temperature, heat capacity and entropy are derived and a phase transition at some critical radius is found. Concerning the entropy, the meaning of *holography* in gravity and possible outcomes for the black hole information paradox are explained.

In section **??**, the Einstein field equations are modified in order to find a dual nonlocal gravity theory that gives the same results as the purely-Einsteinian matter. Such a theory may be called a *quantum improved* General Relativity, as it incorporates short scale improvements in the context of tensor calculus and Riemannian geometry.

Chapter 1

Theoretical background

1.1 General Relativity

In this section, a short derivation of General Relativity (GR) is given. It is the geometrical theory of gravitational interaction from matter and the major framework used in this work. To do so, some core concepts of differential geometry on manifolds are retraced briefly in order to derive the Einstein Field Equations (EFE) by Hamiltonian's principle of least action. Exact definitions of the new vector concept are skipped in favour of condensing the ideas. In this text I follow the notations of [15, 44, 48, 77, 78]. They prefer abstract index notation as a more fundamental approach to introduce Riemannian geometry. In contrast, some tensors may also be derived by "index constraints" as done in [28]. This is less elegant but more straightforward.

1.1.1 Differential Geometry

In curved space geometry, intuition about well-known mathematical symbols like vectors as "position vectors" fails [78]. The mathematical approach is a differential description using the fact that manifolds M are locally flat (they look "nearly" flat). Thus the tangent vector V is introduced as a directional derivative operator. The components of such a vector may be denoted as

$$V(f) = V^{\mu}\frac{\partial f}{\partial x^{\mu}}. \tag{1.1}$$

The vector V maps functions $f \in C^{\infty}(M, \mathbb{R})$ to $\mathbb{R}$. With a fixed point $p \in M$, it defines the tangent vector space V_p. Introducing the dual space V_p^* and the dual dual space $V_p^{**} \cong V_p$ yields to the definition of tensors as a multilinear mappings from vectors and dual vectors into numbers [77].

1.1.2 Covariant Derivation Operator

As for two points $p, q \in M$, the tangent spaces V_p and V_q can not directly be compared. For example, defining for the vector V^μ a traditional derivative (cf. [48, page 208])

$$\frac{\partial V^\mu}{\partial x^\nu} = \lim_{h\to 0} \frac{V^\mu(x^1,\dots,x^\nu+h^\nu,\dots,x^n) - V^\mu(x^1,\dots,x^\nu+h^\nu,\dots,x^n)}{h^\nu} \tag{1.2}$$

fails as even x and $x+h$ may not be compared directly. As a solution, a covariant derivation operator ∇ by means of the parallel transport is derived. This operator will transform like a tensor.

While Wald [77, page 31] designates requirements for the covariant derivation (linearity, Leibnitz rule, index contraction commutativity, consistency with the index free notation and vanishing torsion tensor/commutativity) and derives the existence of a *connection coefficient* Γ^a_{bc}, one can also introduce the connection coefficient as the link in the parallel transport which shall be the "correct" way to denote the derivative (1.2):

$$V^\mu(x \to x+h) := V^\mu(x) - V^\lambda(x)\Gamma^\mu_{\nu\lambda}h^\nu. \tag{1.3}$$

By replacing the traditional difference $V^\mu(x) - V^\mu(x+h)$ by $V^\mu(x) - V^\mu(x \to x+h)$ in equation (1.2), one immediately ends up with the definition of the covariant derivative

$$\nabla_\mu V^\nu = \partial_\mu V^\nu + \Gamma^\nu_{\mu\sigma}V^\sigma. \tag{1.4}$$

The covariant derivative naturally extends when computing derivatives of tensors of arbitrary rank. For a (k,l)-Tensor T the derivative is given (without proof) by

$$\nabla_\alpha T^{\lambda_1\dots\lambda_k}_{\mu_1\dots\mu_l} = \partial_\alpha T^{\lambda_1\dots\lambda_k}_{\mu_1\dots\mu_l} + \sum_{i=1}^{k} \Gamma^{\lambda_i}_{\alpha\beta} T^{\lambda_1\dots\beta\dots\lambda_k}_{\mu_1\dots\mu_l} - \sum_{j=1}^{l} \Gamma^{\beta}_{\alpha\mu_i} T^{\lambda_1\dots\lambda_k}_{\mu_1\dots\beta\dots\mu_l}. \tag{1.5}$$

1.1.3 The Metric

The connection symbol $\Gamma^\alpha_{\beta\gamma}$ introduced in equation (1.3) is still ambigous. As soon as one equippes the manifold with a metric $g_{\mu\nu}$, there is a special choice, constrained by the requirement that scalars shall be invariant under parallel transport (in colloquial terms, scalars are required to be the same in any coordinate system). The inner product of two arbitrary vectors $\boldsymbol{v}$ and $\boldsymbol{w}$ is a scalar and shall therefore also be invariant under any parallel transport $t^\alpha\nabla_\alpha$. This leads to

$$0 \overset{!}{=} t^\alpha \nabla_\alpha g_{\beta\gamma} v^\beta w^\gamma \quad \Rightarrow \quad 0 = \nabla_\alpha g_{\beta\gamma}. \tag{1.6}$$

A connection $\Gamma^\gamma_{\alpha\beta}$ is called *metric compatible* if it fulfills (1.6) and is torsion-free ($\Gamma^\gamma_{\alpha\beta} = \Gamma^\gamma_{(\alpha\beta)}$, see e.g. [15, page 99] for torsion).

This uniquely determined choice of connection symbols is called *Christoffel symbols*. They allow computing the parallel transport and the covariant derivative from the metric:

$$\Gamma^\delta_{\alpha\beta} = \frac{1}{2} g^{\delta\gamma}(\partial_\alpha g_{\beta\delta} + \partial_\beta g_{\alpha\delta} + \partial_\gamma g_{\alpha\beta}). \tag{1.7}$$

1.1.4 Curvature

It is important to remember that for a manifold M there exist different choices of coordinate systems, and only if one found flat space coordinates that are applicable everywhere (that is, $\mathbf{\Gamma} = 0$ for all $p \in M$), the manifold is not curved. This reasoning does not work the other way, as the example of choosing polar coordinates (t, r, ϕ, θ) in flat space shows: Some entries are non-zero (e.g. $\Gamma^{\phi}_{r\phi} = 1/r$), but the space is still flat.

In favour to get a measure for spacetime curvature, one can analyse the "defects" of parallel transport around a closed loop with infinitesimal extend. It will be shown that the change is described by a $(1,3)$-curvature tensor called *Riemann curvature tensor.*

In the present setup (cf. figure 1.1), the vector V^μ is moved around the closed path $a \to b \to c \to d$ with infinitesimal spacings $+\Delta^\mu_1, +\Delta^\mu_2, -\Delta^\mu_1, -\Delta^\mu_2$. One cam determine the missing part $\#$ when coming back to a by explicit computation of the vector V^μ at the space time points:

$$V^\mu(a) = V^\mu(a) \tag{1.8a}$$
$$V^\mu(b) = V^\mu(a \to a + \Delta_1) = V^\mu(a) - V^\alpha(a)\Gamma^\mu_{\beta\alpha}(a)\Delta^\beta_1 \tag{1.8b}$$
$$V^\mu(c) = V^\mu(b \to b + \Delta_2) = V^\mu(b) - V^\gamma(b)\Gamma^\mu_{\delta\gamma}(b)\Delta^\delta_2 \tag{1.8c}$$
$$V^\mu(d) = V^\mu(c \to c - \Delta_1) = V^\mu(c) - V^\epsilon(c)\Gamma^\mu_{\kappa\epsilon}(c)(-\Delta^\kappa_1) \tag{1.8d}$$
$$\#V^\mu(a) = V^\mu(d \to d - \Delta_2) = V^\mu(d) - V^\lambda(d)\Gamma^\mu_{\omega\lambda}(d)(-\Delta^\omega_2) \tag{1.8e}$$

Recursively inserting all equations into each other gives a long expression where all linear terms $\mathcal{O}(\Delta^\nu_i)$ vanish. All third powers $\mathcal{O}(\Delta^\nu_i\Delta^\xi_j\Delta^\rho_k)$ are ignored, so the result is propertional to second order terms $\mathcal{O}(\Delta^\gamma_1\Delta^\delta_2)$ after appropriate index relabeling. Note that the Christoffel symbols (also) depend on the point where they are evaluated at. They can be simply moved e.g. at the first insertion step 1.8b into 1.8c by $\Gamma(b) = \Gamma(a) + \partial_\nu\Delta^\nu_1\Gamma(a)$. One ends up with the definition of the Riemann tensor $R^\mu_{\alpha\beta\gamma}$ as piece of the missing part

$$\#V^\mu(a) = V^\mu(a)\Big(\underbrace{\partial_\beta\Gamma^\mu_{\gamma\alpha} - \partial_\gamma\Gamma^\mu_{\beta\alpha} + \Gamma^\delta_{\gamma\alpha}\Gamma^\mu_{\beta\delta} - \Gamma^\delta_{\beta\alpha}\Gamma^\mu_{\gamma\delta}}_{R^\mu_{\alpha\beta\gamma}}\Big)\Delta^\gamma_1\Delta^\delta_2. \tag{1.9}$$

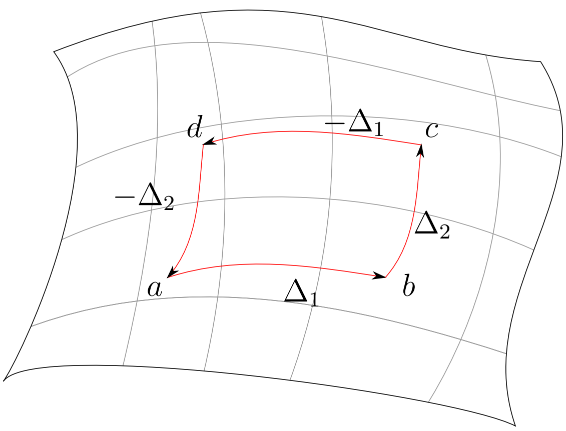

Figure 1.1: Illustration of the closed loop parallel transport on infinitesimal linear displacements Δ^μ_i. When performing the calculation in equation 1.8, on curved spacetimes one finds a defect which defines the Riemann tensor. This means the vector at the beginning (point a) does not match the vector after the loop any more.

By tensor contraction, one can define the simpler Ricci tensor $R_{\mu\nu} = R^{\lambda}_{\mu\lambda\nu}$ and finally the Ricci scalar $R = R^{\lambda}_{\lambda}$. This quantity is also called scalar curvature and it is the simplest invariant that gives information about flatness of space: As soon as $R = 0$ everywhere, the space is flat.

Most significance for the next section has the Einstein curvature tensor

$$G_{\mu\nu} = R_{\mu\nu} + \frac{1}{2} g_{\mu\nu} R. \tag{1.10}$$

1.1.5 Einstein Field Equations

Einstein equations can be derived from a variational principle $\delta S = 0$ on the action S (Hamilton principle). They can also be derived by other means, e.g. symmetry aspects leaving only one choice for combining $G_{\mu\nu}$ and the energy density tensor $T_{\mu\nu}$.

Here, the ansatz will be the action, defined by the Lagrangian $\mathcal{L} = \mathcal{L}_G + \mathcal{L}_M$, that is, the interaction (gravitational) part and the source (matter) part. Those two parts are guessed, and basically taking the curvature scalar R and the trace of the energy density tensor $T = T^{\lambda}_{\lambda}$ appears to be both an intuitive and good choice. The low energy matching is traditionally accomplished by a prefactor κ, so one ends up with the *Einstein-Hilbert-Action* including matter,

$$S = \int \sqrt{-g}\, \mathrm{d}^4 x \left(\frac{R}{2\kappa} + T \right) \tag{1.11}$$

Note that $\sqrt{-g}$, with g the determinant of the metric $g^{\mu\nu}$, is neccessary for the invariant volume element.

Splitting up the integral into two parts S_R and S_T and calculate the variation individually yields, at first for S_R,

$$\delta S_R = \frac{1}{2\kappa} \delta \int \sqrt{-g}\, \mathrm{d}^4 x\; R_{\mu\nu} g^{\mu\nu} = \frac{1}{2\kappa} \int \mathrm{d}^4 x\; R_{\mu\nu} \delta(\sqrt{-g} g^{\mu\nu}) + \frac{1}{2\kappa} \int \mathrm{d}^4 x\; \sqrt{-g} g^{\mu\nu} (\delta R_{\mu\nu}). \tag{1.12}$$

One can show that the integral over the variation of $\delta R_{\mu\nu}$ vanishes (surface integral) while the variation $\delta\sqrt{-g} g^{\mu\nu}$ contributes.

For a full discussion, one typically switches to *tensor densities* which are "salted" with $\sqrt{-g}$ and written in German gothic letters [48]

$$\mathfrak{T}^{\cdots}_{\cdots} = \sqrt{-g}\; A^{\cdots}_{\cdots}, \tag{1.13}$$

where $A^{\cdots}_{\cdots}$ represents a tensor in a local coordinate frame. Using the identity $\delta\sqrt{-g} = -{}^1\!/_2 \sqrt{-g} g_{\mu\nu} \delta g^{\mu\nu}$ yields

$$\delta S_R = \int \mathrm{d}^4 x R_{\mu\nu} (\delta \sqrt{-g} g^{\mu\nu}) = \int \mathrm{d}^4 x \sqrt{-g} \left(R_{\mu\nu} - \frac{1}{2} g_{\mu\nu} R \right) \delta g^{\mu\nu}. \tag{1.14}$$

Secondly, considering S_T, it is

$$\delta S_T = \int \mathrm{d}^4 x\; \sqrt{-g}\, (\kappa T_{\mu\nu})\, \delta g^{\mu\nu}. \tag{1.15}$$

By requiring $\delta_S = \delta S_R + \delta S_T = 0$ and collecting the terms under the integrals one recieves

$$R_{\mu\nu} - \frac{1}{2} g_{\mu\nu} R = \kappa T_{\mu\nu}, \tag{1.16}$$

the *Einstein field equations* (EFE). The low energy matching with the Newtonian potential $\Phi = -GM/r$ allows determining $\kappa = -8\pi G$ (with G the Newton constant, not to be confused with the rarely used trace of the Einstein tensor G^μ_μ).

An astonishing fact of the Einstein field equations is that they allow for deriving all classical predictions of mechanics. The energy conservation law $\nabla_\mu T^{\mu\nu} = 0$ is also intrinsically contained in the Einstein field equations. One can show that in $d = 3+1$ space-time dimensions, the EFE are 10 independent non-linear coupled equations which are only possible to solve analytically for highly symmetric problems.

1.1.6 The Planck Scale

The Planck scale is the name of the mass scale that is inevitably connected with the Einstein field equations (1.16). It can be found with the low energy limit, as from Newtons law follows $[G] = 1/M^2$. It can also be found by

- considering the metric as a dimensionless tensor.
- The curvature scalar R as second derivative of the metric must then have unit $[R] = 1/L^2 = M^2$.
- On the other hand, the energy momentum tensor $T_{\mu\nu}$ in 4 space-time dimensions has dimension $[\mathbf{T}] = M^4$.

It follows that the Einstein field equations look like

$$R_{\mu\nu} - \frac{1}{2} g_{\mu\nu} R = -8\pi \frac{1}{M_{\mathrm{Pl}}^2} T_{\mu\nu} \tag{1.17}$$

with a mass M_{Pl}, the Planck mass. Reinserting units gives a numerical value of $\sim 10^{16}$ TeV. Compared to the mass scales of particle physics, i.e. the QCD scale $\Lambda_{\mathrm{MS}} \sim 220$ MeV or the electroweak scale ~ 100 GeV, the Planck scale is huge. The large ratio of Planck mass over electroweak mass is called the *weak hierarchy problem* of the standard model of particle physics.

As a consequence, gravity can be neglected by particle collision center of mass energies accessible in ground based colliders like the Large Hadron Collider (LHC) at CERN (~ 10 TeV). As a rule of thumb, gravity must be considered when the amount of the order of Planck mass is compressed in a cube with edge length of the order of the Planck length $L_{\mathrm{Pl}} = 1/M_{\mathrm{Pl}} \sim 10^{-35}$ m.

In the next sections, a theory is proposed how to avoid these circumstances, basically by *lowering* the Planck mass to some accessible range with the LHC.

1.2 Exact solutions of General Relativity

There are books collecting and classifying exact solutions (in contrast to numerical solutions or expansions) of Einstein gravity like Griffiths [33] and Stephani [70]. For an introductory overview about the spacetimes developed by Schwarzschild and DeSitter which are presented in this section, Griffiths text book [33] gives the best overview, this section follows the reasoning of Griffiths.

In this section, in favour to the derivation of a quasi-classical source term in section 3.1, the metrics are not derived.

1.2.1 Minkowski space-time

This section is for fixing the notation used in the thesis. Minkowski spacetime (the flat space) is the Einstein solution of the empty space $R_{\mu\nu} = 0$. Working in cartesian coordinates and considering flat space with a $g_{\mu\nu} = \eta_{\mu\nu} = \mathrm{diag}(-1, +1, +1, +1)$ signature, the Minkowski line element can be given as

$$\mathrm{d}s^2 = g_{\mu\nu}\mathrm{d}x^\mu \mathrm{d}x^\nu = -\mathrm{d}t^2 + \mathrm{d}x^2 + \mathrm{d}y^2 + \mathrm{d}z^2, \tag{1.18}$$

with the coordinates $t, x, y, z \in (-\infty, \infty)$. It is convenient to switch to spherical coordinates when a spherical symmetric problem is given (as it is, in this thesis). Spherical coordinates can be given by the transformation rules $x = r\sin\theta$, $y = r\sin\theta\sin\phi$ and $z = r\cos\theta$, with $r \in [0, \infty)$, $\theta \in [0, \pi]$ and $\phi \in [0, 2\pi)$. In these coordinates, the (same) line element reads

$$\mathrm{d}s^2 = -\mathrm{d}t^2 + \mathrm{d}r^2 + r^2(\mathrm{d}\theta^2 + \sin^2\theta \mathrm{d}\phi^2) = -\mathrm{d}t^2 + \mathrm{d}r^2 + r^2\mathrm{d}\Omega_2^2. \tag{1.19}$$

Considering spherical coordinates in flat Minkowski space is a good opportunity to learn about *coordinate singularities*: Apparently, the spherical line element (1.19) exhibits singularities at points where $r = 0$, $\sin\theta = 0$ or $r \to \infty$. But the cartesian coordinate choice (1.18) tells that these singularities are not “real”, because equation (1.18) shows coordinates without singularities, so the apparent singularities are no true singularities. In contrast, a *curvature singularity* is distinguished by a diverging curvature scalar $R = R^\mu_\mu$, and no choice of coordinates can avoid a coordinate singularity at points where a curvature singularity occurs. In the next section, the most simple space-time exposing a single curvature singularity point is encountered.

1.2.2 Schwarzschild metric

The Schwarzschild metric is the solution for the spherically symmetric static point mass distribution

$$\rho_\delta(r) := \frac{M}{4\pi r^2}\delta(r), \tag{1.20}$$

which is — having electrostatics in mind — the most basic distribution one can imagine.

PN: 1. Paper von H.Balasin (Tensordichten, sagt mir nichts!). 2. Laplace und Poisson-Methoden unterscheiden.

The Schwarzschild problem, as can be found in text books [48, 77], is typically divided into the *outer* Schwarzschild metric, which describes the space outside a spherically symmetric static mass distribution where $R_{\mu\nu} = 0$, and the *interior* Schwarzschild metric that describes the space-time inside a perfect fluid.

It is worth mentioning that the outer Schwarzschild metric is derived from $\rho_\delta(r)$, as given in (1.20), but it will be assumed to be the solution outside of any spherical symmetric matter distribution $\rho(r)$. This even holds for non-static (i.e. time dependent) spherical symmetric distributions, e.g. monopole gravitational waves. This is a consequence of the *Birkhoff theorem* which states that any spherically symmetric solution of the vacuum Einstein field equations must be static and *asymptotically* flat (Minkowski for $r \to \infty$). Note that the Birkhoff theorem only holds in $d = 4$ space-time dimensions (cf. the next section about higher dimensional gravity).

The solution of (1.20) is given by the Schwarzschild metric

$$\mathrm{d}r^2 = -(1 - 2\Phi(r))\mathrm{d}t^2 + (1 - 2\Phi(r))^{-1}\mathrm{d}t^2 + r^2\mathrm{d}\theta^2 + r^2\sin^2(\theta)\mathrm{d}\phi^2 \tag{1.21}$$

with the gravitational potential (Newton's potential) $\Phi(r) = GM/r$. Note that r is not the *distance* of the origin $r = 0$, as space time is deformed and r actually gets timelike for $r < 2GM$.

The radius $r_0 = 2GM$ has a special meaning. At r_0, the metric (1.21) has a *coordinate* singularity which is not a curvature singularity, as one can see when switching e.g. to Eddington-Finkelstein coordinates (Tortoise coordinates). What physically happens at r_0 is that light from the space time region enclosed by the $r = r_0$ cannot escape that surface, i.e. it is literally trapped (*trapping* surface). For this reason, one calls this a *black hole* with event horizon radius r_0, as no event that takes place inside the horizon can be seen by an outside observer.

Actually, the Schwarzschild space-time features a curvature singularity at $r = 0$, which was already "announced" by the Dirac delta function, $\rho_\delta(r) \xrightarrow{r\to 0} \infty$. The singularity is shielded by the event horizon, so whatever happens near it cannot be observed outside. In 1969, Roger Penrose formulated the *cosmic censorship hypothesis* which states that curvature singularities are always "hidden" behind an event horizon, so there are no *naked singularities*. In fact, there are solutions of the EFEs with naked singularities, like the hyper-extreme Reissner-Nordström space-time, discussed in section 5.1.6.

Many modifications of the Schwarzschild line element have been investigated, e.g. $g_{00} = 1 - 2GM/r \to \epsilon - 2GM/r$, or by allowing $M \to M(\boldsymbol{x})$, or by including new physics (like electrical charge). Such approaches have been studied [33], and actually $M \to M(r)$ in a way $\delta \to h(r)$ with $h(r)$ a finite delta approximation describes best the roadmap for this thesis. However, in any General Relativity text book, the Schwarzschild metric is alsmost always extended with angular momentum J and/or electric charge Q, as there exist the old and well-known solutions of the Reissner-Nordström (RN) metric ($Q > 0, J = 0$), the Kerr metric ($Q = 0, J > 0$) and the Kerr-Newman metric ($Q, J > 0$). The *no-hair theorem*, formulated by John Wheeler, postulates that all black hole solutions resulting from the Einstein equations (including electromagnetism, so strictly spoken Einstein-Maxwell equations) are fully characterized by only mass M, electrical charge Q and angular momentum J. Actually, this theorem has not been proven and is therefore only a *conjecture* that will be adressed in section **??** again.

While angular momentum is probably the most relevant parameter for astronomical purposes, in this thesis it turns out that the RN metric possesses analogies to the regular black hole solutions that will be derived (section 5.1.6). Note that in this thesis, spinning black holes are not studied. This is not neccessarily bad, since only the final evaporation phases of black holes is concerned. Section **??** will deal with that topic.

1.2.3 De Sitter space-time

Except for the flat Minkowski space time, there are also two (unique) solutions with constant curvature R, which can be derived by the 10 isometries of space-time in four dimensional space-time by the local condition [33]

$$R_{\alpha\beta\gamma\delta} = \frac{R}{12}(g_{\alpha\gamma}g_{\beta\delta} - g_{\alpha\delta}g_{\beta\gamma}). \tag{1.22}$$

Using the Einstein equations with cosmological constant Λ,

$$G_{\mu\nu} + \Lambda g_{\mu\nu} = 8\pi G T_{\mu\nu}, \tag{1.23}$$

these two solutions are real vacuum solutions ($T_{\mu\nu} = 0$), and $R = 4\Lambda$, $R_{\alpha\beta} = \Lambda g_{\alpha\beta}$. Space with $R > 0$ is called *de Sitter* space-time (dS) while space with $R < 0$ is called *anti-de Sitter* space-time (AdS), after the Dutch physicist Willem de Sitter.

There is a set of spherical coordinates that do not cover the complete deSitter space time, but is well enough for the considerations done in this thesis. Robert Mayers calls these the "static patch" coordinates [52], and the gravitational potential is given by

$$V(r) = \frac{\Lambda}{3}r^2 := \left(\frac{r}{\ell}\right)^2. \tag{1.24}$$

In de Sitter space, our coordinates $g_{00} = 1 - r^2/\ell^2$ have a singularity at $r_0 = \ell = \sqrt{3/\Lambda}$. Of course, since $R = 4\Lambda > 0$ everywhere, this is no curvature singularity. Anyway the surface $r = \ell$ forms a horizon. One can show that this is a *cosmological horizon* [33] which reveals a universe expansion speed higher than the speed of light: Events beyond $r > \ell$ cannot reach the observer at $r = 0$ anymore. An exact discussion requires introduction of Friedmann-Lemaître-Robertson-Walker-like (FLRW) coordinates and "struggling" with cosmology, which is beyond the scope of this thesis.

1.3 Extra Dimensions

From the mathematical/geometrical viewpoint, in terms of tensor calculus, the generalization from 4 to d space-time dimensions is trivial: One can write the Einstein equations in d space-time dimensions as

$$R_{MN} - \frac{1}{2} g_{MN} R = -8\pi G T_{MN} \tag{1.25}$$

with capital latin indices (like A, B, M, N) running from $0, 1, \ldots, d-1$ while the lower greek indices (like α, β, μ, ν) refer to the 4d submanifold and run from 0 to 3. Lower latin indices (like a, b, m, n) indicing the 3d spatial submanifold as before $1, 2, 3$. Without indices, bold vectors (like $\boldsymbol{x}$, $\boldsymbol{y}$) shall indicate d-dimensional vectors, while vectors with arrow (like $\vec{x}$, $\vec{y}$) indicate $(d-1)$-dimensional vectors (just the spatial part in a given metric).

1.3.1 The Schwarzschild-Tangherlini black hole

Black holes in higher dimensions are more diverse than in 4d, since more topologies are possible [26], for example ring solutions ("black rings", like Doughnuts). The most simple generalization of the Schwarzschild solution to d dimensions is the *Schwarzschild-Tangherlini* metric (STM). It describes the spherical and static black hole produced by a point like matter source in higher dimensions and was found in 1963 by Tangherlini.

The STM can be described by the line element

$$\mathrm{d}s^2 = (1 - V(r))\mathrm{d}t^2 - (1 - V(r))^{-1}\mathrm{d}r^2 + r^{2+n}\mathrm{d}\Omega^2_{2+n}. \tag{1.26}$$

This line element is a straightforward extension of the 4d Schwarzschild line element (1.21). The gravitational potential is retrieved by replacing the $1/r$ Newtonian radial falloff by $1/r^{d-3}$, getting [26]

$$V(r) = \frac{2}{n+2} \frac{M G_d}{r^{d-3}}, \tag{1.27}$$

with the d-dimensional coupling constant G_d and mass parameter M. The modification of the coupling constant is a crucial reason why extradimensional gravity is done and subject to the following section. The d-dimensional coupling constant G_d will be refered to as G_*, the number of dimensions arises from the context. The gravitational potential may also be written in terms of the horizon radius

$$V(r) = \frac{2}{n+2} \left(\frac{r_H}{r}\right)^{d-3}, \quad \text{with} \quad r_H^{d-3} = \frac{n+2}{2} M G_* \,. \tag{1.28}$$

This notation uncovers the *no more* linear size-mass relation $r_H \propto M$, it is only linear in 4 dimensions.

The Schwarzschild-Tangherlini metric (1.26) will be derived as the point like mass distribution limit in section 3.

1.3.2 ADD-model

In 1998, Nima Arkani-Hamed, Savas Dimopoulos and Gia Dvali (ADD) proposed a model with n large spatial extra dimensions (LXDs or LEDs). This model lives in a $d = 4 + n$ dimensional space-time. The observable four-dimensional universe is called the *brane* (the term comes from membrane), embedded in the higher-dimensional *bulk*. These n extra dimensions are taken to be flat and compactified, like the extra dimension in the KK theory, but the compactification radius R_c is considered *large* compared to the Planck length. Typical values are $R_c \approx 1$mm. This is small enough to agree with non-observed deviations from Newton's law. The idea of the ADD model is, that all Standard Model fields *live* on the brane, that is, do not notice the existence of more than four dimensions. Only gravitons and possibly scalar fields [39] are allowed to propagate everywhere (bulk and brane). See figure 1.2a for a way to imagine brane and bulk space, while figure 1.2b displays a way to imagine compactified extra dimensions.

PN: 3 Gravitative Freiheitsgrade in bulk?

The large extra dimension scenario can solve the weak hierarchy problem of the Standard Model by imposing a new fundamental mass scale M_* which produces the observable 4d Planck mass scale M_{Pl} by integrating out the volume of the extra dimensions. The weak hierarchy problem is the strange fact that the electro-weak energy scale (masses of electro-weak gauge bosons) is about 10^{32} times smaller than the gravity energy scale (Planck mass). In other formulations, it is the question why the Higgs boson is so much lighter than M_{Pl}. The extra dimensional outcome states that one can see only an effective weak coupling constant $G = 1/M_{\mathrm{Pl}}^2$, because it is the result of the integrated out volume of the extra dimensions, where gravity also propagates. This ratio is defined as

$$M_{\mathrm{Pl}}^2 = C_n V_n M_*^{n+2} , \tag{1.29}$$

with V_n the volume of the enrolled extra dimensions, with tori and compactification radii R_c e.g. $V_n = (2\pi R_c)^n$ and a dimensionless prefactor $C_n = \mathcal{O}(1)$.

Note that there are multiple conventions about the prefactor C_n in (1.29). Here it is chosen most like the Han-Lykken-Zhang notation (HLZ), as proposed in the appendix of [18]:

$$C_n = \left(\frac{\Omega_{n+2}}{\Omega_2}\right)^{\frac{1}{n+2}} \tag{1.30}$$

The prefactor C_n is used to compensate higher dimensional numerical contributions from volume integrals. Without extra dimensions ($n = 0$), $M_{\mathrm{Pl}} = M_*$.

In the ADD scenario, these extra dimensions were to be meant *large* in extend, that is, in the milimeter scale. Thus, the fundamental couping reaches the TeV scale even with one extra dimension. This opens the door for experimental tests, as the center of mass energy of the Large Hadron Collider (LHC) at cern is in the same order of magnitude (10 TeV).

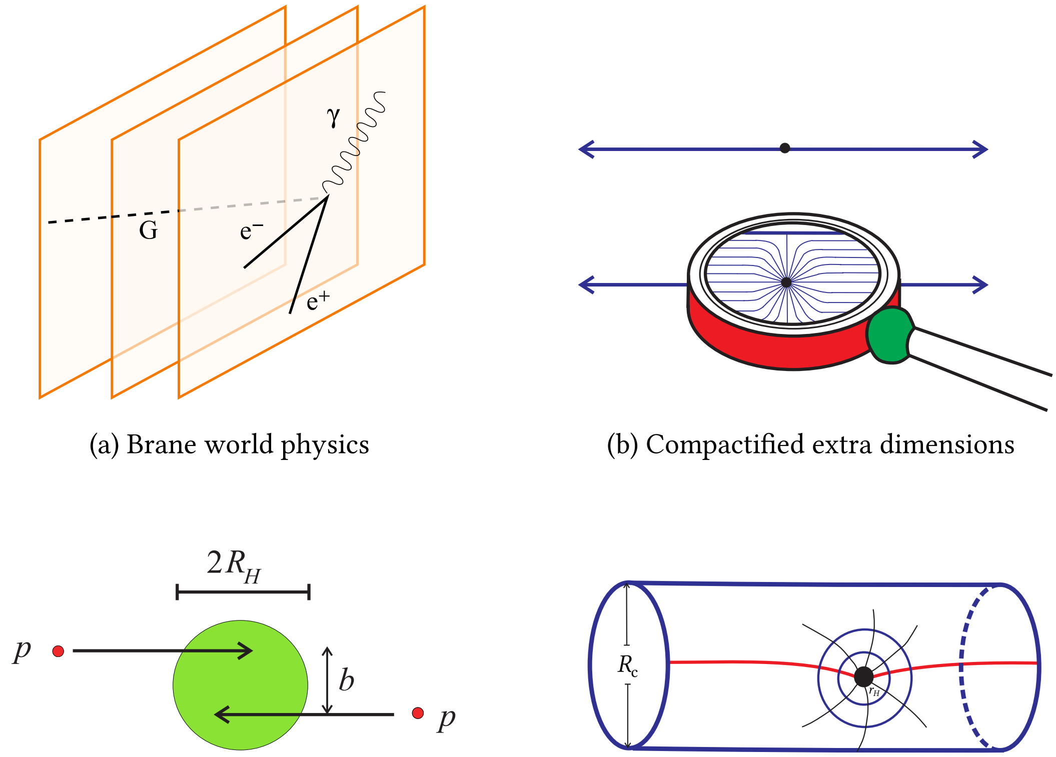

(a) Brane world physics (b) Compactified extra dimensions

(c) Hoop conjecture (d) Quantum Black Hole

Figure 1.2: Illustrations on how to imagine large extra dimensions and brane world physics.
(a) The (orange) 4d branes are displayed as 2d surfaces, while one extra dimension is displayed horizontally. While the QED process takes place on the brane, and neither electron, positron and photon can escape the brane, the graviton is allowed to freely traverse the whole spacetime.
(b) The compactification picture shows where one faces extra dimensions even in real life: When zooming in, the one dimensional horizontal line shows a vertical substructure. At big distances, the extra dimensions are not noticable.
(c) The hoop conjecture illustration shows how to imagine a particle collision with impact parameter $b < 2R_H = 2L_*$ which produces a black hole with event horizon $2R_H$.
(d) A black hole with $r_H \ll R_c$, that is, the BH is much smaller than the compactification radius of the tori, does not notice the extra dimensional periodic boundary geometry.
Pictures taken and adapted from [18, 35, 45].

1.4 Black Holes in Large Extra Dimensions

1.4.1 Production

There is no accelerator on earth which can probe quantum gravity at the 4d planck scale $\sim 10^{16}$ TeV, as already mentioned in section 1.1.6. The ADD scenario implies a mechanism how black holes in particle accelerators can be produced.

By means of the *hoop conjecture* (figure 1.2c), black holes are produced as soon as $M_{\text{center of mass}} \sim M_*$. As $L_* \ll R_c$, no problems arise with the special enrolled nature of the spatial extra dimensions (figure 1.2d): The black hole is very small compared to the extra dimensional tori, so it locally looks $3+n$-spherically symmetric [35].

The production rate is governed by a geometrical cross section approximation

$$\sigma(M) \sim \pi r_H^2. \tag{1.31}$$

This experimental signature is the main motivation for investigating black holes in large extra dimensions.

1.4.2 Evaporation

Mini black holes produced in particle colliders evaporate by Hawking radiation, because their lifetime is very short, compared to their astronomical counterparts. The evaporation process is typically categorized in four phases [11, 35, 45]:

(a) **Balding phase**. In this phase the black hole looses the *hair* which consist of asymetries (multi-pole moments and gauge fields, if applicable). It is expected that the BH goes throught the balding phase very rapidly [79]. At the end of this phase, the BH is axisymmetric and rotating. This kind of BH is described by the Kerr-Newman metric.

(b) **Spin down phase**. The black hole radiates away all of its angular momentum and some mass. The evaporation is understood in terms of Hawking and Unruh-Starobinsky radiation. At the end of this phase, the BH is spherical symmetric and nonrotating. This kind of BH is described by the Schwarzschild metric.

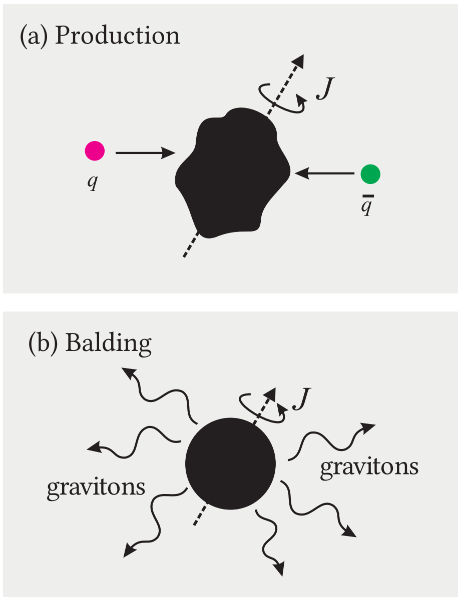

Figure 1.3: Sketch of the phases, modified from [35]

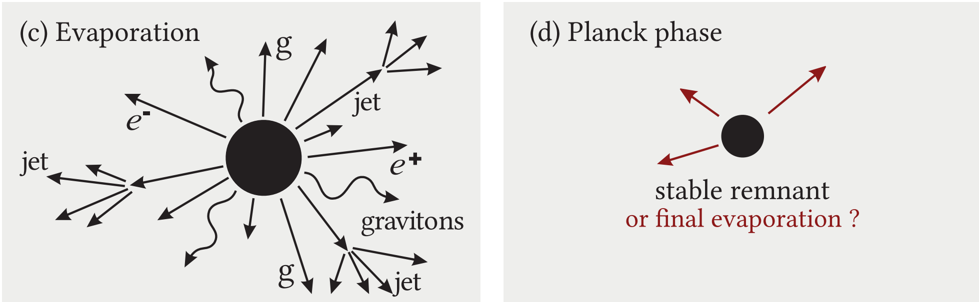

Figure 1.4: Sketch of the evaporation phases, modified from [35].

(c) **Schwarzschild phase**. The black hole is spherical and still radiates by Hawking radiation (monopole radiation pattern).

  At the end of this phase, the semiclassical thermodynamics, based on the Hawking temperature

$$T_H = \frac{\hbar\kappa}{2\pi} = \frac{\hbar}{8\pi GM}, \tag{1.32}$$

  get more and more *ill defined*. The evaporating black hole gets hotter and hotter and evventually emits particles with the same order of mass as the black hole mass. The thermodynamical canonical ensemble gets wrong because the Black hole cannot be in a stable equilibrium with its surrounding heat bath any more [29].

(d) **Planck phase**. The black hole mass reaches the Planck mass and quantum gravity effects get strong. In this phase, $r_H \sim L_*$ and the semiclassical picture breaks down. There are two widely beliefed opportunities: The black hole completely evaporates away to particles of the Standard Model, or it gets a stable configuration, the *black hole remnant*.

Chapter 2

Minimal length in physics

One of the tenets of high energy physics is the association of the failure of a theory at scales where the theory predicts singularities. It is common belief that nature is nonsingular in the same way (classical) physics is supposed to be "smooth" everywhere. Accordingly, the problem of the Schwarzschild black hole is the curvature singularity in the origin which may be back-traced to the Dirac delta distribution composing the matter source $\delta(\boldsymbol{x})$. The dirac distribution is a good model (in the sense of a matter profile) as seen from far from the origin, while it fails at small distance to the origin.

Most quantum gravity approaches address this problem by *nonlocality*. The nonlocality is typically intermediated by a minimal length scale which serves as energy scale when nonlocal effects become strong.

2.1 The black hole—particle duality

At shortest scales there is a tangible particle-black hole *duality*, illustrated in figure 2.1a. On the quantum mechanical side, each particle with mass (=energy) m can be assigned to a length scale. From quantum mechanics, candidates are the *de Broglie wavelength* and the *Compton wavelength*. For particles with speed of light, the de Broglie wavelength $\lambda_B = h/p$ becomes the Compton wavelength $\lambda_C = \hbar/mc$. As we consider energy scales $pc \propto M_{\text{Pl}}$, the velocity limit $v \to c$ is justified.

THe compton wavelength for quantum mechanical particles suggests $L_{\text{particle}} \sim 1/m$, as the red curve in figure 2.1a indicates (The mass m for a particle with $v = c$ is just $m = pc^2$). On the other hand, the black hole picture in four space-time dimensions assigns to each mass distribution a length by means of the Schwarzschild event horizon $r_H = 2GM/c^2$, so $L_{\text{black hole}} \sim m$, as the blue curve indicates. These two curves cross at the Planck scale $L_{\text{particle}} \sim L_{\text{black hole}} \sim \sqrt{\hbar c/G} := L_{\text{Pl}}$ (numerical factors are suppressed in this picture).

Trace as a gedankenexperiment a particle in an accelerator where its energy (velocity) is increased, resulting in a better length scale resolution (particle compression, red arrow). At the Planck scale M_{pl}, suddenly by the *hoop conjecture* one expects the particle to become a black hole, and further energy (i.e. acceleration) increases the size of the object (again). The resulting

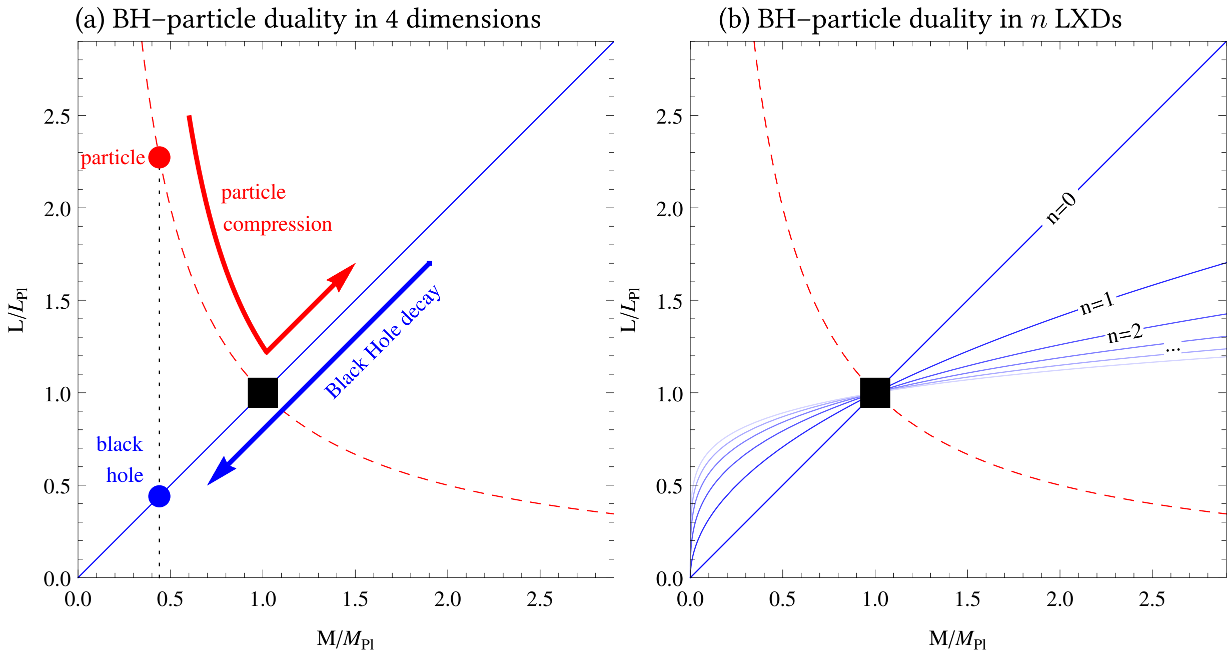

Figure 2.1: Length-vs-mass pictures for the Schwarzschild(-Tangherlini) space time (blue lines) vs the quantum mechanical picture (red dashed line)

black hole is quite unstable and decays by Hawking evaporation (blue arrow). As there is no *inverse hoop conjecture* in particle physics, nothing prevents the Schwarzschild black hole from evaporating at scales below the Planck scale. One ends up with a situation where two theories predict two different sizes for the same system.

Note that in the extra dimensional scenario, the black hole mass–length ratio is no more propertional, but $L_{\text{black hole}} \sim \sqrt[1+n]{m}$. The situation is displayed for different choices of n in figure 2.1b. The modified mass–length relation does not change the qualitative nature of the black hole–particle duality, for each number of extra dimensions the above statement holds.

2.2 Self-Completeness

There are two ways out of the black hole–particle ambiguity: Either General Relativity breaks down and must be replaced by a completely different theory, or it can be saved by some kind of *completeness*. In figure 2.2, a solution is sketched: By modifying the gravitational event horizon in a way that it smoothly merges into the particle picture, one gets a unique particle–black hole interpretation and a *minimum length scale* of physics L_{Pl}. In this theory, there is literally no way to probe distances below L_{Pl} as it is either circumvented by quantum mechanical uncertainity or black hole production.

Gravity is called *self complete* if the validity of the Einstein field equations (EFE) is recognized at any energy scale (i.e. mass scale M at figure 2.1), but it is *self protecting* against minimal length singularities. This is imposed by completing the EFE by a nonlocal contribution. It is motivated by fundamental principles like the generalized uncertainty principle, noncommuting geometry or theories like loop quantum gravity and string theory. Appendix A.2 gives a short overview about these theories.

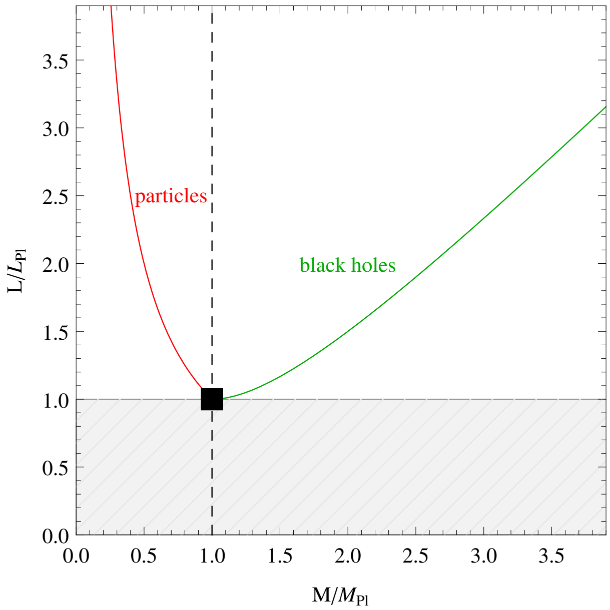

Figure 2.2: Self complete gravity: The red line displays the unaltered length scale associated with quantum particles, while the green line is an exemplary placeholder for a quantum gravity improved black hole horizon. The picture suggests a "smooth" transition at the Planck scale $M = M_{PL}$, $L = L_{Pl}$. In this way, the length scales $L < L_{Pl}$ are no more physically accessible.
This picture shall be understood as the goal of the short scale improved black hole metrics which are subject of the following chapters.

2.3 Nonlocal gravity

The nonlocal contributions to the geometric part of the Einstein field equations are introduced with a bilocal operator $\mathcal{A}^2$ which mediates *nonlocal* effects in space-time. $\mathcal{A}^2$ is a function of the generally covariant D'Alambert operator $\Box = g^{\alpha\beta}\nabla_\alpha\nabla_\beta$ associated with an energy scale $\Lambda = 1/L$ which displays the length at which short distance effects get important. $\mathcal{A}^2(\Box/\Lambda^2)$ is a dimensionless and generally covariant operator. It enters the Einstein field equations on the right hand side of Einstein equations

$$G_{\mu\nu} = 8\pi G\, \mathcal{A}^{-2}(\Box/\Lambda^2)T_{\mu\nu} := 8\pi G\mathcal{T}_{\mu\nu}. \tag{2.1}$$

The non-classical matter distribution $\mathcal{T}_{\mu\nu} = \mathcal{A}^2 T_{\mu\nu}$ is described by the nonlocal operator. By multiplying the inverse $\mathcal{A}^2$ from the left hand side, the *dual theory* is found:

$$\mathcal{A}^2(\Box/\Lambda^2)G_{\mu\nu} := \mathcal{G}_{\mu\nu} = 8\pi G\, T_{\mu\nu}. \tag{2.2}$$

In the dual theory, the nonlocality was *shifted* to the geometrical part (the Einstein tensor) of the field equations, while the matter part remains purely classical. This theory seems more fundamental than the semiclassical matter distribution.

Note the difference between equation (2.1) and (2.2): While the field equations (2.1) represents classical gravity coupled to a quantum mechanical source term $\mathcal{T}_{\mu\nu}$, the field equations

(2.2) describe equations for nonlocal spacetime $\mathcal{G}_{\mu\nu}$ coupled to a classical source term $T_{\mu\nu}$ after "modified rules" of general relativity. These two interpretations are (mathematically and physically) equivalent [51, 55].

The action of the nonlocal field theory is obtained by the modified Ricci scalar $\mathcal{R}$ in the modified Einstein tensor $\mathcal{G}_{\mu\nu} = \mathcal{R}_{\mu\nu} - \frac{1}{2} g_{\mu\nu}\mathcal{R}$. The nonlocal Ricci tensor defines the gravitational action and a variational derivation as in section 1.1.5 can be done just by replacing $R \to \mathcal{R}$.

2.3.1 Acting on the Dirac delta distribution

The nonlocal effect of $\mathcal{A}^2$ can be separated by displaying the Ricci scalar with a Dirac delta distribution

$$\mathcal{R}(x) = \mathcal{A}^2(\Box_x/\Lambda^2)R(x) = \int \mathrm{d}y\ \mathcal{A}^2(\Box_x/\Lambda^2)\delta(x-y)R(y). \tag{2.3}$$

By means of the momentum representation of the dirac distribution $\delta(x) = \int \mathrm{d}p\ e^{ipx}$, the nonlocal operator $\mathcal{A}^2$ can be displayed in momentum space:

$$\mathcal{R}(x) = \int \mathrm{d}y\ R(y) \int \mathrm{d}p \mathcal{A}^2(-p^2)e^{ip(x-y)}. \tag{2.4}$$

2.4 The generalized uncertainty principle

The generalized uncertainty principle (GUP) proposes a modification of the Heisenberg uncertainty principle

$$\Delta x\, \Delta p \geq \frac{\hbar}{2}. \tag{2.5}$$

As the Heisenberg uncertainty principle is a consequence of the quantum mechanical commutator relation

$$[\boldsymbol{x}, \boldsymbol{p}] = i\hbar, \tag{2.6}$$

the GUP is usually introduced by complementing this commutator relation for momentum and/or position dependent terms [41],

$$[\boldsymbol{x}, \boldsymbol{p}] = i\hbar(1 + \alpha\boldsymbol{x}^2 + \beta\boldsymbol{p}^2). \tag{2.7}$$

This yields a modified uncertainty relation of the form

$$\Delta x\, \Delta p \geq \frac{\hbar}{2}\left(1 + \alpha\boldsymbol{x}^2 + \beta\boldsymbol{p}^2 + \alpha\langle\boldsymbol{x}\rangle^2 + \beta\langle\boldsymbol{p}\rangle^2\right). \tag{2.8}$$

Restricting to the case $\alpha = 0$ allows to find a Hilbert Space representation [41] in momentum space. Solving relation (2.8) for exact equality for Δp requires for exact momentum measurement $\langle p\rangle = 0$ a minimal position uncertainty

$$\Delta x \geq \hbar\sqrt{\beta}. \tag{2.9}$$

It is possible to derive an identity operator in momentum space for $\alpha = 0$, it is [41]

$$1 = \int_{-\infty}^{+\infty} \frac{\mathrm{d}p}{1+\beta p^2} |p\rangle\langle p| \,. \tag{2.10}$$

This enables computing the Schwarzschild black hole in the GUP scenario. To do so, the GUP must be stated for vector operators. It follows that (2.10) basically holds for any number $m \in \mathbb{N}$ of spatial dimensions [37]

$$1 = \int_{-\infty}^{+\infty} \frac{\mathrm{d}^m p}{1+\beta p^2} |p\rangle\langle p| \quad \text{with } p = \|p\| \,. \tag{2.11}$$

The modified position space integration measure defines the nonlocal operator $\mathcal{A}^{-2}$ for the (quantum-modified) matter part of the GUP Schwarzschild black hole. It is introduced by means of the momentum representation of the Dirac delta distribution which constructs the Schwarzschild black hole:

$$\mathcal{T}_{\mu\nu} = -M\mathcal{A}^{-2}(\Box)\delta^3(\vec{r}) \stackrel{!}{=} -\frac{M}{(2\pi)^3} \int \frac{d^3p}{1+\beta p^2} e^{i\vec{x}\cdot\vec{p}} \tag{2.12}$$

The nonlocal GUP operator in 4d spacetime therefore reads

$$\mathcal{A}(\Box) = (1-\Box)^{1/2} \tag{2.13}$$

and fulfills $\mathcal{A} \to 1$ when $\Box \to 0$. The GUP effect (2.12) can be computed etc., this is done in [37] and the next chapter.

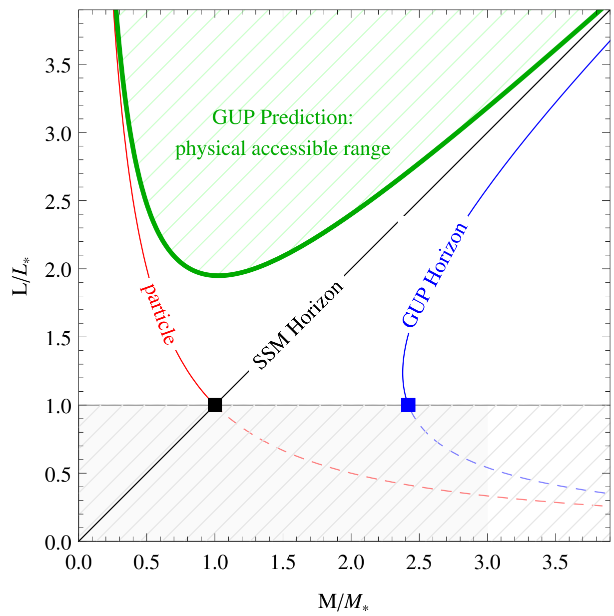

Figure 2.3: The outer horizon of the spherical static black hole in the GUP scenario (blue), compared to the classical Schwarzschild prediction (black). The green range indicates the accessible range predicted by the uncertainty relation (2.8). The lower bounds of the compton wavelength and GUP black hole horizon allow a greater accessible physical region. In any way, distances below $L < L_*$ cannot be probed.

Chapter 3

Quasi-classical black holes

In this chapter, a rather unspecified class of generic black hole solution is discussed. It is constructed by a quasi-classical source term which is modeled by a *smeared* dirac delta distribution. In the static radial symmetric setup, we can compute the modifications from the ordinary Schwarzschild setup. In this chapter, a concrete choice for the smearing will not be made. It is introduced only in a fashion $\Theta(r) \to H(r)$ with $\Theta(r)$ the Heaviside step function and $H(r)$ an approximation function, characterized by a regulator $\tilde{r}_0$ with dimension of length. As we will derive a nonlocal operator for this class of black holes in the end of the chapter, $\tilde{\Gamma} = {}^1\!/_{\tilde{r}_0}$ turns out to be the energy scale where modifications to General Relativity apply. These modifications are coded in $H(r)$, and it depends on the form of $H(r)$ if the modifications can improve the low distance regime of General Relativity.

3.1 From a quasi-classical source term to the metric

In this section, the metric for any static spherical symmetric gravitational potential $V(r)$ in $d = n+4$ space time dimensions will be derived. The only further requirement is large distance matching of the Schwarzschild potential $V(r) = 2GM/r$. This is equivalent to starting with a static isotropic matter density $\rho(r)$ and requiring $\lim_{r\to\infty} \rho(r) = 0$.

The ansatz for the solution is the following $d = n + 4$ dimensional spherical symmetric and static metric, described by its line element

$$\begin{aligned} \mathrm{d}s^2 &= -e^{\nu(r)}\mathrm{d}t^2 + e^{-\nu(r)}\mathrm{d}r^2 + r^2\mathrm{d}\Omega^2_{n+2} && (3.1)\\ &= -\left(1 - V(r)\right)\mathrm{d}t^2 + \left(1 - V(r)\right)^{-1}\mathrm{d}r^2 + r^2\mathrm{d}\Omega^2_{n+2} && (3.2)\end{aligned}$$

with Ω_{n+2} the surface line element of an $(n+3)$ sphere (for details about the surface sphere, see appendix **??**). The spherical coordinates are given by $x_\mu = (x_0, \vec{x}) = (x_0, r, \phi, \theta_1, \ldots, \theta_{n+2})$, but it is written i instead of θ_i ($i = 1, \ldots, m$ and $m := n + 2$) in the indices to improve readability, refering to the diagonal coefficients in the metric as

$$g_{AB} = \mathrm{diag}\left(g_{00}(r), -g_{00}^{-1}(r), g_{\phi\phi}(r,\phi), g_{11}(r,\theta_1), \ldots, g_{mm}(r,\theta_m)\right). \tag{3.3}$$

This notation is the same as in [65].

The argumentation follows the derivation of the inner Schwarzschild solution, as can be found in General Relativity textbooks: The property $-g_{00} = g_{11}^{-1}$ is required for flat space at large distances.

Given the matter density and the metric ansatz, the stress tensor T^{NM} can be determined. Due to the symmetry of the problem, it can already be stated as

$$T^{NM} = \mathrm{diag}\left(T^{00}, T^{rr}, T^{\phi\phi}, T^{11}, T^{22}, \ldots, T^{mm},\right) = \mathrm{diag}\left(-\rho, -\rho, p, p, \ldots, p\right), \tag{3.4}$$

following [57,65]. Now switching to a $(1,1)$ type tensor for $\mathbf{T}$ yields the conservation of energy equation as $\nabla_N T^N_M = 0$ with

$$T^A_B = g_{BC}T^{AC} = g_{BB}T^{AB} = \mathrm{diag}(g_{00}T^{00}, g_{rr}T^{rr}, \ldots, g_{mm}T^{mm}). \tag{3.5}$$

The conservation equation $\nabla_N T^N_M = 0$ is now computed for all d possible values of the free index M. Starting with the $M = r$ case gives the equation (no sum convention here)

$$0 = \nabla_0 T^0_r + \nabla_r T^r_r + \sum_i \nabla_i T^i_r. \tag{3.6}$$

The covariant derivative ∇_N and the Christoffel symbol Γ^C_{AB} must be computed (see appendix E for the definitions). The summands of (3.6) are given by

$$\nabla_0 T^0_r = \partial_0 T^0_r + \Gamma^0_{0D}T^D_r - \Gamma^D_{0r}T^0_D = \frac{1}{2}g^{00}T^r_r\partial_r g_{tt} + \frac{1}{2}g^{00}T^0_0\partial_r g_{tt} \tag{3.7a}$$

$$\nabla_r T^r_r = \partial_r T^r_r + \Gamma^r_{rD}T^D_r - \Gamma^D_{rr}T^r_D = \partial_r T^r_r \tag{3.7b}$$

$$\forall i: \quad \nabla_i T^i_r = \partial_i T^i_r + \Gamma^i_{iD}T^D_r - \Gamma^D_{0r}T^i_D = \frac{1}{2}g^{ii}T^r_r\partial_r g_{ii} + \frac{1}{2}g^{ii}T^0_0\partial_r g_{ii} \tag{3.7c}$$

One ends up with the explicit equation

$$0 = \partial_r T^r_r + \frac{1}{2}g^{00}\left(T^r_r - T^0_0\right)\partial_r g_{00} + \frac{1}{2}\sum_i g^{ii}\left(T^r_r - T^i_i\right)\partial_r g_{ii} \tag{3.8}$$

By construction of T^A_B, the term $T^r_r - T^0_0 \sim \rho - \rho = 0$ vanishes. The remaining contribution from each angle i is

$$g^{ii}\partial_r g_{ii} = \frac{1}{r^2\sin^i(\theta_i)}\partial_r\left(r^2\sin^i(\theta_i)\right) = \frac{2}{r}, \tag{3.9}$$

where $\sin^i(x) = (\sin(x))^i$ displays the ith power of $\sin(x)$. By summing up $d-2$ equal terms (3.9), all remaining energy momentum components are determined to

$$T^i_i = T^0_0 + \frac{r}{n+2}\partial_r T^0_0 = \rho + \frac{r}{n+2}\partial_r\rho. \tag{3.10}$$

As a result, the $M = r$ case of the energy conservation law $\nabla_N T^N_M = 0$ already determined the energy momentum tensor. It is not shown here that the other $d-1$ energy conservation equations do not contribute any further information.

In order to solve the Einstein equation, in addition to the energy momentum tensor one needs the Ricci tensor as additional ingredient. It is given as the contraction of the Riemann tensor

$$R_{\mu\nu} = \partial_\lambda \Gamma^\lambda_{\nu\mu} - \partial_\nu \Gamma^\lambda_{\lambda\mu} + \Gamma^\lambda_{\mu\gamma}\Gamma^\gamma_{\nu\mu} - \Gamma^\lambda_{\nu\gamma}\Gamma^\gamma_{\lambda\mu}, \tag{3.11}$$

see Appendix E.1 for the values of all Christoffel symbols. The Ricci tensor is again diagonal, with the entries, as (1,1) type tensor,

$$R^0_0 = R^r_r = -\frac{e^\nu}{2}\left(\partial^2_r \nu + (\partial_r \nu)^2 + (n+2)\frac{\partial_r \nu}{r}\right) = \frac{1}{2}V''(r) - \frac{n+2}{2}\frac{V'(r)}{r} \tag{3.12a}$$

$$\forall i: \quad R^i_i = \frac{1+n-e^\nu\left(1+n+r\partial_r\nu\right)}{r^2} = (1+n)\frac{V(r)}{r^2} + \frac{V'(r)}{r}. \tag{3.12b}$$

The Ricci scalar is then given by

$$R = R^N_N = \frac{(n+2)V(r)}{r^2} + V''(r). \tag{3.13}$$

Now one can write out the Einstein equations in a trace reversed form, in $(1,1)$ tensor notation for d dimensions:

$$R^B_A = \frac{1}{M_*^{n+2}}\left(T^B_A - \delta^B_A \frac{T^C_C}{n+2}\right) \tag{3.14}$$

Since $\mathbf{R}, \mathbf{T}, \delta$ are diagonal, the Einstein equations reduce to d non-zero equations where only two equations differ from each other, identified by their indexes $A, B = r, r$ and $A, B = i, i$. The latter gives the following first order differential equation for $V(r)$:

$$V'(r) + \frac{n+1}{r}V(r) = \frac{1}{M_*^{n+2}}\frac{r\rho(r)}{n+2} \tag{3.15}$$

The general solution of the metric for any $\rho(r)$ is given by the integral

$$V(r) = \frac{1}{r^{n+1}}\left(\frac{1}{(n+2)M_*^{n+2}}\int_{c_1}^{r} x^{n+2}\rho(x)\mathrm{d}x + c_2\right) \quad \text{with} \quad c_1, c_2 = \mathrm{const} \tag{3.16}$$

The boundary values $V(0)$ and $V'(0)$ give rise to the two integration contants c_1 and c_2. Physically, they allow the low-energy matching of the theory. In the context of this thesis, c_1 is important for discussion about minimal lengths.

3.2 A smeared point-like matter density

The matter density choice to be inserted into (3.16) is based on the Schwarzschild-Tangherlini point-like static and spherically symmetric density

$$\rho(r) = \frac{M}{\Omega_{n+2}\, r^{n+2}}\delta(r) = \frac{M}{\Omega_{n+2}\, r^{n+2}}\frac{\mathrm{d}\Theta(r)}{\mathrm{d}r}, \tag{3.17}$$

with the Dirac delta distribution $\delta(r)$ and the Heaviside unit step function

$$\Theta(r) = \begin{cases} 0 & \text{when} \quad r < 0 \\ 1 & \quad\quad\quad\; r \geq 0 \end{cases}. \tag{3.18}$$

The occurence of the Heaviside function in the Schwarzschild source term (3.17) is now replaced by a *smeared* version we refer to as $H(r)$. This function $H(r)$ is supposed to encode all nonlocal effects of the theory. The generic *Schwarzschild-like* energy density is therefore

$$\rho(r) = \frac{M}{\Omega_{n+2}\, r^{n+2}} \frac{\mathrm{d}H(r)}{\mathrm{d}r}. \tag{3.19}$$

Inserting (3.19) into the integral 3.16 gives us the gravitational potential with n large extra dimensions as

$$\boxed{V(r) = \frac{1}{2+n} \frac{M}{M_*^{n+2}} \frac{H(r)}{r^{n+1}}.} \,. \tag{3.20}$$

Here, M_* is the fundamental Planck mass, and M is a constant that will be identified as mass.

3.2.1 The Mass

Question: Shall I mention the bad definition of the mass, sinc the line element in integral (3.21) is actually **wrong** and should be $\sqrt{-g}\mathrm{d}^{n+3}x$? Current papers (e.g. Ansoldis Review about regular BHs) do not discuss this, but some textbooks about GR do. Do you have literature where this is discussed for our class of QG black holes?

The mass contained inside a $(3+n)$-sphere (the object will be referred to as $\mathcal{B}(r)$) with radius r is given by the integral

$$m(r) = \int\limits_{\mathcal{B}(r)} \rho(x)\mathrm{d}^{n+3}x = M \int\limits_0^r H'(r) = MH(r). \tag{3.21}$$

From the mathematical viewpoint, the mass M is just a constant that may be used to fulfill the horizon equation $V(r) = 1$. Therefore I set

$$M = (n+2)M_*^{n+2} \frac{r_H^{n+1}}{H(r_H)}, \tag{3.22}$$

so when plugging into the metric

$$V(r) = \frac{1}{n+2} \frac{M}{M_*^{n+2}} \frac{H(r)}{r^{n+1}}, \tag{3.20 revisited}$$

the horizon equation $V(r) = 1$ is fulfilled at $r = r_H$. The physical meaing of M is the mass of a black hole of radius r_H [58]. When substituting $n+1$ powers of M_* by $M_* = 1/L_*$, one can easily relate

$$\boxed{M = (n+2) \left(\frac{r_H}{L_*}\right)^{n+1} \frac{1}{H(r_H)} M_*} \,. \tag{3.23}$$

3.2.2 The regulator

The amount of *smearing* accomplished by the function $H(r)$ must be mathematically encoded in a constant that can be brought in relation to r, so it shall be of dimension length or energy. For example, consider the Gaussian delta approximation

$$\delta_\sigma(r) = \frac{1}{\sqrt{2\pi\sigma}} \exp\left(-\frac{r^2}{2\sigma}\right), \quad \delta(r) = \lim_{\sigma\to 0} \delta_\sigma(r). \tag{3.24}$$

as a canidate for $H'(r) := \delta_\sigma(r)$. The variance σ, also refered to as the *width* of the distribution, is the regulator of the metric constructed when inserting the cumulative normal distribution function $H(r) := \Phi(r) \propto \int_{-\infty}^r e^{-x^2/2\sigma} \mathrm{d}x$ into (3.20).

In the physical models in the next chapters, the *width* (from now on the symbol $\tilde{r}_0$ will be generally used) will be linked to a physical length scale by imposing principles like self-encoding.

In favour to take the limit $H(r) \to \Theta(r)$, one has to examine the limit of the regulator $\tilde{r}_0 \to 0$. Accordint to the finite values $\Theta(r) = 1$ and $\delta(r) = 0$ for $r > 0$, for any nonzero radius, the limit $\tilde{r}_0 \to 0$ is accomplished by the replacement rules

$$H(r) \to 1, H'(r) \to 0, H''(r) \to 0, \ldots. \tag{3.25}$$

This of course also holds for products like $H(r)H'(r) \to 0$.

3.3 Geometry

The mass M and gravitational potential $V(r)$ were determined for arbitrary $H(r)$. For specific choices of $H(r)$, one is able to do a discussion about event horizons ($g_{00} = 1 - V(r) \overset{!}{=} 0$) and evventually draw a conformal diagram. This is done for two models in sections 4.1 and 5.1. Here, the discussion will be a general one about special features of any metric described by $H(r)$.

3.3.1 Remnants

Nonlocal matter distributions described by $H(r)$ exhibit extremal configurations which can be identified with the two *remnant equations*:

$$\begin{cases} g_{00}(r_0) & = 0 \quad (3.26a) \\ \partial_r\big|_{r=r_0} g_{00}(r) & = 0 \quad (3.26b) \end{cases}$$

The first equation (3.26a) ensures the metric has a horizon at r_0. The second equation (3.26b) requires the metric to have an extremal value at r_0. The latter also states that the remnant temperature, which is propertional to $\partial_r g_{00}(r)$, shall vanish at r_0. This motivates the name *black hole remnant* for the black hole with horizon radius $r_H = r_0$: It is stable and decays no more. This is discussed in section 3.4. At this point, note that this kind of black hole remnant is called a *cold* remnant.

When inserting the generic potential (3.20), the remnant equations give

$$g_{00}(r_0) = 0 = 1 - \frac{1}{2+n}\frac{M}{M_*^{n+2}}\frac{H(r_0)}{r_0^{n+1}} \tag{3.27a}$$

$$\partial_r|_{r=r_0}\, g_{00}(r) = 0 = H'(r_0) - (n+1)\frac{H(r_0)}{r_0}. \tag{3.27b}$$

If the second remnant equation (3.27b) is fulfilled *only* depends on the shape of $H(r)$. As $H(r)$ is supposed to approximate a step function, chances are good that (3.27b) is fulfilled for *any* reasonable $H(r)$. Therefore, remnants are a property of nonlocal gravity. Physical meaningful remnants which are stable also have to fulfill (3.27a).

3.3.2 Curvature finitness

The Ricci scalar is according to (3.12) given by

$$R(r) = R_N^N = \frac{(n+2)V(r)}{r^2} + V''(r) \tag{3.28a}$$

$$= \frac{2}{2+n}\frac{M}{M_*^{2+n}}\frac{(2+n)^2H(r) - 2(1+n)rH'(r) + r^2H''(r)}{r^{3+n}} \tag{3.28b}$$

A profile $H(r)$ can produce a non-singular black hole origin if the nominator in (3.28b) has a taylor expansion at least of order r^{3+n}. When expanding $H(r)$ and its derivatives in a series expansion around $r = 0$ as

$$H(r) = \sum_{n=0}^{\infty}\frac{H^{(n)}(0)}{n!}r^n \approx H(0) + H'(0)r + \frac{1}{2}H''(0)r^2, \tag{3.29}$$

$$H'(r) = \sum_{n=0}^{\infty}\frac{H^{(n+1)}(0)}{n!}r^n \approx H'(0) + H''(0)r \tag{3.30}$$

$$H''(r) = \sum_{n=0}^{\infty}\frac{H^{(n+2)}(0)}{n!}r^n \approx H''(0) \tag{3.31}$$

one can determine the leading term (biggest power of r) from the nominator in (3.28b) as

$$\begin{aligned}(2+n)^2H(r) - 2(1+n)rH'(r) + r^2H''(r) &\sim (2+n)^2H(0)\\ &+ (3+2n+n^2)H'(0)r + (1/4n^2 - n)H''(0)r^2 \propto H(0).\end{aligned} \tag{3.32}$$

A regular black hole therefore fulfills the condition

$$H(r) = \mathcal{O}(r^{3+n}) \quad \text{at origin } \; r = 0. \tag{3.33}$$

3.3.3 Energy conditions

Energy conditions in General Relativity are a tool to put constraints on matter distributions (that is, energy-momentum tensors) in a way how some expects them to behave. They are formulated from a classical viewpoint and *not* deduced from Einstein field equations or other first principles. Roughly speaking, they generalize the statement that one does not observe negative masses or regions of negative mass distribution.

Approaches to Quantum Gravity regularly violate energy conditions, and by examining how and where they violate these conditions, one understands about the quantum nature in General Relativity. For example, one expects energy conditions violate around the black hole center, e.g. violations occur in a region $r \lesssim L_*$ while they hold for $r \gtrsim L_*$. As Ansoldi notes, this is cannot be taken for granted in a non linear theory as General Relativity is [2].

We check the following energy conditions (EC):

- **Null EC**, defined that for every (future) *null* vectors x^μ the observed matter density

$$\rho_{\text{obs}} = T_{AB} x^A x^B \tag{3.34}$$

is non negative, $\rho_{\text{obs}} \geq 0$. In words, this means a matter density ρ_{obs} observed by a *light ray* must be positive. A null vector fulfills $x_A x^A = -x_0^2 + x_1^2 + \sum_{i=2}^{3+n} x_i^2 = 0$, and if it is a *future* null vector, $x_A > 0 \,\forall$ possible indices A. Since $T_{AB} \sim \operatorname{diag}(-\rho, -\rho, p, \ldots, p)$ we get

$$\rho_{\text{obs}} \sim -\rho x_1^2 + \sum_{i=2}^{3+n} p x_i^2 = -\rho x_1^2 + p(x_0^2 - x_1^2) = -(\rho + p)x_1^2 + p x_0^2 \overset{!}{\geq} 0 \tag{3.35}$$

The negative contribution is governed by

$$f_{\text{weak}}(r) := \rho + p = 2\rho + \frac{r}{n+2}\partial_r \rho. \tag{3.36a}$$

$$= \frac{2M}{\Omega_{n+2}} \left(\frac{2H'(r)}{r^{n+2}} + \frac{1}{n+2} \frac{H''(r)}{r^{n+1}} \right) \tag{3.36b}$$

In regions where $f_{\text{weak}}(r) > 0$, it is violated. For $H \to \Theta$, (3.36b) is exactly 0 except at the origin.

- **Strong EC** requires basically the same for any (future) *timelike* vector x^μ. We find it violated when

$$f_{\text{strong}}(r) = (2+n)p > 0, \tag{3.37}$$

with the same comment as the Null EC.

- **Dominant EC** requires for any (future pointing) timelike or null vector x^μ that $-T^A_B x^B = -T^A_A x^A = y_A$ is a future timelike or null vector.

Law	Thermodynamics	black holes
0.	T constant on a body in thermal equilibrium	κ constant on horizon of (stationary) BH
1.	$\mathrm{d}E = T\mathrm{d}S - p\mathrm{d}V + \mu \mathrm{d}N$	$\mathrm{d}M = \frac{\kappa}{8\pi}\mathrm{d}A + \Omega_H \mathrm{d}J + \Phi \mathrm{d}q$
2.	$\delta S \geq 0$	$\delta A \geq 0$
3.	$T = 0$ cannot be reached	$\kappa = 0$ cannot be reached

Table 3.1: The laws of thermodynamics correspond with black hole thermodynamics

3.4 Thermodynamics

3.4.1 Hawking Temperature

The Hawking temperature $T_H = \kappa/4\pi$ is defined by means of the surface gravity $\kappa = \partial_r g_{00}|_{r=r_H}$ at the black hole horizon r_H. One gets for generic $H(r)$ the temperature

$$T_H = \frac{1}{4\pi}\left(\frac{1+n}{r_H} - \frac{H'(r_H)}{H(r_H)}\right). \tag{3.38}$$

Taking the Schwarzschild limit $H \to \Theta$ means $H'/H \to 0$, so one evventually gets the well known 4d Schwarzschild temperature $T = 1/(4\pi r_H)$. The H'/H term is the quantum correction which has to cure the diverging behaviour of the first summand $\sim 1/r_H$ in the temperature if the theory shall be a useful Quantum Gravity approach. This leads to the requirement

$$\frac{H(r)}{H'(r)} = \mathcal{O}(r) \quad \text{at origin } r = 0. \tag{3.39}$$

3.4.2 Heat capacity

The heat capacity is an extensiv thermodynamical property, defined as a measure of the heat added to an object resulting from a temperature change, in terms

$$C = \frac{\Delta Q}{\Delta T}. \tag{3.40}$$

For black hole thermodynamics, one can identify $Q = M$ and use the Hawking temperature just derived to compute the heat capacity. The heat capacity can be computed by reusing $T(r_H)$ and $M(r_H)$ when inserting a $1 = \partial r_H/\partial r_H$ and computing

$$C = \frac{\partial M}{\partial T_H} = \frac{\partial M}{\partial r_H}\left(\frac{\partial T_H}{\partial r_H}\right)^{-1} = \frac{\partial M}{\partial z_H}\left(\frac{\partial T_H}{\partial z_H}\right)^{-1}. \tag{3.41}$$

For generic $H(r)$, inserting temperature (3.38) and mass (3.23), one can do the elaborate computation and ends up with the compact expression

$$C = -\frac{4\pi r_H^{n+2}}{M_*^{n+2}} \frac{(n+1)H(r_H) - r_H H'(r_H)}{r_H^2 H(r_H) H''(r_H) - r_H^2 H'(r_H)^2 + (n+1) H(r_H)^2}. \tag{3.42}$$

By simply letting $H, H', H'' \to 0$ according to section 3.2.2, one ends up with the diverging heat capacity of ordinary Schwarzschild black hole:

$$\begin{tikzcd} C \arrow[r, "H \to \Theta"] \arrow[d, "n \to 0"'] & -4(1+n)\pi r_H^{2+n}/M_*^{2+n} \arrow[d, "n \to 0"] \\ -4\pi r_H^2 G \frac{H - r_H H'}{r_H^2 H H'' - r_H^2 H'^2 + H^2} \arrow[r, "H \to \Theta"'] & -4\pi r_H^2 G \end{tikzcd} \tag{3.43}$$

Depending on $H(r)$, the heat capacity possibly undertakes changes of sign, where a phase transition takes place ($C \to \pm\infty$). Radii here $C(r) \to \pm\infty$ are called critical radii and labeled r_C. At such a point, the black hole temperature $T_H(r_C)$ (eq. 3.38) is maximal:

$$\partial_{r_H} T_H|_{r_H = r_C} = 0 \Leftrightarrow z_C = \sqrt{\frac{1+n}{H'(z_C) - H''(z_C)H(z_C)}} H(z_C). \tag{3.44}$$

As $H(z) \to \Theta(z)$, the critical point goes to infinity. This corresponds to the fact that the Schwarzschild metric has no critical point.

3.4.3 Entropy

Entropy is a measure of information, and there are many definitions. In statistical mechanics, entropy is typically defined as the amount of information needed to describe the physical state of a thermodynamical system. It therefore counts all micro states which define an emerging macroscopic state.

In the context of black holes, entropy is maybe the most interesting quantity, since it deals with the *information paradox* of black holes. It is the issue what happens with information (i.e. physical states) that crosses the event horizon.

The Hawking-Bekenstein entropy is defined via the Hawking Temperature T_H as

$$S = \int \frac{\mathrm{d}M}{T_H}. \tag{3.45}$$

The entropy defining integral can also be subsituted like in the heat capacity in the section before, giving for generic H a compact expression:

$$\boxed{S(r) = \int \frac{\mathrm{d}M}{T} = \int \mathrm{d}r_H \left(\frac{1}{T} \frac{\mathrm{d}M}{\mathrm{d}r_H} \right) = 4\pi m_n \int \mathrm{d}r_H \frac{r_H^{1+n}}{H(r_H)}} \tag{3.46}$$

Approaching the limit $H \to \Theta$, one gets the Schwarzschild entropy curve

$$4\pi m_n \int \mathrm{d}r_H \, r_H^{1+n} = \frac{4\pi m_n}{1+n} r_H^{2+n} \xrightarrow{n \to 0} 8\pi G \, r_H^2 \tag{3.47}$$

Answer to your comment considering the Entropy S: *From NCBH I got the gamma, this sounds to be wrong*, according to the $1/H(r_H)$ in the denominator of (3.46):
I pressume my result is right. I might insert a chapter discussing GUP and NCBHs in a short as candidates for $H(r)$. I then expect $H(r) \sim \gamma\left(\frac{3}{2}, \frac{r^2}{4\theta}\right)$ according to eq. (61) in your 2008 NCBH review [53] http://arxiv.org/abs/arXiv:0807.1939.

3.5 Nonlocal operator

In this chapter, I want to derive a nonlocal operator $\mathcal{A}^{-2}(\boldsymbol{x})$ for the given smearing models $H(r)$. For $L_* \to 0$, this operator is supposed to vanish $\mathcal{A}^{-2} \to 1$. This section ties up with the introduction of nonlocal operators given in the previous chapter according to [51, 55].

The operator is linked to $H(r)$ with a Fourier transformation. Working in momentum space allows one to easily compute the inverse. The smeared energy-momentum tensor reads

$$\mathcal{T}_0^0 = M\mathcal{A}^{-2}(\Box)\delta^{3+n}(\vec{x}). \tag{3.48}$$

It produces the matter density given in (3.19),

$$\mathcal{T}_0^0 = \frac{M}{\Omega_{n+2}\, r^{n+2}} \frac{\mathrm{d}H(r)}{\mathrm{d}r}. \tag{3.49}$$

Matching equations (3.48) and (3.49) means

$$\boxed{\mathcal{A}^{-2}(\Box)\delta^{3+n}(\vec{x}) = \frac{1}{\Omega_{n+2} r^{n+2}} \frac{\mathrm{d}H(r)}{\mathrm{d}r}}\,. \tag{3.50a}$$

Writing the dirac delta by its plane wave momentum space representation $\delta(\vec{x}) = \int \mathrm{d}^{3+n}p\, e^{+ipx}$ on the left hand side and inserting a $1 = \mathcal{F}^{-1}\mathcal{F}$ by means of a double fourier transformation on the right hand side allows computing a solution for the operator in momentum space by means of a fourier transformation of the right hand side:

$$\Leftrightarrow \int \mathrm{d}p^{3+n}\, \mathcal{A}^{-2}(\Box)\, e^{ipx} = \frac{1}{\Omega_{n+2} r^{n+2}} \frac{\mathrm{d}H(x)}{\mathrm{d}x} \tag{3.50b}$$

$$\Leftrightarrow \int \mathrm{d}^{3+n}p\, \mathcal{A}^{-2}(p^2)\, e^{ipx} = \int \mathrm{d}^{3+n}p\, \overbrace{\left(\frac{1}{(2\pi)^{2+n}} \int \mathrm{d}^{3+n}z \frac{1}{\Omega_{n+2}\|z\|^{n+2}} \frac{\mathrm{d}H(\|z\|)}{\mathrm{d}\|z\|} e^{-ipz}\right)}^{\tilde{\mathcal{T}}_0^0(p)} e^{ipx} \tag{3.50c}$$

$$\Leftrightarrow \mathcal{A}^{-2}(p^2) = \frac{1}{(2\pi)^{2+n}\Omega_{n+2}} \int \mathrm{d}^{3+n}z \frac{1}{z^{n+2}} \frac{\mathrm{d}H(z)}{\mathrm{d}z} e^{-ipz} \tag{3.50d}$$

Note that, by concept, the operator $\mathcal{A}^{-2}$ is dimensionless. It is therefore valid to switch the coordinate system $(r, p) \to (z, q)$ without prefactors, where $z = r/L$, $q = pL$ are dimensionless coordinates with arbitrary length scale L.

3.5.1 Higher-dimensional Fourier Transformation

To solve (3.50d), one can integrate out all extra dimensional angles and effectively reduce the higher-dimensional fourier transformation of the radial symmetric function to a one dimensional one. Calling $V(r) := \frac{H'(r)}{r^{n+2}}$ the higher dimensional Fourier kernel, an effective one-dimensional Fourier transformation is be derived in this section. This is motivated by the well-known three dimensional procedure which is easier to read and given in appendix D.1.

Start with the $N = n + 3$-dimensional fourier transformation and rewrite it into conventional polar coordinates:

$$\hat{V}(p) = \frac{1}{(2\pi)^{3+n}} \int \mathrm{d}^{3+n} r \; e^{-i\vec{r}\cdot\vec{p}} V(r) \tag{3.51a}$$

$$= \frac{1}{(2\pi)^{3+n}} \int_0^\infty \mathrm{d}r \; r^{2+n} \int_0^{2\pi} \mathrm{d}\varphi \prod_{i=1}^{n+1} \int_0^\pi \mathrm{d}\theta_i \sin^i(\theta_i) \; e^{-i\vec{r}\cdot\vec{p}} V(r) \tag{3.51b}$$

Now use the angle θ_1 for identification with the inner scalar product angle $\vec{r}\cdot\vec{p} := rp\cos\theta_0$. Subsitute $\int_0^\pi \mathrm{d}\theta_1 \sin(\theta_1) = -\int_{-1}^{+1} \mathrm{d}\cos\theta := \int_{-1}^{1} \mathrm{d}x$. Integrating out *all other* n angles θ_i as well as the angle φ gives a $\Omega_{2+n}/2$ contribution, as the $n+3$-sphere volume is given by $\int \mathrm{d}^{3+n} r = \int \mathrm{d}r \Omega_{n+2} r^{n+2}$. Divide it by the missing factor $\int_0^\pi \mathrm{d}\theta \sin(\theta) = 2$, used for the scalar product substitution. One ends up with

$$= \frac{1}{(2\pi)^{3+n}} \frac{\Omega_{n+2}}{2} \int_{-1}^{+1} \mathrm{d}x \int_0^\infty \mathrm{d}r \; r^{2+n} V(r) \; e^{-irpx} \tag{3.51c}$$

$$= \frac{1}{(2\pi)^{3+n}} \frac{\Omega_{n+2}}{2} \int_0^\infty \mathrm{d}r \; r^{2+n} V(r) \left[\frac{1}{-ipr} e^{-iprx} \right]_{-1}^{+1} \tag{3.51d}$$

$$= \frac{1}{(2\pi)^{3+n}} \frac{\Omega_{n+2}}{2} \frac{i}{p} \left(\int_0^\infty \mathrm{d}r \; r^{1+n} V(r) e^{-ipr} - \int_0^\infty \mathrm{d}r \; r^{1+n} V(r) e^{+ipr} \right) \tag{3.51e}$$

In favour to write this line as an effective one dimensional Fourier transformation, transform the second integral in line (3.51e), first by switching the integral borders, $\int_0^\infty \mathrm{d}r = -\int_\infty^o \mathrm{d}r$, second by variable substitution $r := -r'$. This inserts an alternating minus, depending on n, as $r^{1+n}\mathrm{d}r = (-1)^{1+n}(r')^{1+n}(-1)\mathrm{d}r' = (-1)^n r' \mathrm{d}r'$. Note the substitution also toggles the sign of the integral borders, allowing to combine both integrals to

$$= \frac{1}{(2\pi)^{3+n}} \frac{\Omega_{n+2}}{2} \frac{i}{p} \int_{-\infty}^\infty \mathrm{d}r \; r^{1+n} \left[V(r)\Theta(r) + (-1)^n V(-r)\Theta(-r) \right] e^{-ipr} \tag{3.51f}$$

$$= \frac{1}{2\pi} \int_{-\infty}^\infty \mathrm{d}r \; v(r) \; e^{-ipr}. \tag{3.51g}$$

One derives an effective one dimensional Fourier transformation of the effective function

$$v(r) := \frac{1}{(2\pi)^{2+n}} \frac{\Omega_{2+n}}{2} \frac{i}{p} r^{1+n} \left[V(r)\Theta(r) + (-1)^n V(-r)\Theta(-r) \right]. \tag{3.52}$$

Note that the Heaviside step function $\Theta(z)$, which was used to combine the integrals from line (3.51e) to one in (3.51f) is understood on the complex plane as

$$\Theta(z) = \Theta(Re\, z). \tag{3.53}$$

The requirement (3.53) must be only exactly fulfilled at the evaluation points of the integral, that is, the poles of $v(r)$. Therefore, $\Theta(z)$ may be weaker defined. See appendix D for more details.

Issues may arise with holomorphy when Cauchy theorem is applied. This is discussed further in the appendix, realizing that solving the integral on the complex plane works in three dimensions, so it shall work in any higher number of dimensions. Note that this approach was also successfully applied to a GUP-inspired nonlocal operator in an onging work [46].

3.5.2 Inverting the bilocal smearing operator

It is possible to solve the $\mathcal{A}^{-2}$ integral (3.50d) by rewriting it to an one-dimensional one. Inserting

$$V(r) = \frac{1}{\Omega_{n+2} r^{n+2}} \frac{\mathrm{d}H(r)}{\mathrm{d}r} \tag{3.54}$$

into equation (3.51f) results in the compact expression, valid for any dimension n:

$$\mathcal{A}^{-2}(p^2) = \frac{1}{(2\pi)^{3+n}} \frac{i}{2p} \int_{-\infty}^{\infty} \mathrm{d}r \frac{H'(|r|)}{r} e^{-ipr}. \tag{3.55}$$

This equation can be solved with the residue theorem. Since in (3.55), $r \equiv \|\vec{r}\| \geq 0$ and $p \equiv \|\vec{p}\| \geq 0$, there is only one integration contour for Jordan's lemma. For the forward Fourier transformation $\mathcal{F}_1$, as seen in (3.55), the contour is determined by requiring (for some constant $\# > 0$ representing the momentum)

$$\lim_{r \to \pm i\infty} e^{-ipr} = 0 \;\Rightarrow\; e^{-i(+\#)(\pm i\infty)} = e^{\pm\infty\#} = 0 \;\Rightarrow\; r \to -i\infty, \tag{3.56}$$

i.e. it is closed on the lower half complex plane ($Im\, r < 0$). For the inverse Fourier transformation $\mathcal{F}_1^{-1}$, it is closed on the upper half complex plane ($p \to i\infty \Leftrightarrow Im\, p > 0$).

Concluding, equation (3.55) allows deriving the inverse bilocal operator by inserting a specific choice of $H(r)$.

Chapter 4

The holographic black hole in higher dimensions

Building on the previous chapter, a special choice of $H(r)$ defines the *holographic black hole* in n large extra dimensions:

$$h(r) = \frac{r^{2+n}}{r^{2+n} + \tilde{r}_0^{2+n}}. \tag{4.1}$$

$\tilde{r}_0$ is a regulation constant of dimension length that is discussed in the next sections. For $n \to 0$, the profile (4.1) reduces to the four dimensional profile first studied by Nicolini and Spalluci in [59].

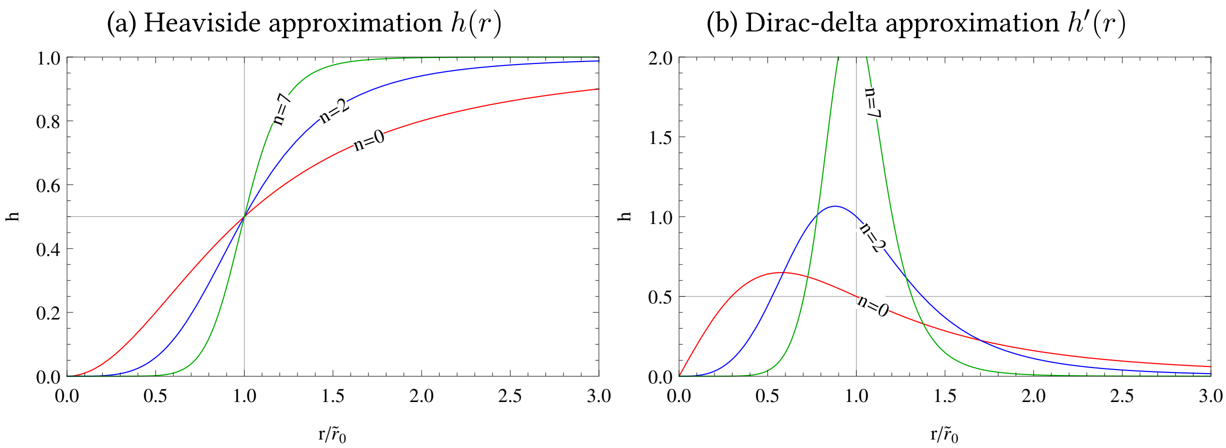

Figure 4.1: The Heaviside (a) and Dirac delta (b) approximation profile $h(r)$ against it's built in length scale $\tilde{r}_0$ for a different number of large extra dimensions n. One sees that $\tilde{r}_0$ plays the role of the *width* of the profile. By choice, it is a kind of "half-life scale", as can be computed when computing $h(\tilde{r}_0) = 1/2$. Note also that increasing n create sharper distributions. For $n \to \infty$, the curve resembles a displaced step function $h_{n\to\infty}(r) = \Theta(r - \tilde{r}_0)$. This reflects the fact that all volume in a ∞-sphere lives on the surface.

Inserting $h(r)$ into the generic gravitational potential (3.20) creates for a fixed n and $\tilde{r}_0$ a geometry, uniquly determined by its mass M:

$$V(r) = \frac{1}{2+n}\frac{M}{M_*^{n+2}}\frac{r}{r^{2+n}+\tilde{r}_0^{2+n}}. \tag{4.2}$$

The gravitational potential (4.2) spawns a class of black hole geometries which is subject of this chapter.

Note that this profile is an *ab-initio* proposal, and especially the higher dimensional continuation is "guessed". The special feature is that *there is no further ingredient than General Relativity*. There is no need to stress a more advanced theory like String Theory or loop quantum theory to generate the metric defined by (4.2). It will be shown that the holographic metric does not cure the curvature singularity in the origin, but features logarithmic corrections to the black hole entropy. The higher dimensional modification will be justified by yielding the required entropic corrections in any number of dimensions.

4.1 Geometry

4.1.1 Horizons

The event horizon equation, considering r_H being the event horizon, requires

$$0 = g_{00}(r_H) \quad \Rightarrow \quad 0 = z^{2+n} - z\,m_n + 1, \tag{4.3}$$

with $m_n = 1/(n+2)M/M_*^{n+2}$ and $z = r/\tilde{r}_0$. The number of (physically meaningful) solutions depends on m_n, that is, on the black hole mass M. For any n, there are three possible solutions, plotted in figure ??:

$M < M_*$ The mass is too small to create a black hole. The physical object is a vacuum, self-gravitating particle-like structure which is stable.

$M > M_*$ There are two horizons with radii $r_\pm$. In figure ??, they are indicated by red dots. Physically, one can argue that the outer horizon r_+ is the more relevant one, since it *shields* the black hole inner structure. Mathematically, r_- is a Cauchy horizon, and in the region $r_- < r < r_+$, where $g_{00} < 0$ and $g_{rr} > 0$, the coordinates r and t switch their meaning (cf. section 5.1.6).

There are no meaningful compact analytic expressions for the values of $r_\pm$, expcept for the holographic metric and without extra dimensions ($n = 0$), as already given in [59]:

$$r_\pm = GM \pm \sqrt{GM^2 - 4}. \tag{4.4}$$

For $n > 0$ and especially for the self-regular metric, the roots of (??) can simply be determined numerically.

Note that for $M \gg M_*$, r_+ approaches the Schwarzschild-Tangherlini horizon.

$M = M_*$ The two horizons merge to a single horizon which is called *extremal* or *degenerate* horizon $r_\pm = r_0$ and identified with the extremal mass M_*. In figure 4.2a, the green line displays the coefficient g_{00} with extremal mass, showing a single horizon, indicated by the green dot. Figure 4.2b displays the extremal configuration in higher dimensions.

4.1.2 The self-encoding remnant

The extremal black hole configuration $M = M_*$ is a feature of nonlocal matter densities, and in the present class of black hole geometries, it is simultaneously able to exhibit another feature, namely *self-encoding* of the extremal radius r_0 in the built in length scale $\tilde{r}_0$.

The extremal radius is found by inserting $h(r)$ into the second remnant equation (3.27b):

$$\boxed{r_0 = \tilde{r}_0 \left(\frac{1}{1+n}\right)^{\frac{1}{2+n}}} \tag{4.5}$$

Equation (4.5) allows to connect the length scale $\tilde{r}_0$ introduced as “built in” length scale in the holographic profile to a physical length scale r_0. This equation can be used to eliminate $\tilde{r}_0$ from the holographic profile (4.1) in favour of the physical meaningful r_0:

$$h(r) = \frac{r^{2+n}}{r^{2+n} + \tilde{r}_0^{2+n}} = \frac{r^{2+n}}{r^{2+n} + (1+n) r_0^{2+n}}. \tag{4.6}$$

Note that the *self-encoding* principle requires that the size of the remnant r_0 should be identical to the fundamental length scale of the physical theory l_0. For gravity in 4d space time, the only fundamental length scale is given by the coupling constant (Newtons constant) G which defines the Planck length $L_{\text{Pl}} = \sqrt{G} \approx 10^{-35}\,\text{m}$. In 4d, (4.5) assures this is true, as already stated in [59]:

$$r_0 \overset{!}{=} l_0 = L_{\text{Pl}} = \tilde{r}_0. \tag{4.7}$$

With extra dimensions, there is the reduced Planck length L_* which is the actual fundamental length scale l_0, since the observable Planck length L_{Pl} is just a large-distance effective one. To express $h(r)$ only in terms of L_*, require $r_0 \overset{!}{=} l_0 \equiv L_*$ and find

$$\tilde{r}_0 = (1+n)^{\frac{1}{2+n}}\, L_*\,. \tag{4.8}$$

Implementing the self-encoding profile into the holographic profile (4.6) gives a profile which is contains nothing more than the universal physical constant L_*:

$$h(r) = \frac{r^{2+n}}{r^{2+n} + (1+n) L_*^{2+n}} \tag{4.9}$$

When computing $M(r_0)$, the self-encoding of the fundamental mass scale M_* is expected, that is, $M(r_0) = M_*$. It is $h(L_*) = 1/(2+n)$ and thus, by construction,

$$M(L_*) = \frac{1}{n+2}\left(\frac{L_*}{L_*}\right)^{1+n} \frac{1}{h(L_*)} M_* = M_*. \tag{4.10}$$

(a) g_{00} in $n = 0$ for different masses M.

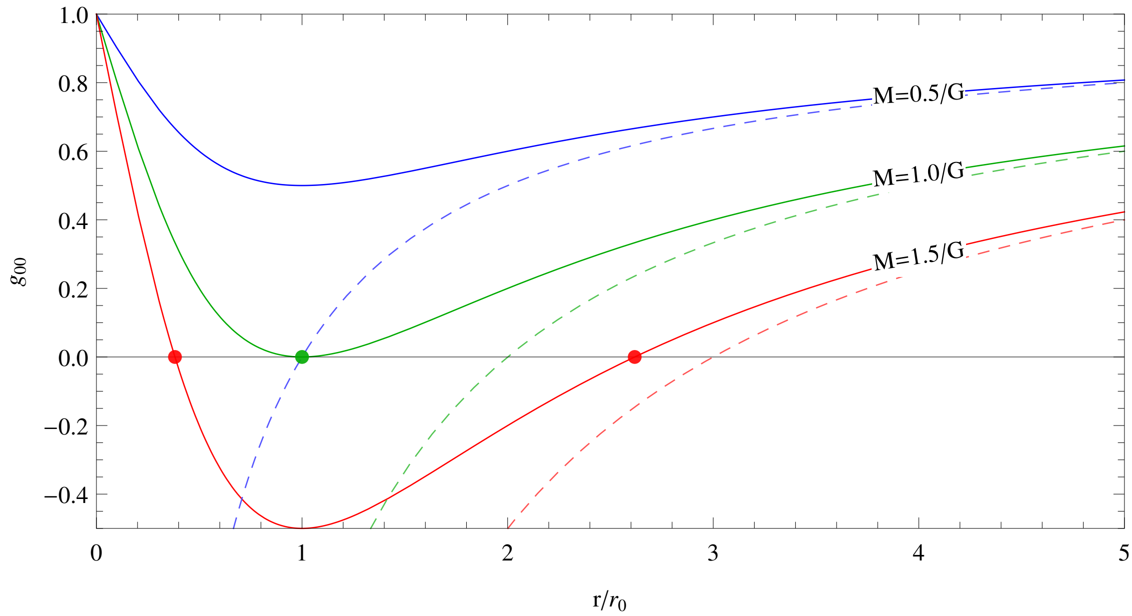

(b) g_{00} for $M = M_*$ in different dimensions n.

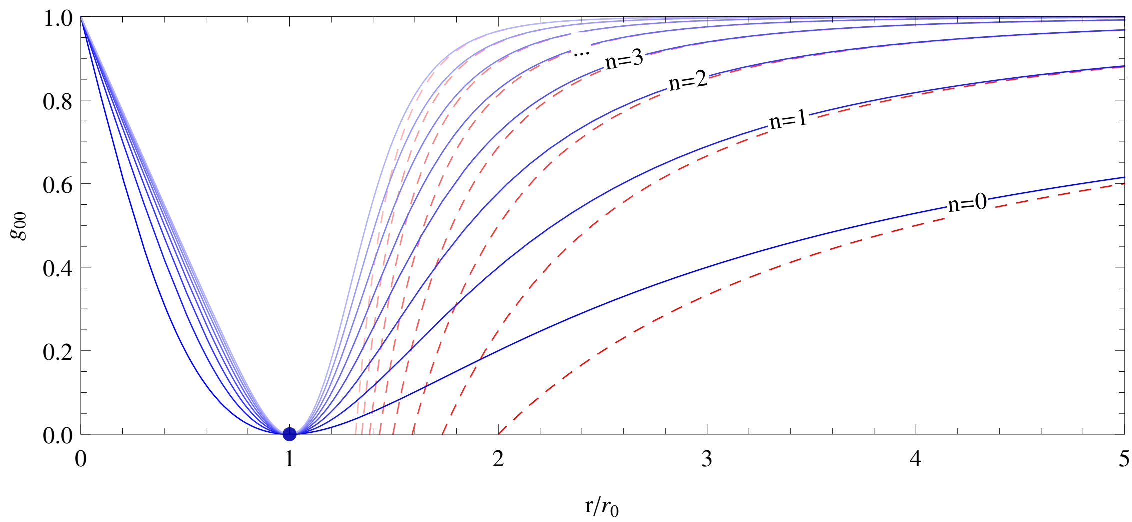

Figure 4.2: The holographic gravitational potential. The upper panel 4.2a shows different geometries based on the black hole mass. The three curves represent a smaller than critical-mass (blue), critical mass (green) and heaviest mass (red).
The lower panel 4.2b shows the higher dimensional extension for the self-encoding masses M_*. All curves are scaled for the individual L_* according to the numerical values given in table 4.1. Compared to the fourdimensional metric (fig. 4.2a), one can see that the picture basically *stays the same*. In this figure, the curves qualitatively get "sharper" with increasing n, which corresponds to the increasing surface to volume ratio of n-spheres, which is a purely geometrical effect.
In any case, the dashed line corresponds to the equivalent Schwarzschild metric.

n	0	1	2	3	4	5	6	7
$\tilde{r}_0/L_*$	1.00	0.79	0.76	0.76	0.76	0.77	0.78	0.79
$L_*/\tilde{r}_0$	1.00	1.26	1.32	1.32	1.31	1.29	1.28	1.26
$(\tilde{r}_0/L_*)^2$	1.00	1.59	1.73	1.74	1.71	1.67	1.63	1.59

Table 4.1: Numerical results for eq. (4.5): The ratio of the arbitrary constant $\tilde{r}_0$ given in the initial $h(r)$ formulation vs. the real minimal length L_*. This table does **not** display the self-encoding horizon radius $r_0 = L_*$, remnant masses $M_* = 1/L_*$ and reduced coupling (Newtons) constant $G_* = M_*^2$. These numbers are **not** given in multiples of $L_P = \sqrt{\hbar G/c^3} \approx 10^{-35}$ m, the 4d Planck unit, but they are dimensionless.

These are not numbers in Planck units, but they display the ratio from eq (4.5). It is absolutely arbitrary and has no physical meaning. Therefore I wonder which kind of numbers you would like to see here. I can show the minimal length scales defined by ADD, $M_{\text{Pl}}^2 \cong V_n M_*^{n+2}$ for $n \in \{0, 1, 2...\}$, but this has nothing to do with the holographic model!

4.1.3 Minimal length

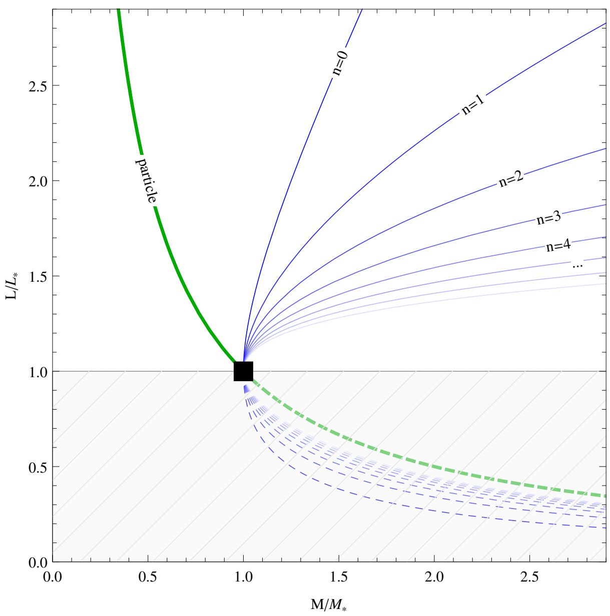

Figure 4.3: The two horizons of the holographic black hole stand out in this plot as the upper and lower branches of the blue curves. While the upper branch represents the

4.1.4 Curvature singularity

According to the curvature considerations for general profiles $H(r)$ in section 3.3.2, the holographic metric is still diverging. One can give an estimation for $R(0)$ based on the taylor expansions of the holographic profile $h(r)$ at $r = 0$:

$$h(r) = (r/L)^{2+n} + \mathcal{O}\left((r/L)^{2(2+n)}\right), h'(r) \approx (r/L)^{1+n}, h''(r) \approx (r/L)^n \tag{4.11}$$

Inserting this into $R(r)$ for $H(r)$, equation (3.28b), gives $H(0) \approx L/r$. The holographic black hole has therefore still a curvature singularity at the origin.

4.2 Thermodynamics

The thermodynamics of the holographic black hole arise from the equations given in section 3.4. By inserting the holographic profile $h(r)$ in the equations derived for general $H(r)$, the quantities in this section are derived.

4.2.1 Hawking Temperature

The Hawking Temperature of a holographic black hole with radius r_H in n LXDs is determined by (3.38) to

$$T_H = \frac{1}{4\pi r_H}\left(1 + n - (2+n)\frac{(L_*/r)^{(2+n)}}{1+(L_*/r)^{(2+n)}}\right). \tag{4.12}$$

Figure 4.4 shows the temperature of the black holes. Comparing with the appropriate Schwarzschild black hole in n dimensions, the first thing to be noticed is the difference of the two curves which becomes large below $r \lesssim 3L_*$ or $r \lesssim {}^3/_2 r_C$, with the critical temperature r_C as defined in the next section. There is a maximum temperature at the critical radius r_C (indicated by the dots in fig. 4.4, numerical values are given in table 5.2), and for smaller radius the black hole cools down until it reaches zero temperature at r_0. One therefore speaks of a *cold* remnant.

4.2.2 Heat capacity

The heat capacity of a holographic black hole with radius r_H in n LXDs is determined by 3.42 to

$$C = -\frac{4\pi r_H^{2+n}}{M_*^{n+2}}\frac{\left(r_H^{-n}+r_H^2\right)^2\left((1+n)r_H^2 - r_H^{-n}\right)}{\left(4+3n+n^2\right)r_H^{n-4}+r_H^{2n-2}-(1+n)r_H^6}. \tag{4.13}$$

The critical radius can be determined by evaluating the extremal temperature condition and inserting the current black hole model into (3.44):

$$r_C = 2^{\frac{1}{n+2}}\left((2+n)\sqrt{n^2+2n+5} - n^2 + 3n - 4\right)^{-\frac{1}{n+2}} L_* \tag{4.14}$$

4.2.3 A Phase transition

Eventually, having computed g_{00}, T and C, one is able to compare those quantities for black hole stability discussion. Figure 4.6 illustrates the curves and different phases, exemplary for the holographic black hole. Considering the sign of the heat capacity, three phases can be distinguished:

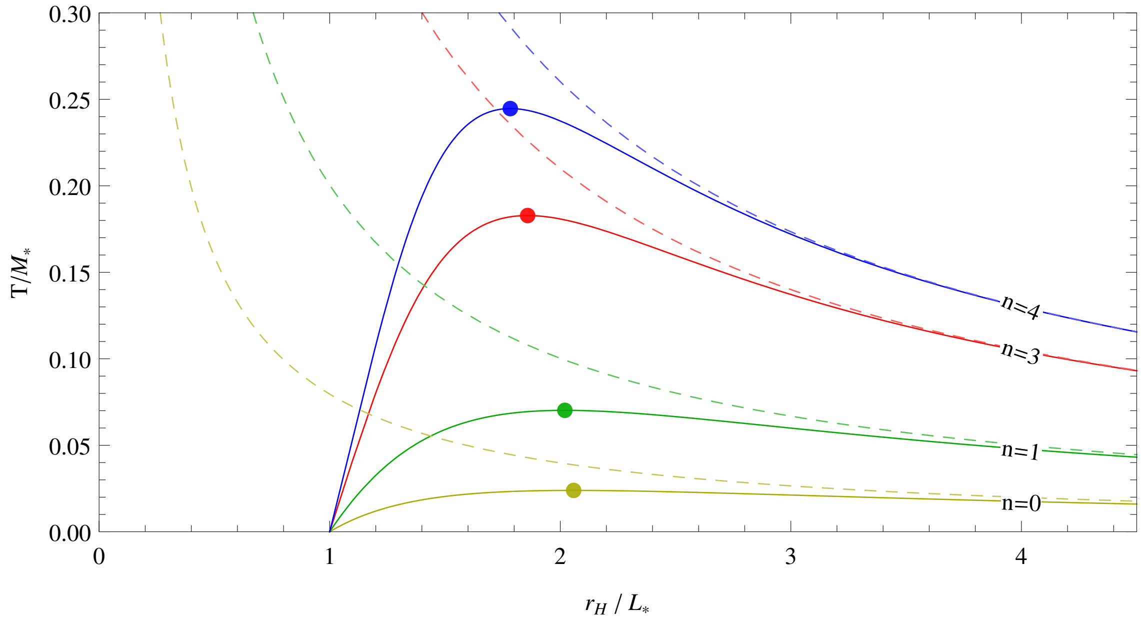

Figure 4.4: Temperature of the holographic black hole, compared to the dashed-line Schwarzschild-Tangherlini black hole temperature, in a different number of dimensions. The circles indicate the critical radii (eq. 4.14) where maximal temperatures occur.

n	0	1	2	3	4	5	6	7
r_C	2.060	1.600	1.480	1.410	1.360	1.330	1.300	1.280
$T(r_C)$	0.024	0.070	0.124	0.183	0.245	0.309	0.375	0.443

Table 4.2: Critical radii r_C for different dimensions and maximum temperatures. All values are given in nd Planck units (as multiples of L_*).

$r > r_C$. The heat capacity is negative, the system is instable: Losing mass by radiation makes it hotter and hotter. This behaviour is well described by the Schwarzschild metric.

When reaching $r \to^+ r_c$, in the modified metrics this process stagnates, the temperature rises no more. Now a phase transition takes place at r_C, the system gets stable.

$r_0 < r < r_C$. The heat capacity is positive and the black hole system is stable. Losing mass now results in losing temperature. The system heavily deviates from the classical Schwarzschild solution. The Temperature decreases until it evventually reaches zero.

$r < r_0$. This phase is physically never accessed, as the system got stable at r_0. The self-complete paradigm also ensures that no black holes cannot be generated at these distances, as smaller length scales then r_0 are not accessible.

Thermodynamics in this area are nonsense: There is a negative temperature $T < 0$ and the system is instable again, since $C < 0$.

(a) Heat capacity C for different n, scaled against individual L_*

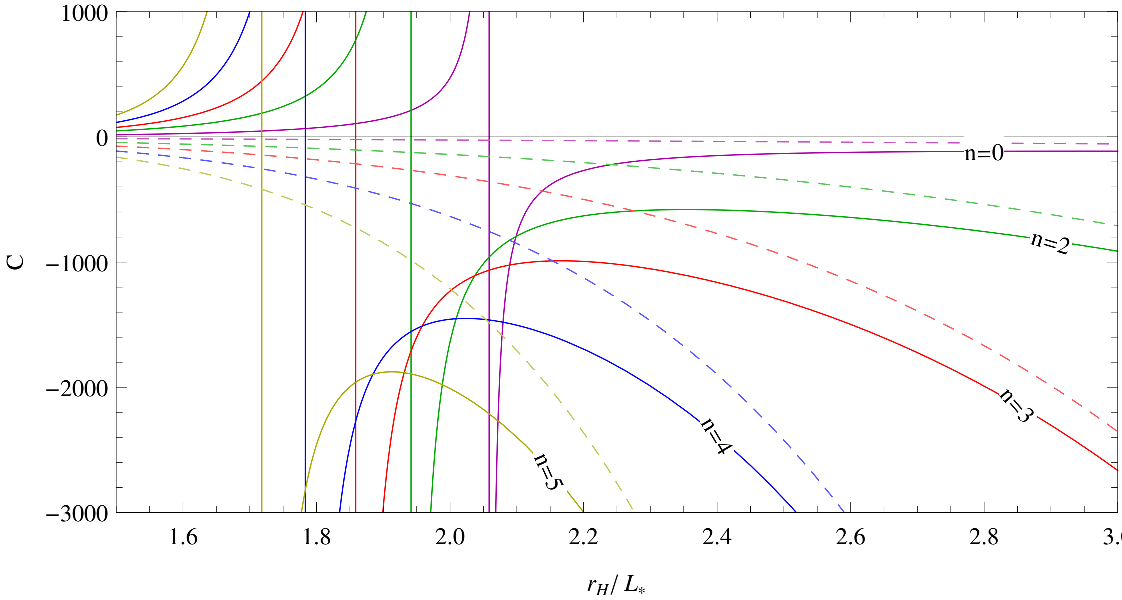

(b) Heat capacity C for different n, scaled against L_* and shifted around r_C

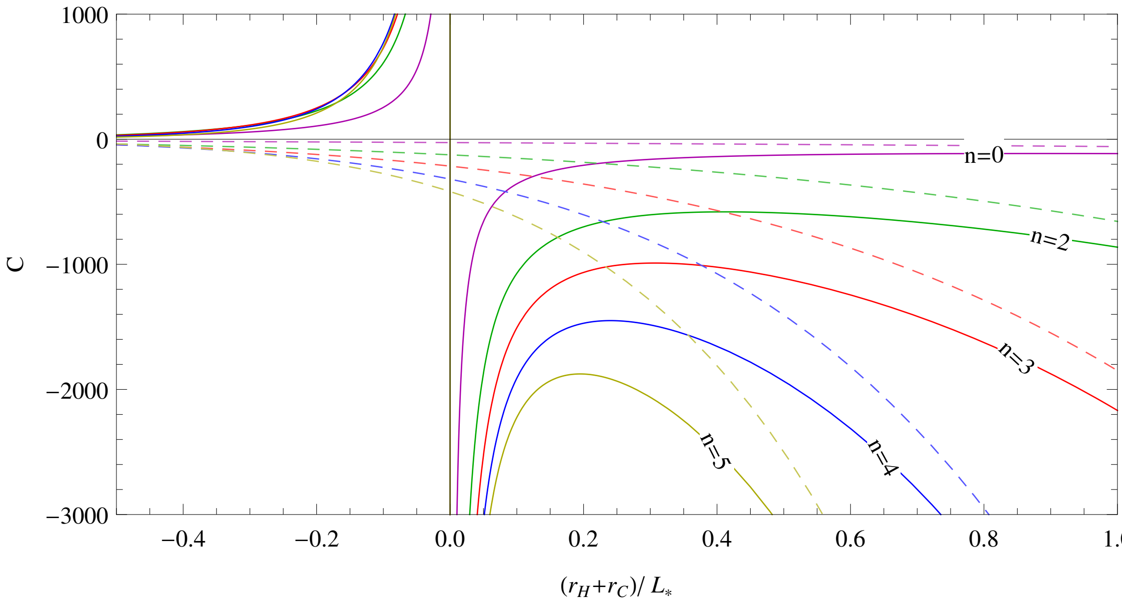

Figure 4.5: The heat capacity of the holographic black hole for different extra dimensions n, as a function of the black hole size r_H. The dashed line corresponds to the heat capacity of the classical Hawking-Beckenstein black hole in n extra dimensions.

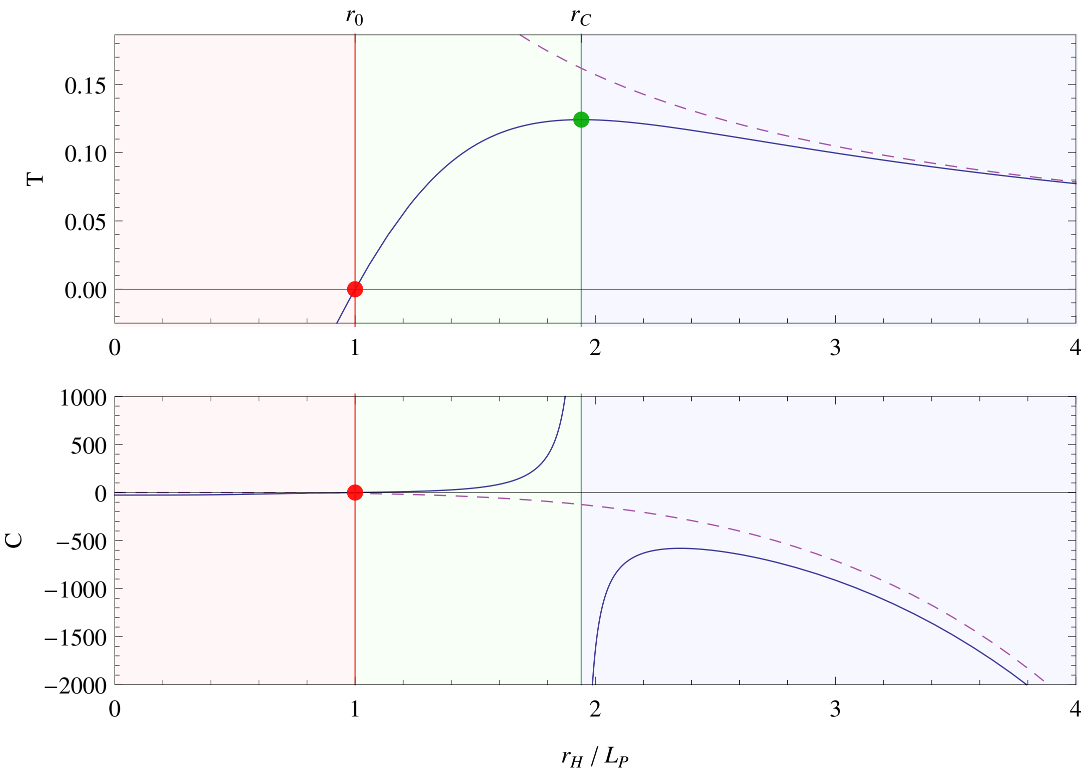

Figure 4.6: Comparison of temperature (top panel) and heat capacity (bottom panel) on the same scale. Here, $n = 2$, but the plot looks systematically the same in all dimensions. The dashed curves are the corresponding Schwarzschild behaviour.
Regarding the sign of the heat capacity (Sign $C = \pm 1$), there are three different states, indicated by colors and seperated by r_0 (red line) and r_C (green line).

4.2.4 Entropy

Compared to that curve, for the holographic model in n dimensions the entropy integral (3.46) has the value

$$S_h(r) = 4\pi m_n \left(\frac{r^{n+2}}{n+2} + \log(\frac{r}{L_*}) \right) . \tag{4.15}$$

Note the *logarithmic quantum corrections*. They motivate the label *holographic* for the $h(r)$-smeared metric.

4.2.5 The area quantization picture

The black hole area theorem dates back to Wheeler 1973 and is a recasting of the Schwarzschild

Please **skip this section** 4.2.5, it still needs to be improved.

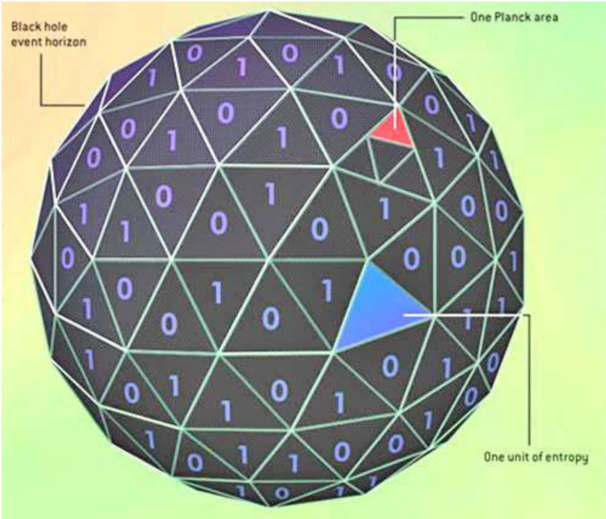

Figure 4.7: An artistic interpretation of the holographic principle, as it illustrated an science magazine article by Jacob Bekenstein [9]. The black hole entropy is quantizied in terms of Planck units. A Planck area (blue) has $A/4$ units of entropy (red).

black hole entropy in terms of the horizon area $A = 4\pi r_H^2$, and therewith

$$S = 2\pi \frac{A}{A_0} \quad \text{with } A_0 = 4\pi L_P^2. \tag{4.16}$$

In the same spirit, we can recast the holographic metric black hole (4.15) as

$$S_h(A_+) = \frac{\pi}{A_0}(A_+ - A_0) + \pi \log(A_+/A_0), \tag{4.17}$$

with $A_+ = \Omega_{n+2} r_+^{2+n}$ and $A_0 = \Omega_{n+2} L_*^{2+n}$.

By means of a taylor expansion $\log(x) \approx (x-1) + \mathcal{O}\left((x-1)^2\right)$ around $x = 1$, one sees the entropy vanishes for $A_+ \to A_0$, which encodes the physical fact that the Planck size remnant can be only realized in one configuration [59]. We therefore interpret it as an *ground state* for a quantized area spectrum

$$A_+ = A_{n-1} = nA_0 = 4\pi n L_*^2, \tag{4.18}$$

to express A_+ (literally) stores n basic units of information. Wheeler created a new term for this concept of *bits* and *bytes*: One byte consists of 4π bits. This is also shown in figure 4.7.

The area quantization also motivates to a discrete mass spectrum and the analysis of a transition from a (semi-)classical regime to a quantum regime with different kinds of decay: thermal decay vs. quantum decay with discrete quanta emission. The higher dimensional extension does not change the picture drawn in [59].

The area quantization concept was also studied by Dvali [22, 23].

4.3 Modified field equations

In the holographic model, insert $h(r)$ to derive from (3.55) the expression (note there is no need for powers of L when switching to dimensionless coordinates)

$$\mathcal{A}^{-2}(q^2) = \underbrace{\frac{2+n}{(2\pi)^{3+n}} \frac{i}{2q}}_{f_0} \int_{-\infty}^{\infty} \mathrm{d}z \left[\underbrace{\frac{z^n}{(1+z^{2+n})^2}}_{f_+} \Theta(z) + \underbrace{\frac{(-1)(-z)^n}{(1+(-z)^{2+n})^2}}_{f_-} \Theta(-z) \right] e^{-iqz}. \tag{4.19}$$

The poles of f_+ are the same as for f_-, just mirrored at the imaginary axis $Re(z) = 0$, in symbols $f_+(z) = -f_-(-z)$. The poles of f_+ are given by

$$\left(1+z^{2+n}\right)^2 = 0 \quad \Leftrightarrow \quad z = (-1)^{\frac{1}{2+n}} = \exp\left\{\frac{i\pi + 2\pi i k}{n+2}\right\} \quad \forall k \in \mathbb{N}_0. \tag{4.20}$$

There are $n+1$ unique poles, each to be counted twice due to the power of 2 in the denominator of f_+. Due to the integration contour (3.56), only the $\frac{n+1}{2}$ unique poles in the region $Im(z_0) \leq 0$ are taken into account. For f_+, only the $\frac{n+1}{4}$ poles in the region $Re(z_0) \geq 0$ are visible. Identify these poles by their set of angles in the complex phase,

$$\Phi_n = \left\{\varphi = \arg(z) \;:\; 1 + z^{n+2} = 0 \wedge Im(z) \leq 0 \wedge Re(z) \geq 0\right\} \tag{4.21}$$

$$= \left\{\varphi = \pi \frac{1-2k}{n+2} \;:\; k \in \mathbb{N}_0 \wedge k \leq \frac{n}{4}\right\}, \tag{4.22}$$

and write $e^{i\Phi_n} = \{z = e^{i\varphi} : \varphi \in \Phi_n\}$ to denote the set of complex numbers associated with Φ_n. Note the number of angles $|\Phi_n| = \lfloor \frac{n+1}{4} \rfloor$ is a step function, so it is unlikely that a more compact expression than the subsequent one can be derived for general n.

All poles $z_0 \in e^{i\Phi_n}$ are of 2nd order, the residues are therefore given by

$$\operatorname*{Res}_{z\to z_0} f_+(z)e^{iqz} = \lim_{z\to z_0} \frac{\mathrm{d}}{\mathrm{d}z}(z-z_0)^2 f_+(z)e^{iqz} = \frac{\operatorname{sign}(z_0)\bar{z}_0}{(n+2)} e^{iz_0 q}(1 - iz_0 q) \tag{4.23}$$

and enter the holographic $\mathcal{A}^{-2}$ integral from (4.19) in a way that

$$\begin{aligned}\int \mathrm{d}z \left(f_+(z)\Theta(z) + f_-(z)\Theta(-z)\right) e^{iqz} = (2\pi i)(-1)\cdot \\ \cdot \left(2 \sum_{z_0 \in e^{i\Phi_n}} \operatorname*{Res}_{z\to z_0} f_+(z) + 2 \sum_{z_0 \in e^{\Phi_n}} \operatorname*{Res}_{z\to z_0} f_-(z)\right).\end{aligned} \tag{4.24}$$

Note that due to symmetry of the poles, there are either poles z_0 (produced by f_+) and $-z_0$ (produced by f_-) which residues sum to the expression

$$\operatorname*{Res}_{z_0} f_+ e^{izq} + \operatorname*{Res}_{-z_0} f_- e^{izq} = \operatorname*{Res}_{z_0} f_+ e^{izq} - \operatorname*{Res}_{z_0} f_+ e^{-izq} = \frac{2i\bar{z}_0}{(2+n)^2} \sin(z_0 q), \tag{4.25}$$

or the f_+ and f_- share a common pole at $z_0 = -i$, then

$$\operatorname*{Res}_{-i} f_+ e^{izq} = \frac{i}{n+2} e^{+q}(1-q). \tag{4.26}$$

Note that poles at $z_0 = -i$ only occur at integer $n/4$, that is $n = 0, 4, 8, \ldots$. In favour to give a closed form result, one therefore cannot always apply the simplification rules (4.25) and (4.26). The overall result is given by

$$\boxed{\mathcal{A}^{-2} = \frac{(2\pi)^{2+n}}{q} \sum_{\varphi \in \Phi_n} \operatorname{sign}(z_0) \bar{z}_0 e^{iz_0 q}(1 - iz_0 q)} \tag{4.27}$$

with $z_0 = e^{i\varphi}$. Without extra dimensions ($n = 0$) is the only case where a purely real result can be given, for $n > 0$ complex phases always survive in (4.27). For $n = 0$ we get (with $q = pL$):

$$\mathcal{A}^{-2} = \frac{1}{4\pi} \left(\frac{e^{-q}}{q} + e^{-q} \right). \tag{4.28}$$

Reinserting L and sending $L \to 0$ gives $\mathcal{A}^{-2} \to 1/4\pi$. (There is missing some 4π here to ensure $\mathcal{A}^{-2} \to 1$).

Chapter 5

The self-regular black hole in higher dimensions

In this chapter, another black hole model is proposed, defined by a special choice of $H(r)$ in the scope of chapter 3, the *self-regular black hole* in n large extra dimensions:

$$h_\alpha(r) = \frac{r^{3+n}}{(r^\alpha + \tilde{r}_0^\alpha/2)^{\frac{3+n}{\alpha}}}. \tag{5.1}$$

This profile contains two constants α and $\tilde{r}_0$. The regularization constant $\tilde{r}_0$ was already discussed and has the same meaning in this model like in the one before. The α is a dimensionless constant that, as it will turn out, couples together the two fundamental theories encoded in this black hole model.

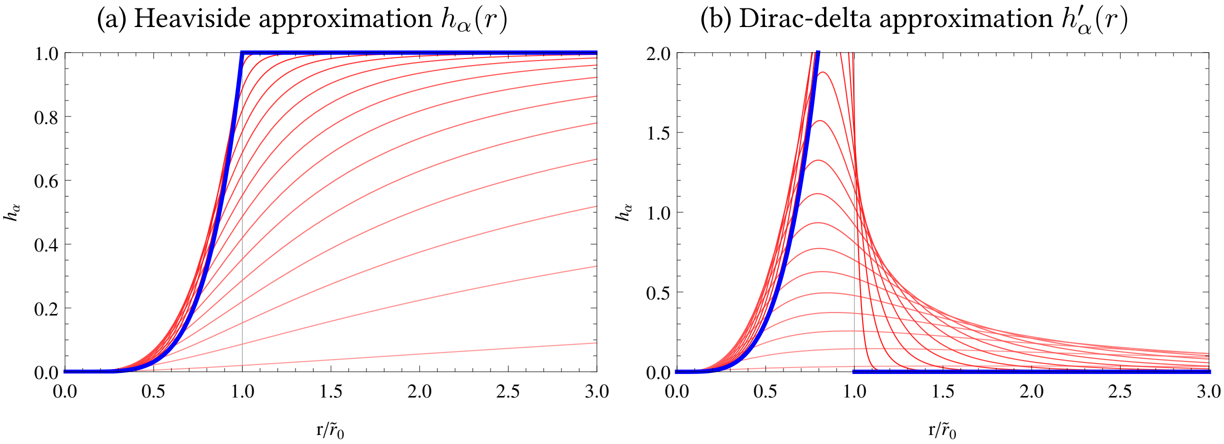

Figure 5.1: The Heaviside (a) and Dirac delta (b) approximation profile $h_\alpha(r)$ against it's built in length scale $\tilde{r}_0$ for different choices of α and fixed nn. Red color saturation indicates increasing α, while the thick blue curve represents $\alpha = \infty$. See appendix B for details of the graph.

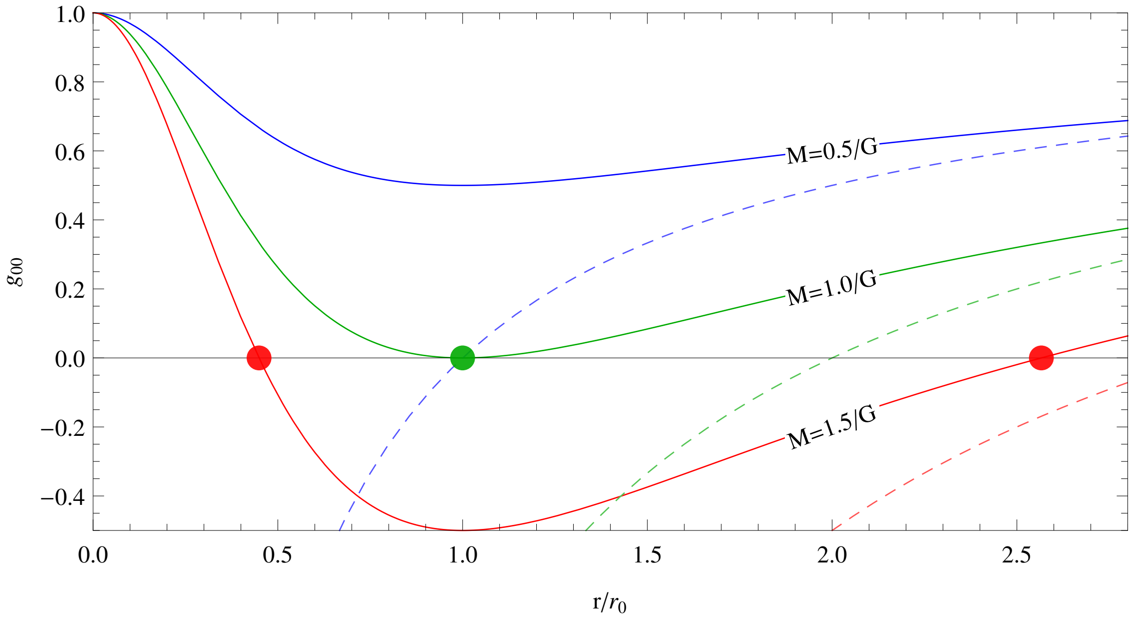

Figure 5.2: g_{00} for the self-regular, self-encoding ($\alpha = \alpha_0$) black hole in 4d ($n = 0$). The three curves represent a smaller than critical-mass (blue), critical mass (green) and a too heavy mass (red). In any case the dashed line corresponds to the equivalent Schwarzschild metric. Note the different behaviour as $z = r/r_0 \to 0$ compared to the holographic figure 4.2a.

5.1 Geometry

Compared to the holographic black hole, the self-regular black hole excells in its outstanding geometric features, while it does not possess the thermodynamic features one expects from a quantum gravity.

5.1.1 Horizons

The event horizon equation, considering r_H being the event horizon, requires $0 = g_{00}(r_H)$. For the self-regular black hole, the horizons r_H are given by the root of the polynomial

$$0 = z^2(z^\alpha + 1/2)^{(3+n)/\alpha} - m_n \tag{5.2}$$

with $m_n = 1/(n+2)M/M_*^{n+2}$ and $z = r/\tilde{r}_0$. The number of (physically meaningful) solutions depends on m_n, that is, on the black hole mass M. For any n, there are three possible solutions, plotted in figure 5.2:

$M < M_*$ The mass is too small to create a black hole. The physical object is called a *G-lump* after Dymnikova [24] and represents a vacuum, self-gravitating, regular, particle-like structure [2].

$M > M_*$ There are two horizons with radii $r_\pm$. In figure 5.2, they are indicated by red dots. Physically, one can argue that the outer horizon r_+ is the more relevant one, since it

n	0	1	2	3	4	5	6	7
α_0	1.755	4.285	7.081	9.333	10.642	11.128	11.098	10.805
$\tilde{r}_0/L_*$	1.	0.851	0.856	0.862	0.86	0.851	0.839	0.825
$L_*/\tilde{r}_0$	1.	1.176	1.168	1.16	1.163	1.175	1.192	1.212
$(\tilde{r}_0/L_*)^2$	1.	0.724	0.733	0.743	0.739	0.725	0.704	0.681

Table 5.1: Numerical results for equation (5.3).

These are not numbers in Planck units, but they display the ratio from eq (??). It is the same situation like in table 4.1, there is no physical content in this table.

shields the black hole inner structure. Mathematically, r_- is a Cauchy horizon, and in the region $r_- < r < r_+$, where $g_{00} < 0$ and $g_{rr} > 0$, the coordinates r and t switch their meaning (cf. section 5.1.6).

There are no meaningful compact analytic expressions for the values of $r_\pm$, but the roots of (??) can simply be determined numerically.

Note that for $M \gg M_*$, r_+ approaches the Schwarzschild-Tangherlini horizon.

$M = M_*$ The two horizons merge to a single horizon which are called $r_\pm = r_0$. This is the *extremal* radius, identified with the extremal mass M_*. In figure 5.2, the green line displays the gravitational potential with extremal mass, showing a single horizon, indicated by the green dot.

5.1.2 The self-regular self-encoding remnant

As the holographic model, the self-regular black hole exhibits an extremal configuration $M = M_*$. The extremal radius r_0 is retrieved with the remnant equation (3.27b) to

$$r_{0,\alpha} = \tilde{r}_0 \left(\frac{1}{1+n}\right)^{\frac{1}{\alpha}}. \tag{5.3}$$

Equation (5.3) allows to connect the length scale $\tilde{r}_0$ introduced for self-regular model to a physical length scale r_0. Note that the *self-encoding* principle requires that the size of the remnant r_0 should be identical to the fundamental length scale of the physical theory l_0. For gravity in 4d space time, the only fundamental length scale is given by the coupling constant (Newtons constant) G which defines the Planck length $L_{\text{Pl}} = \sqrt{G} \approx 10^{-35}\,\text{m}$. In 4d, (??) assures this is true, as already stated in [59]:

$$r_0 \overset{!}{=} l_0 = L_{\text{Pl}} = \tilde{r}_0. \tag{5.4}$$

With extra dimensions, there is the reduced Planck length L_* which is the actual fundamental length scale l_0, since the observable Planck length L_{Pl} is just an effective one. To express

$h(r)$ and $h_\alpha(r)$ only in terms of L_*, require $r_0 \overset{!}{=} l_0 = L_*$ and find

$$\tilde{r}_0 = (1+n)^{\frac{1}{\alpha}} L_* \,. \tag{5.5}$$

When computing $M(r_0)$, the self-encoding of the fundamental mass scale M_* is expected, that is, $M(r_0) = M_*$. This allows fixing α. Using the mass (3.23), it reads

$$M(r_H) = \underbrace{\frac{1}{n+2}\left(\frac{3+n}{2}\right)^{\frac{3+n}{\alpha}}}_{\overset{!}{=}1} \left(\frac{r_0}{L_*}\right)^{n+1} M_* = M_* \quad \text{with } \alpha = \alpha_0 \tag{5.6}$$

This gives us the self-encoding value for the α parameter:

$$\alpha_0 = \frac{3+n}{\ln(2+n)} \ln \frac{3+n}{2}. \tag{5.7}$$

We refer to the self-regular black hole with $\alpha = \alpha_0$ as the self-encoding and self-regular black hole.

5.1.3 Minimal length

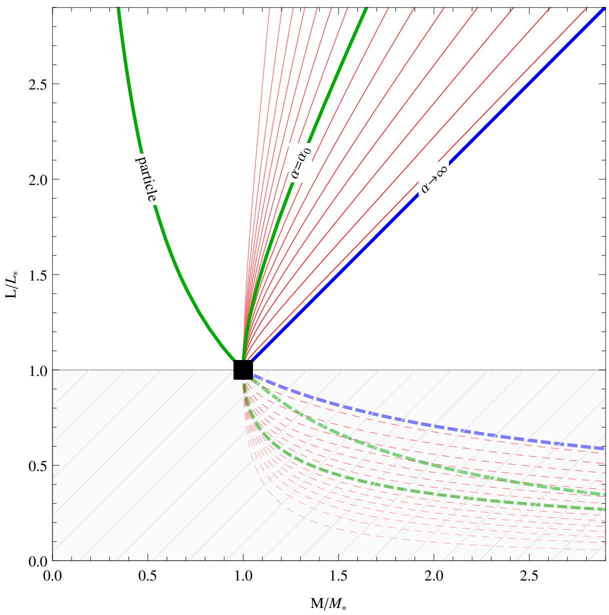

Figure 5.3: The two horizons of the self-regular black hole in $n = 0$ with different choices of α stand out in this plot as the upper and lower branches of the red curves.

5.1.4 The regular core

According to the curvature considerations for general profiles $H(r)$ in section 3.3.2, the self-regular metric offers a non-diverging curvature at the origin. One can give an estimation for $R(0)$ based on the taylor expansions of the self-regular profile $h_\alpha(r)$ at $r = 0$:

$$h_\alpha(r) = ({}^r/{}_{L_*})^{3+n} + \mathcal{O}\left(({}^r/{}_{L_*})^{2(3+n)}\right), h'_\alpha(r) \approx ({}^r/{}_{L_*})^{2+n}, h''_\alpha(r) \approx ({}^r/{}_{L_*})^{1+n} \tag{5.8}$$

Inserting this into $R(r)$ for $H(r)$, equation (3.28b) gives a finite value for $R(0)$ as soon as $\alpha > 0$, c.f. figure 5.4. This is the reason for the name of the "self-regular metric". In general, black holes with no curvature singularity at the origin are called "regular" [?, 2].

To be skipped. The following text until the end of section 5.1.4 still needs to be improved.

To learn more about the origin of the regularity, one can investigate the limit $\alpha \to \infty$, plotted in figure 5.5. At $\alpha \to \infty$, the two phases of the black hole clearly stand out. For simplicity, one should discuss the case in $n = 0$ and $M = M_*$. It is

$$\lim_{\alpha\to\infty} g_{00} = \begin{cases} 1 - 2GMr^2 & , r < L \\ 1 - \frac{2GM}{r} & , r > L. \end{cases} \tag{5.9}$$

Recognize the de Sitter space gravitational potential from section 1.2.3,

$$g_{00} = 1 - \frac{\Lambda}{3} r^2, \qquad \text{(1.24 revisited)}$$

with positive cosmological constant $\Lambda = {}^2\!/\!_3\, GM$ and positive constant curvature $R = 4$ (cf. figure 5.4). This is called the de Sitter *core* since for physical meaningful theories, $r < \infty$.

What is the meaning of the cosmological vacuum solution like de Sitter in the context of Quantum black holes? EFE relate space-time $G_{\mu\nu}$ to matter density $T_{\mu\nu}$. In this thesis, the term *dual theory* will be frequently encountered, which means shifting contributions between $G_{\mu\nu}$ and $T_{\mu\nu}$. In this context, the dual theory to de Sitter space-time as a solution of EFEs with cosmological constant and zero energy momentum tensor $T_{\mu\nu}$ is EFE without cosmological constant but shifted contributions inside the energy momentum tensor. This idea goes back to Dymnikova [24], but is also already discussed in text books as vacuum polarisation [48, p. 411]. In the quantum picture, this is interpreted as the *Quantum Vacuum* and is characterized by its *outward pressure* we were encountered with already at the time of the derivation of the black hole, equation (3.10) that defines the tangential pressure as

$$p = \rho + \frac{r}{n+2} \partial_r \rho > 0. \tag{5.10}$$

One can imagine this type of pressure as the one driving a fermi gas and refer to it as degeneracy pressure. This kind of pressure also prevents the G-lump from collapsing in its own gravitational inward pressure. For a review about regular interiors of Schwarzschild-like black holes with $T^0_0 = T^1_1$, see also [25].

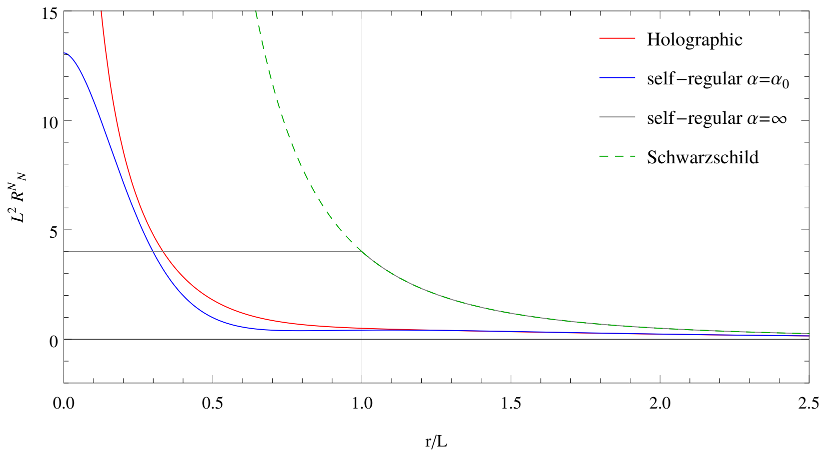

Figure 5.4: The curvature scalar R for $n = 0$, $GM = 1$, $\alpha = 3\alpha_0$ holographic (red) and self-regular model (blue). While the curvature diverges for the holographic black hole, any value of the self-regular black hole archieves a finite value $R(0)$.

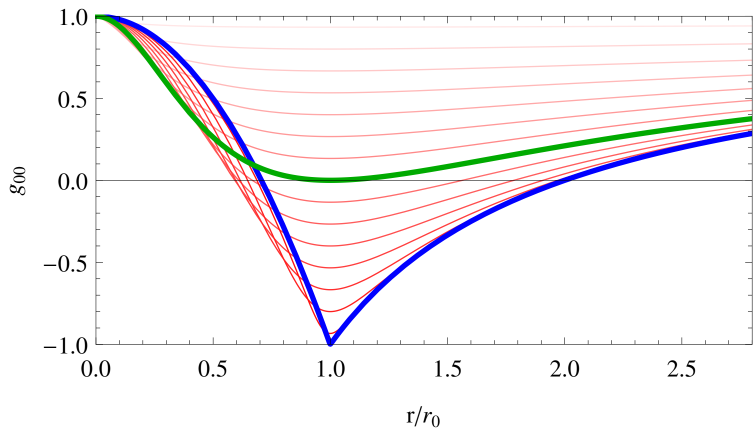

Figure 5.5: g_{00} for $M = 1$ and different choices of $\alpha \in \{0, 20\}$. The blue curve shows the limit $\alpha \to \infty$. Color saturation encodes the α scale. The special self-encoding choice $\alpha = \alpha_0$ is highlighted as green line (as in fig. 5.2). For details of the α choice, see Apx. B.

5.1.5 The Bardeen black hole

The Bardeen black hole (reviewed e.g. in [2]) was one of the first regular black hole solutions examined in literature. It is described by the gravitational potential

$$V(r) = \frac{2Mr^2}{(r^2+e^2)^{3/2}} = 2\frac{M}{e}\frac{1}{(1+e^2/r^2)^{3/2}}. \tag{5.11}$$

The Bardeen metric is a special case of the self-regular black hole with parameters

$$n = 0, \alpha = 2 \quad \text{and} \quad \tilde{r}_0 = 2^{1/\alpha}e, \tag{5.12}$$

where e is an electric charge (the Coulomb constant $(4\pi\epsilon_0)^{-1} \equiv 1$). Apparently, the Bardeen black hole is not self-encoding, as $\alpha_0 \neq 2$.

The Bardeen black hole was found to cure the nacked singularities of the Reissner Nordström (RN) black hole. While this thesis does not cover charged black holes, the geometry of the RN black hole is tightly connected to the self-regular black hole. The RN metric describes a static nonrotating black hole with electrical charge e in $d = 4$ (with $G = 4\pi\epsilon_0 = c = 1$) and its gravitational potential is given by

$$V(r) = \frac{2M}{r} - \frac{e^2}{r^2} = 2\frac{M}{e}\frac{z-1}{z^2} \quad \text{with } z = r/e. \tag{5.13}$$

Figure 5.6 compares the RN black hole with the Bardeen black hole. In this figure, one sees that the hyper-extreme case $M < e$ is replaced by G-lumps, giving flat space for $M/e \to 0$. This cures both the naked singularity as well as the repulsive gravity regime ($g_{00} > 1$).

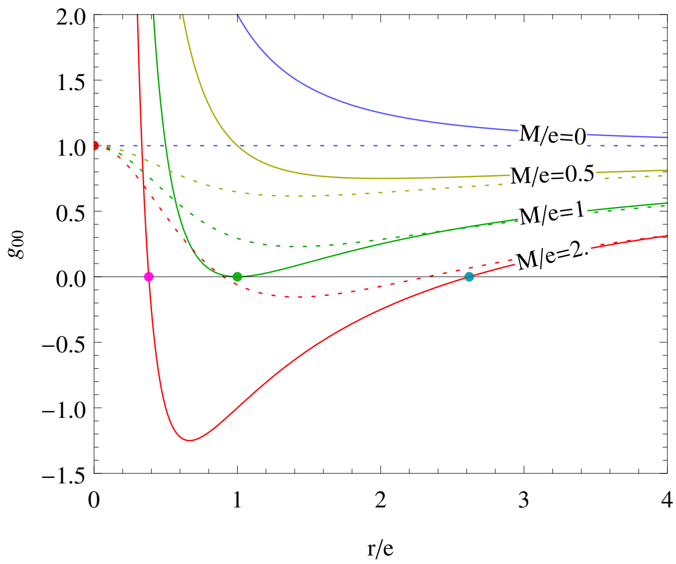

Figure 5.6: The Reissner-Nordström gravitational potential for different mass-charge ratios M/e, compared with the Bardeen solution for the same mass-charge ratios (dashed lines).

Further details and analogies are discussed in the next section about the conformal structure of the self-regular black hole.

5.1.6 Conformal Structure

It is often helpful to transform coordinates in a way that the global structure of space-time is mapped on a finite diagram. If this mapping is conformal (preserving angles locally) and two-dimensional, such diagrams are called *(Carter-)Penrose diagrams* [33, 48, 77].

The three Penrose diagrams that represent the three possible space-times presented in section 5.1.1 are displayed in figure 5.7. It is the diagram of a *regular black hole* which resembles the structure of the *Reissner Nordström* (RN) black hole.

One can discuss the Penrose diagrams shortly without going into detail how to find the maximally extended space-time that describes space-time everywhere, taking up the distinction of cases in section 5.1.1. Figure 5.7 contains three panels:

(a) The G-lump is probabily the biggest archievement for the description of a charged black hole (RN), as it cures the naked singularity, while it is not the object of interest in this context.

(b) The conformal diagram for the maximally extended black hole is periodic on the vertical axis on infinite extend ("isometric" regions). There are three classes of regions: the untrapped and asymptotically flat space time region **I**. The timelike region of trapped surfaces **II**, characterized by $r_- < r < r_+$, connects outer **I** and core **III** regions. The again space-like and untrapped region **III** is hyperbolic, as dominated by de Sitter behaviour. Note that in this space-time, it is possible to *wrap around the universe* by starting from **I**, travelling **II** and **III** and leaving the black hole near zone again over **II** to **I**, all inside a causal light-cone with $45°$ angles.

(c) The extremal situation also made the singularity accessible from outside by travelling from region **I** to **III**. This is cured with a regular origin.

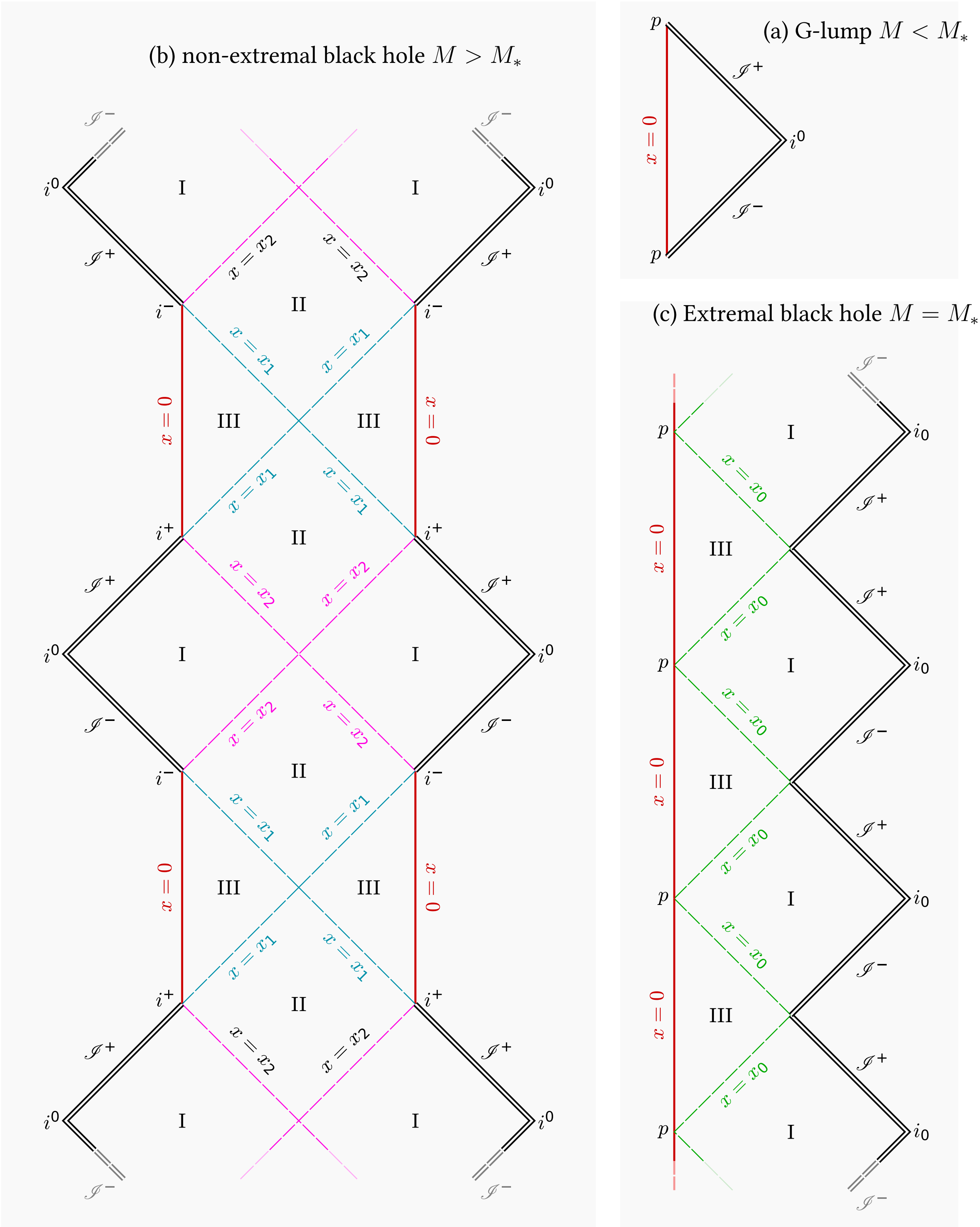

Figure 5.7: The penrose diagrams of the regular black holes, after [2,34,51]. x is a dimensionless coordinate $x = r/\tilde{r}_0$ and $x_2 = r_+/\tilde{r}_0$ is the outer horizon, while $x_1 = r_-/\tilde{r}_0$ is the inner horizon. $x_0 = r_0/\tilde{r}_0$ is the extremal horizon.

n	0	1	2	3	4	5	6	7
r_C	1.970	1.460	1.340	1.290	1.260	1.250	1.230	1.220
$T(r_C)$	0.024	0.074	0.131	0.191	0.254	0.319	0.386	0.454

Table 5.2: Critical radii r_C and maximum temperature $T(r_C)$ for different dimensions, for the self-encoding ($\alpha = \alpha_0$) self-regular black hole. Values are given in d-dim Planck units (multiples of L_*).

5.2 Thermodynamics

This chapter is dedicated the derivation and discussion of the temperature, stability and entropy of the black hole remnant. This means the non-extremal black hole configurations are no more discussed here.

5.2.1 Hawking Temperature

The Hawking Temperature of a self-regular black hole with radius r_H in n LXDs is determined by (3.38) to

$$T_H = \frac{1}{4\pi r_H}\left(1 + n - \frac{(L/r)^{4+n}}{1 + \frac{1}{\alpha}(L/r)^{3+n}}\right). \tag{5.14}$$

Below $r \lesssim 3L_p$, the temperature differs significantly from the Schwarzschild temperature. There is a maximum temperature at a critical radius r_C (indicated by the dots in fig. 5.8, numerical values are given in table 5.2), and for smaller radius the black hole cools down until it reaches zero temperature at r_0. The self-holographic metric produces therefore *cold* remnants.

5.2.2 Heat capacity

The heat capacity of a self-regular black hole with radius r_H in n LXDs is determined by 3.42 to

$$C = -\frac{4\pi r_H^{2+n}}{M_*^{n+2}} \frac{2^{-\frac{3+n}{\alpha}}\left(2 + r^{-\alpha}\right)^{\frac{3+n}{\alpha}+1}\left(r^{-\alpha} - (1+n)\right)}{r^{-2\alpha} - 2(1+n) + r^{-\alpha}(1 + 3\alpha + n\alpha - 1)}. \tag{5.15}$$

The critical radius for $h(r_C)$ and $h_\alpha(r_{C,\alpha})$ can be determined by evaluating the extremal temperature condition (3.44):

$$r_C = 2^{\frac{1}{\alpha}}\left(\sqrt{(3+n)(3+n+\alpha(2+3\alpha+(\alpha-2)n))} + (n-1) - \alpha(3+n)\right)^{-\frac{1}{\alpha}} L_*\,. \tag{5.16}$$

The critical radius was used to rescale the abscissa in figure 5.9, so $(r_H - r_C)r_0$ is displayed. Thus it is easier to compare C for a different number of dimensions. Numerical values for r_C are given in table 5.2.

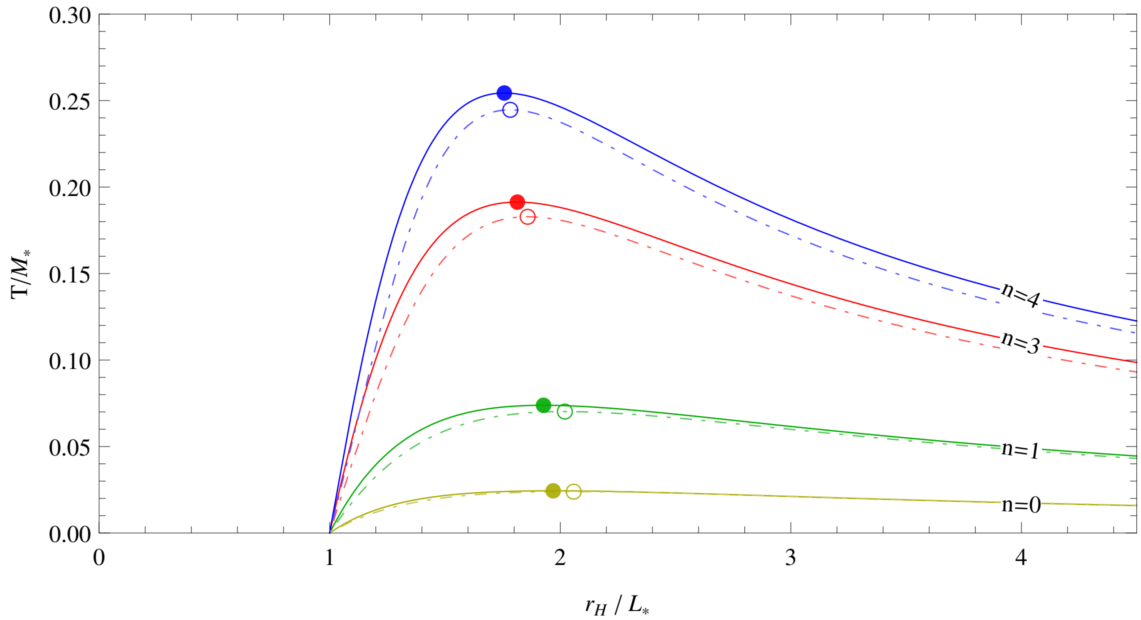

Figure 5.8: Temperature of the self-encoding self-regular black hole for different extra dimensions n (solid curves) in comparison to the holographic black hole temperatures (dot-dashed curve).

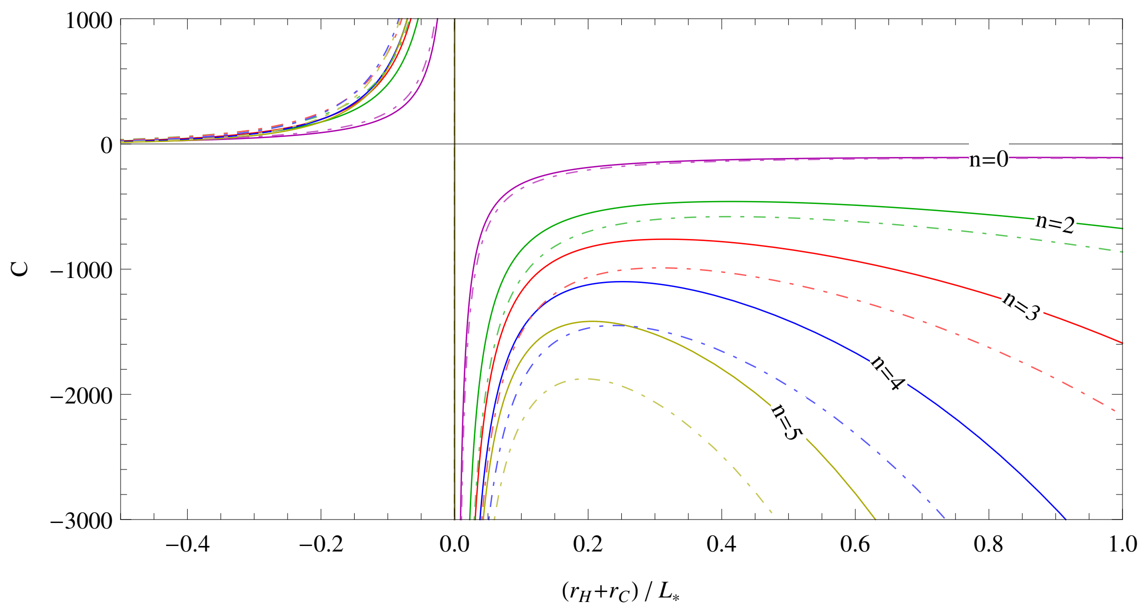

Figure 5.9: Heat capacity of the self-encoding ($\alpha = \alpha_0$), self-regular black hole (solid lines) compared with the holographic black holes (dot dashed lines), in different extra dimensions n. For each curve, the x-axis is shifted to the corresponding critical radius r_C (given by eq. 5.16) and scaled by the horizon length r_0 (given by eq. 5.3).

5.2.3 Entropy for self-encoding

The self-encoding metric also does not possess a logarithmic entropy correction, but a hypergeometrical one:

$$S = \frac{4\pi m_n}{n+2}\left(r^2 + {}_2F_1\left(-\frac{2+n}{\alpha}, -\frac{3+n}{\alpha}, 1-\frac{2+n}{\alpha}; -\frac{1}{2r^\alpha}\right)\right) \tag{5.17}$$

5.3 Modified field equations

For sef-encoding model, insert $h_\alpha(r)$ into the integral for $\mathcal{A}^{-2}$ as given in (3.55). For convenience, switch to a new dimensionless notation, $L' := L/2^{1/\alpha}$ and $z = r/L'$, $q = pL'$. With that notation, all poles will have radius 1. The integral reads:

$$\mathcal{A}^{-2}(q^2) = \underbrace{\frac{3+n}{(2\pi)^{3+n}}\frac{i}{2q}}_{f_0}\int_{-\infty}^{\infty}\mathrm{d}z\left[\underbrace{\frac{z^{1+n}}{(1+z^\alpha)^{\frac{3+n}{\alpha}+1}}}_{f_+}\Theta(z) + \underbrace{\frac{(-1)(-z)^{1+n}}{(1+(-z)^\alpha)^{\frac{3+n}{\alpha}+1}}}_{f_-}\Theta(-z)\right]e^{-iqz}. \tag{5.18}$$

As with the holographic model, I chose $f_+(z) = -f_-(-z)$ and will therefore discuss only f_+. Its poles are given by

$$(1+z^\alpha)^{\frac{3+n}{\alpha}+1} = 0 \quad\Leftrightarrow\quad z = (-1)^{1/\alpha} = \exp\left\{\frac{i\pi + 2\pi i k}{\alpha}\right\} \quad \forall k \in \mathbb{N}_0. \tag{5.19}$$

For arbitrary choices of $\alpha \in \mathbb{R}_{\geq 0}$, as they were physically discussed in section **??**, the poles multiplicity in (5.19) is not an integral number. For the poles determination, this is not a problem, but for calculating residues it is.

Equation for nth order singularities of a function $g(z)$:

$$\operatorname*{Res}_{z\to a} g(z) = \frac{1}{(n+1)!}\lim_{z\to a}\frac{\partial^{n-1}}{\partial z^{n-1}}\left((z-a)^n g(z)\right) \tag{5.20}$$

Ways to solve that for $n := \frac{3+n}{\alpha}$: Fractional calculus...

I will **remove** this section, as I was not able to compute the nonlocal operator for the self-regular black hole. **I am still free for hints how to solve the integral**.

Chapter 6

Discussion and Conclusion

In this thesis, two self-encoding black hole geometries with their extra dimensional generalization are presented. The discussion was preceded by an introducion about the topics General Relativity, exact solutions, higher dimensional gravity scenarios and the quest for Quantum Gravity, namely by enumerating six Quantum Gravity theories that predict black holes.

Considering the geometry of the two self-encoding black holes, the concept of the black hole *remnant* is introduced and the parallel to the charged Reissner-Nordström black hole is showed. The de Sitter core as quantum vacuum source of outward pressure, stemming against the gravitational collapse, is introduced. For the self-encoding non-regular black hole, in this work refered to as the holographic black hole, the curvature singularity is hidden behind a horizon. This incorporates with the minimal length scenario, where distances smaller than the remnant size L_* and bigger than the reduced Planck mass M_* can not be probed. Physics in the trans-Planckian regime therefore gets unaccessible and shielded.

Regarding the thermodynamics of the self-encoding black holes, the remnants are found to be *cold* and *stable* in terms of a vanishing temperature and heat capacity. One finds logarithmic quantum corrections for the self-encoding holographic black hole in agreement with Loop Quantum Theory and String Theory. The holographic picture leads to area quantization and finally gives rise to an emergent gravity interpretation, explaining the gravitational force as entropic force.

As a last step, the *dual* theory to the self-encoding black holes is constructed. By means of finding the nonlocal operator that, applied on a Dirac delta distribution, produces just the desired distortion. This is a doorway of bringing the theory on a more fundamental level.

An appealing property of the geometries in this work is that one can do “paper and pen physics” without relying on numerical computations from the beginning. With the distinct feature of extra dimensions, this work pushes the underlying work forward on the “route to testable predictions” [59].

Appendix A

Adjacent physical theories

A.1 Alternative extradimensional gravity approaches

Vermutlich finales Abstellgleis für die wenig hilfreichen Alternativtheorien für Extradimensionen, wobei RS noch am ehesten mit ADD zu tun hat, aber im Haupttext nicht vor ADD erwähnt werden soll. Dieser Text liest sich am besten nach der Rezeption des Haupttextbereichs über das ADD-Modell. Als geschichtlicher Background passt er eigentlich ganz gut in den Anhang.

A.1.1 Kaluza Klein theory

Extending gravity to higher dimensions has a long history. First suggestions go back to Nordström and Kaluza [32] that proposed extra dimensions to unify gravity and electromagnetism. In 1921, they published a formulation today known as *Kaluza Klein theory* (KK theory), where Kaluza introduced one space-like extradimension and a scalar field ϕ (corresponding to a new particle). KK theory is capable of be producing both Einstein field equations and Maxwell equations at once. This works with any four dimensional metric $g_{\mu\nu}$ which is put in the five dimensional extension according to

$$g_{MN} = \begin{bmatrix} g_{\mu\nu} e^{\phi/\sqrt{3}} + e^{-\phi^2} A_\mu A_\nu & e^{-\phi^2} A_\nu \\ e^{-\phi^2} A_\mu & e^{-\phi^2} \end{bmatrix}. \tag{A.1}$$

To clarify the notation: In equation (A.1), a block matrix notation was used to build up the 5×5 "matrix" g_{MN} by means of the 4×4 matrix $g_{\mu\nu}$. The fifth colum is spanned by four entries $e^{-\phi^2} A_0, \dots, e^{-\phi^2} A_3$ and $e^{-\phi^2}$, while the fifth row is spanned by four entries $e^{-\phi^2} A_0, \dots, e^{-\phi^2} A_3$ and $e^{-\phi^2}$.

The Einstein field equations (1.25) for $d = 5$ are a system of 25 equations that decouple to three independent field equations: The ordinary 4d Einstein equations with a modified (effective) 4d energy momentum tensor $\tilde{T}_{\mu\nu}$,

$$R_{\mu\nu} - \frac{1}{2} g_{\mu\nu} R = -8\pi G \tilde{T}_{\mu\nu}, \quad \text{with } \tilde{T}_{\mu\nu} = \frac{1}{4} e^{-\sqrt{3}\phi} F_{\mu\sigma} F^\sigma_\nu + \frac{\partial_\mu \phi \partial_\nu \phi}{2}. \tag{A.2}$$

The Maxwell's equations for the field A_μ, which read

$$\partial_\mu \partial^\nu A^\mu - \partial_\mu \partial^\mu A^\nu = 0. \tag{A.3}$$

And a relativistic equation for the scalar field ϕ:

$$\partial_\mu \partial^\mu \phi = \frac{-\sqrt{3}}{4} e^{-\sqrt{\phi}} F_{\mu\nu} F^{\mu\nu}. \tag{A.4}$$

Note that in this theory, the gravitational coupling constant G remained untouched ($G_d := G_4$). The fifth dimension is supposed to be compactified on *microscopic* scales (cf. figure 1.2).

A.1.2 Randall-Sundrum scenario

The Randall-Sundrum (RS) model was proposed in 1999 and also implies the existence of one large spatial extra dimension. In contrast to KK, the fifth dimension has constant negative curvature (AdS). The five dimensional line element is given by [40]

L_* definieren **PN**

$$\mathrm{d}s^2 = e^{-2kr_c|y|} g_{\mu\nu} \mathrm{d}x^\mu \mathrm{d}x^\nu + r_c^2 \mathrm{d}y \tag{A.5}$$

with $g_{\mu\nu}$ the 4d space time, $k \sim 1/L_*^2$ a parameter of the order of the fundamental Planck scale, y the extra coordinate and r_c the compactification radius of the extra dimension. The RS metric can be derived like KK from the 5d EFEs with negative cosmological constant.

The RS (and KK) scenario are mentioned only for the sake of completeness and to show alternatives to the following ADD model which is the first one proposing *large* extra dimensions. Historically, the RS model is one year younger than the ADD model and also addresses the Hierarchy Problem by giving rise to an effective 4d Planck mass

$$M_{\mathrm{Pl}}^2 = (1 - e^{-2kr_c}) M_*^3 / k. \tag{A.6}$$

The deviation and discussion of the model is beyond the scope of this work. See e.g. [40] for a review in the context of micro black holes.

An diesem letzten Absatz wird klar wie absurd dieses Kapitel ist.

A.2 Quantum Gravity black holes

This section gives a two-page overview about black holes in different Quantum Gravity approaches and their relationship to this work. It primarily follows the "six families of black holes" proposed in [60] and closes with *String theory*, which is certainly the most popular candidate for QG.

A.2.1 Non-local gravity black holes

Aus diesem Abschnitt wird das NONLOCAL GRAVITY-Kapitel gemacht.

These approaches are based on a nonlocal field theory by means of a nonlocal contribution to the geometric part of the Einstein field equations. In [51, 54], this is done with a derivation operator $\mathcal{F}^{-2}(\Box)$ acting on the Einstein tensor in a way that

$$\mathcal{F}^{-2}(\Box_{\mathbf{x}}/\Lambda_G^2)\left(R_{\mu\nu}-\frac{1}{2}g_{\mu\nu}R\right)=8\pi G_N T_{\mu\nu}, \tag{A.7}$$

with a function $\mathcal{F}^{-2}$ of the generally covariant D'Alambert operator $\Box_{\mathbf{x}}$ acting on space-time vectors $\mathbf{x}$ which is scaled by the energy scale Λ_G of that theory, resulting in a dimensionless operator $\Box_{\mathbf{x}}/\Lambda_G^2$.

This goes back to nonlocal action modifications in gravity proposed by Barvinsky [7, 8]. Actually, such an approach is also used for curing divergences and formulating a pertubative super-renormalizable theory of Quantum Gravity [50].

A.2.2 Noncommutative black holes

You should say something about NCG (it comes from string theory). Hier findet Nicolini dass alles verbessert werden muss.

Noncommutative geometry suggests a "fuzzy" spacetime by imposing a commutation relation on the quantum-mechanical position operator $\boldsymbol{x}^\mu$. In terms, this reads

$$[\boldsymbol{x}^\mu,\boldsymbol{x}^\nu]=i\theta^{\mu\nu} \tag{A.8}$$

with the matrix $\theta^{\mu\nu}>0$ imposing the "discretization" of space-time. This idea leads to a space-time uncertainty and finally to a gaussian energy density approach as dirac replacement in the noncommutative inspired Schwarzschild solution,

$$\rho_\theta(r)=\frac{M}{(4\pi\theta)^{3/2}}e^{-r^2/4\theta}. \tag{A.9}$$

From this equation one can read that $r\sim\sqrt{\theta}$ corresponds to the length scale where noncommutative effects get strong. Funny enough, the metric produced by (A.9) possesses a regular core like the one we will contrive in this chapter [57].

A in-depth review about Noncommutative black holes is [53]. The first extradimensional extension from Rizzo 2005 [65] actually determines the syntax and conventions used in this thesis.

A.2.3 Generalized Uncertainty Principle black holes

The generalized uncertainty principle is perhaps the closest approach to create a "matching" picture 2.2. It can be formulated by suggesting as well a modified Compton scale as a generalized event horizon [13, 14] and states, in the simplest form

$$\Delta x \Delta p \geq \frac{\hbar}{2}\left(1 + \alpha x^2 + \beta p^2\right). \tag{A.10}$$

Note that for $\alpha = \beta = 0$, this is the Heisenberg uncertainty principle. By means of a Hilbert space representation [41], for $\alpha = 0$ on can deduce a modified momentum integration measure where $p \sim \sqrt{\beta}$ plays the role of a high energy regulator, and this can be used to compute the GUP-Schwarzschild black hole with energy density [37, 38]

$$\rho_\beta(r) = \frac{M}{(2\pi)^3} \int \frac{\mathrm{d}^3 p}{1 + \beta p^2} e^{i\boldsymbol{x}\cdot\boldsymbol{p}}. \tag{A.11}$$

Suprisingly, there also is a link to this thesis: Densities like (A.11) have been extended to higher dimensions [46], and the integration technique to solve nonlocal operators introduced in chapter **??** turned out to be successful to compute fourier transformations of GUP operators.

A.2.4 Loop Quantum black holes

Loop Quantum Gravity (LQG) is the competitor for String Theory that has the major advantage of preserving *background-independence*, as this is a major pillar of General Relativity. Therefore, LQG cannot be a pertubative expansion of Quantum GR by means of $\tilde{g}_{\mu\nu} = g_{\mu\nu} + h_{\mu\nu}$, since this would distinguish a special fixed classical background metric $g_{\mu\nu}$. The main principle in LQG is general covariance paired with quantum principles. Contemporary formulations use a graph as basic principe, a network (the "foam") with spacetime points as vertices and a discrete minimal length distance as edges and therefore refined the building word *loop* QG. According to Asthekar, "loops play no essential role in the theory now, for historical reasons, this name is widely used"; there lies the close relationship to lattice gauge theories, as closed loops resemble Wilson plaquettes [66, 76].

It is a long way from Loop Quantum Gravity to Loop Quantum black holes (LQBHs), and contemporary research about LQBHs is fairly less "descriptive" than the black holes modified by the principled mentioned before. See e.g. Modesto [49] who, amongst other things, finds out after a lengthy calculation that the Schwarzschild curvature singularity is no more present in LQBH.

Note that a particularly significant result is a fundamental explanation of the black hole logarithmic entropy correction that was predicted by Wilson. The logarithmic black hole entropy term will be discussed in depth in section **??**.

See the texts of Thiemann [74, 75] and Ashtekar [3] for an pedagogical review about LQG. For a pedagocigal introduction with focus on spin foams, see [63].

A.2.5 Asymptotically safe gravity black holes

Asymptotically safe gravity is built on a running coupling $G(k)$ which is the result of renormalization group treatments; general covariance is maintained with this approach. The basic idea is to make gravity an effective theory at momentum scale k and therefore be safely able to do physics with momenta $k' \gg k$.

Applied to black holes, $G(r)$ takes the place of Newton's contant in the Schwarzschild metric [27]. Thus it is possible to get black hole remnants that resemble the holographic profile we encounter in the next sections.

For introductory papers, see e.g. Reuter [12, 64] and the review [61] by the same author.

A.2.6 Black holes in String Theory

String Theory is the theory of quantum-mechanical relativistic one-dimensional "vibring strings" (like waves), and according to the popular picture, different excitation energies correspond to different point-like particles postulated by the standard model of particle physics. The term "String Theory" is usually used similary to superString Theory, that is, String Theory including supersymmetry (SUSY, a symmetry that relates each boson to its superpartner, the fermion, and vice versa). The existence of extra dimensions, as introduced in section **??**, is actually predicted by String Theory. String Theory is most criticised because its large number of solutions and especially because the dependence on a background spacetime which explicitly breaks general covariance. On the other hand, String Theory only needs one fundamental minimal length scale ℓ_0 and may be treated pertubatively.

Considering black holes, String Theory is especially able to make statements about extremal black hole situations, as we will encounter in the next chapter. The enticing recast of an extremal black hole as a *particle* is unique to String Theory. String Theory also predicts a logarithmic entropy correction as LQG does.

String Theory is handled e.g. in the book of Kiefer [43], black holes in String Theory are discussed in [47]. Probably a good closing overview over all approaches gives the review article [42].

Appendix B

Distribution profiles at a glance

The choice $H(r) = h(r)$ is called *holographic model* and the choice $H(r) = h_\alpha(r)$ is called *self-encoding model* in this thesis. They are distinguished by the index α on the h. Of course, one could also introduce a symbol like $h_n(r)$ to account the fact that the models scale with n, so eventually the symbol is arbitrary.

In this appendix, we give the full forms in the dimensionless notation $z = r/L$. Since the models $H(r)$ represent a smeared Theta function, they are dimensionless, and the identity $h(r) = h(r/L)$ shall represent the fact that $h(r)$ is actually a function of r/L and can be expressed in the dimensionless coordinate $h(z)$:

$$h(r) = \frac{r^{2+n}}{r^{2+n} + L^{2+n}} \qquad h(z) = \frac{1}{1 + \left(\frac{1}{z}\right)^{2+n}} = \frac{z^{2+n}}{z^{2+n} + 1} \tag{B.1}$$

$$h_\alpha(r) = \frac{r^{3+n}}{\left(r^\alpha + L^\alpha/2\right)^{\frac{3+n}{\alpha}}} \qquad h_\alpha(z) = \frac{1}{\left(1 + \left(\frac{1}{z}\right)^\alpha/2\right)^{\frac{3+n}{\alpha}}} \tag{B.2}$$

The derivatives appear in many places and are therefore denoted here. Since $\frac{\mathrm{d}f}{\mathrm{d}r} = \frac{\mathrm{d}f}{\mathrm{d}z}\frac{\mathrm{d}z}{\mathrm{d}r} = \frac{1}{L}\frac{\mathrm{d}f}{\mathrm{d}z}$, we can always substitute $H'(r) = H'(z)/L$. It is important to remember this fact: $H'(r) \neq H'(z)$. In the end, this is because the Lagrange differential operation notation H' is not unique.

$$h'(r) = \frac{(2+n)\, r^{1+n} L^{2+n}}{\left(r^{2+n} + L^{2+n}\right)^2} \qquad h'(z) = \frac{(2+n)\left(\frac{1}{z}\right)^{3+n}}{\left(1 + \left(\frac{1}{z}\right)^{2+n}\right)^2} = (2+n)\frac{h^2(z)}{z^{3+n}} \tag{B.3}$$

$$h'_\alpha(r) = \frac{(3+n) L^\alpha r^{n+2}\left(\frac{L^\alpha}{2} + r^\alpha\right)^{-\frac{n+3}{\alpha}}}{L^\alpha + 2r^\alpha} \qquad h'_\alpha(z) = \frac{\frac{3+n}{2}\left(\frac{1}{z}\right)^{\alpha+1}}{\left(1 + \left(\frac{1}{z}\right)^\alpha/2\right)^{\frac{3+n}{\alpha}+1}} \tag{B.4}$$

The dimensional analysis allows to resemble the powers of L in any expression written in terms of z. For example, the quantity $H'(z)/z$ has the unit $1/L^2$ and therefore $H'(z)/(zL^2) = H'(r)/r$.

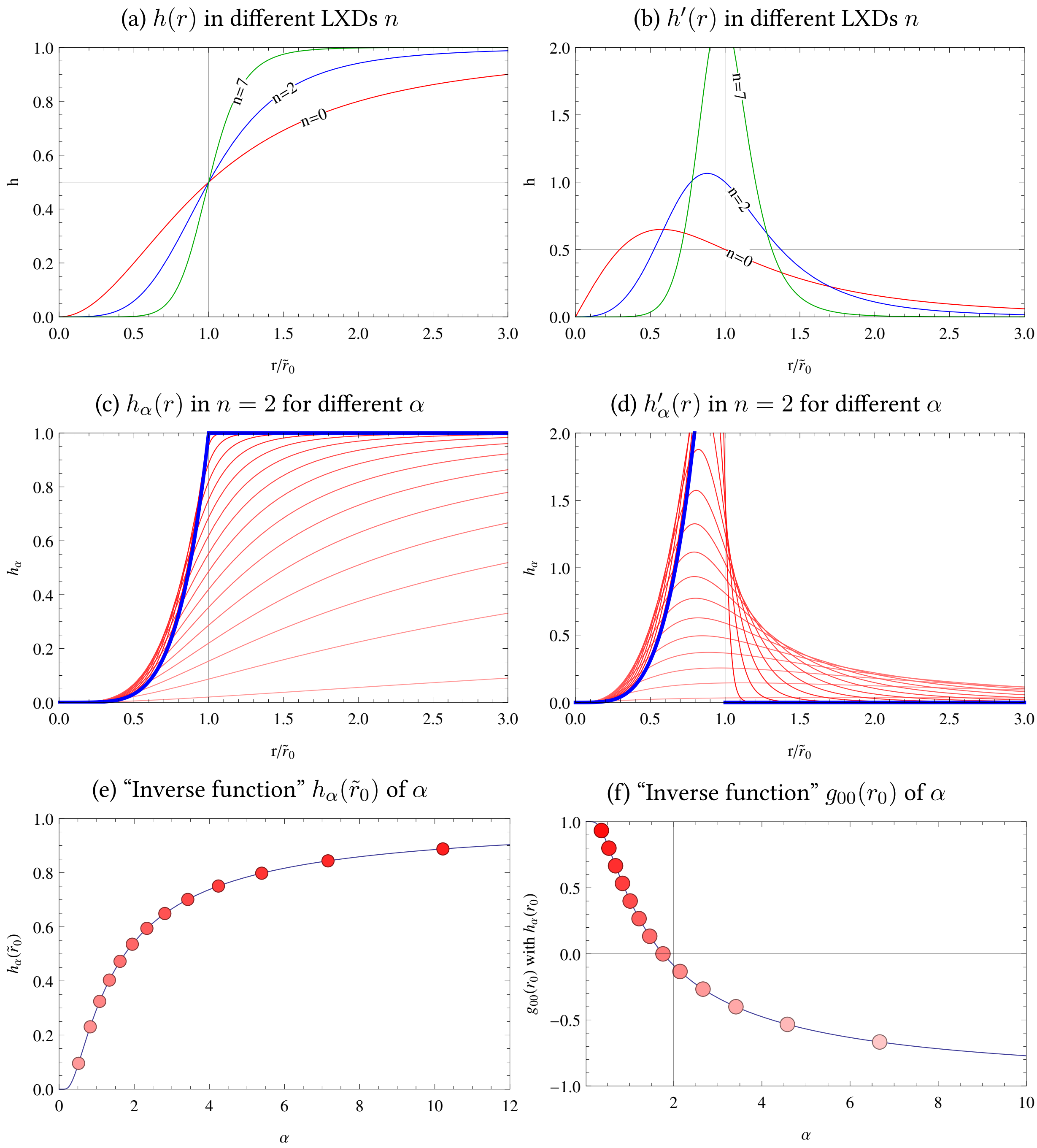

Figure B.1: Plots of the profiles $h(r)$ and $h_\alpha(r)$ as well as their derivatives. The panels B.1e and B.1f show the choices of α that result in uniformly spaced curves when choosing a set of α values for plotting $h_\alpha(\tilde{r}_0)$ or $g_{00}(r_0)$.

Appendix C

n-spheres

To point the emergence of n-spheres in this thesis, we evaluate the d-dimensional volume integral in eucledian space in spherical coordinates $k_i = (r, \phi, \theta_1, \ldots, \theta_{d-2})$, following Wagner [76]:

$$\int \mathrm{d}^d r = \int_0^\infty \mathrm{d}r\ r^{d-1} \underbrace{\int_0^{2\pi} \mathrm{d}\phi \prod_{j=1}^{d-2} \int_0^\pi \mathrm{d}\theta_j\ \sin^j(\theta_j)}_{=a_{n-2},\text{ since }(n-2)-\text{Surface}} = \frac{2\pi^{d/2}}{\Gamma\left(\frac{d}{2}\right)} \int_0^r \mathrm{d}r\ r^{d-1} := \Omega_{d-1} r^d := V_d \tag{C.1}$$

where $\Gamma(x)$ is the Euler Gamma function, given by

$$\Gamma(x) = \int_0^\infty \mathrm{d}t\ t^{x-1} e^{-t} \quad \text{; incomplete version:} \quad \gamma(s, x) = \int_0^x t^{s-1} e^t \mathrm{d}t, \quad \Gamma(1/2) = \sqrt{\pi}, \tag{C.2}$$

and the integration of the $d-2$ angles is done with the help of the identities

$$B(x, y) = \int_0^1 \mathrm{d}t\ t^{x-1}(1-t)^{y-1} = \frac{\Gamma(x)\Gamma(y)}{\Gamma(x+y)} \tag{C.3}$$

$$\int_0^\pi \theta_j\ \sin^j(\theta_j) = \frac{\sqrt{\pi}\,\Gamma\left(\frac{j+1}{2}\right)}{\Gamma\left(\frac{j+2}{2}\right)}. \tag{C.4}$$

The n-sphere S_n with radius r is defined in an n-dimensional manifold (in this work always the eucledian space) by the set

$$S_n = \{\ |\boldsymbol{x}| = r\ \mid\ \boldsymbol{x} \in \mathbb{R}\ \} \tag{C.5}$$

In this work, the n-sphere is important for integration in spherical coordinates without angular dependence (isotropy or spherical symmetry). Integrating out the angles in a d-dimensional volume integration results in the surface area of the $(d-1)$-sphere, embedded in the d-dimensional space.

Formulas to remember for the volume of an n-ball and its corresponding $(n-1)$-sphere:

$$V_n = r^n \frac{\pi^{n/2}}{\Gamma\left(\frac{n}{2}+1\right)} \quad \text{and} \quad A_{(n-1)} = \frac{\mathrm{d}V_n}{\mathrm{d}r} = \frac{\pi^{n/2}}{\Gamma\left(\frac{n}{2}+1\right)} n r^{n-1} = 2\frac{\pi^{n/2}}{\Gamma\left(\frac{n}{2}\right)} r^{n-1} \tag{C.6}$$

There also exists recursion relations for determining V_n, A_n by their lower dimensional values. For the sake of completeness, I also give definitions of the Gamma function Γ:

$$\begin{aligned}\Gamma(x) &= (x-1)! \\ \Gamma(x+1) &= x\Gamma(x)\end{aligned} \quad \text{Prefactors:} \quad \begin{aligned} V_n &= v_n r^n \\ A_n &= a_n r^n \end{aligned} \quad \text{Recursion:} \quad \begin{aligned} v_0 &= 1, \quad v_{n+1} = a_n/(n+1) \\ a_0 &= 2, \quad a_{n+1} = 2\pi v_n \end{aligned} \tag{C.7}$$

I typically split the r-dependence in favour to dimensionless constants by $A_n = \Omega_n r^n$ and $V_n = \mathcal{V}_n r^n$. For numerical values see table C.1.

d	0	1	2	3	4	5	6
$\mathcal{V}_d$	0	2	π	$\frac{4}{3}\pi$	$\frac{1}{2}\pi^2$	$\frac{8}{15}\pi^2$	$\frac{1}{6}\pi^3$
Ω_d	0	2	2π	4π	$2\pi^2$	$\frac{8}{3}\pi^2$	π^3

Table C.1: Volume and surface area prefactors of d-Spheres.

Appendix D

Details of the spherical symmetric d dimensional FT

This appendix ties up with section 3.5.1, where the d-dimensional Fourier Transformation is reduced to a one dimensional one for functions $V(\vec{x})$ which fulfill $V(\vec{x}) = V(|\vec{x}|)$.

The 3d case is actually well known in literature and is given here just for completeness and simpler readability in section D.1. In section D.2, we discuss about entire function aspects of $\Theta(z)$.

D.1 Review of the 3d Fourier transformation

We start the derivation in $d = 3$ total spatial dimensions ($\vec{r} \in \mathbb{R}^3$). Let $V = V(r)$ with $r = |\vec{r}|$ be a radially symmetric potential. Then it's fourier transformation is given by:

$$\hat{V}(p) = \frac{1}{(2\pi)^3} \int \mathrm{d}^3 r \, e^{-i\vec{r}\cdot\vec{p}} \, V(r) \tag{D.1a}$$

$$= \frac{1}{(2\pi)^3} \int_0^\infty \mathrm{d}r \int_0^\pi r^2 \sin\theta \, \mathrm{d}\theta \int_0^{2\pi} \mathrm{d}\varphi \, V(r) \, e^{-ipr\cos\theta_2} \tag{D.1b}$$

In line (D.1b) we already wrote the scalar product with an inner angle θ_2. We now substitute the radial angle θ (the θ which is part of $\vec{r} = (r, \theta, \varphi)$) integration with a $\cos\theta$ integration. This can be done because $\frac{\mathrm{d}\cos\theta}{\mathrm{d}\theta} = -\sin\theta$ and so $\int_0^\pi \sin\theta \mathrm{d}\theta = -\int_{-1}^{1} \mathrm{d}\cos\theta := \int_{-1}^{1} \mathrm{d}x$. We now identify $\cos\theta := x$ with $\cos\theta_1$ because they share the same domain, actually $\theta, \theta_1 \in \{0, \pi\}$ (this is a standard procedure, one can also argue with rotating the coordinate systems). Integrating out $\int_0^{2\pi} \mathrm{d}\varphi = 2\pi$ in mind, we continue with:

$$
\begin{aligned}
&= \frac{2\pi}{(2\pi)^3} \int_{-1}^{+1} \mathrm{d}x \int_0^\infty \mathrm{d}r\, r^2\, e^{-irpx} V(r) && \text{(D.1c)}\\
&= \frac{1}{(2\pi)^2} \int_0^\infty r^2\, \mathrm{d}r\, V(r) \left[\frac{1}{-ipr} e^{-iprx}\right]_{-1}^{+1} && \text{(D.1d)}\\
&= \frac{1}{(2\pi)^2} \frac{i}{p} \int_0^\infty r\, \mathrm{d}r\, V(r) \left\{e^{-ipr} - e^{+ipr}\right\} && \text{(D.1e)}\\
&= \frac{1}{(2\pi)^2} \frac{i}{p} \left\{\int_0^\infty r\, \mathrm{d}r\, V(r) e^{-ipr} - \int_0^\infty r\, \mathrm{d}r\, V(r) e^{+ipr}\right\} && \text{(D.1f)}
\end{aligned}
$$

In line (D.1f), we splitted the integral, and we now make two recastings: At first, switching the integral borders, which inserts one minus: $\int_a^b = -\int_b^a$ in (D.1g). Second, another substitution of the integration parameter $r := -r'$ and therefore $\mathrm{d}r = -\mathrm{d}r'$. The two minus signs kill each other in (D.1h), so $r\mathrm{d}r = r'\mathrm{d}r'$. After substitution, we will call r' again r, which is totally valid.

$$
\begin{aligned}
&= \frac{1}{(2\pi)^2} \frac{i}{p} \left\{\int_0^\infty r\, \mathrm{d}r\, V(r) e^{-ipr} + \int_\infty^0 r\, \mathrm{d}r\, V(r) e^{+ipr}\right\} && \text{(D.1g)}\\
&= \frac{1}{(2\pi)^2} \frac{i}{p} \left\{\int_0^\infty r\, \mathrm{d}r\, V(r) e^{-ipr} + \int_{-\infty}^0 r'\, \mathrm{d}r'\, V(-r') e^{-ipr'}\right\} && \text{(D.1h)}\\
&= \frac{1}{(2\pi)^2} \frac{i}{p} \int_{-\infty}^\infty r\, \mathrm{d}r\, e^{-ipr} \;\{V(r)\Theta(r) + V(-r)\Theta(-r)\} && \text{(D.1i)}\\
&= \frac{1}{(2\pi)^2} \frac{i}{p} \int_{-\infty}^\infty \mathrm{d}r\; \{rV(|r|)\}\; e^{-ipr} && \text{(D.1j)}\\
&= \frac{1}{2\pi} \int_{-\infty}^\infty \mathrm{d}r\, v(r)\, e^{-ipr} && \text{(D.1k)}
\end{aligned}
$$

We derived an effective one dimensional fourier transformation of the new function ("kernel")

$$
v(r) := \frac{i}{2\pi} \frac{r}{p} V(|r|) \tag{D.2}
$$

For shortness, my usual definition of $v(r)$ differs from the one given in (D.2) in terms of non-complex prefactors. For the discussion, equation (D.1i) is the best starting point, as it contains the Heaviside step functions $\Theta(\pm r)$.

The most important issue with this calculation is the question of holomorphy. In these lines, $\Theta(z)$ must be understood as

$$
\Theta(z) = \Theta(Re\, z). \tag{D.3}
$$

This definition is intrinsically nonholomorphic. On the other hand, as soon as Θ is implemented as a smeared distribution, like continuing the integral of a Dirac delta approximation like the Cauchy distribution, this might be cured. Anyway, there is no ordering relation $\leq_{\mathbb{C}}$ in the complex numbers, so the theta is likely to behave differently on the complex plane. In three dimensions this approach is well known and works.

Whats about the real and complex parts of this fourier transformation? By construction, $V(|r|)$ is an even function (definition: $f(x) = f(-x)$ is even, $-f(x) = f(-x)$ is odd). Therefore $r\ V(|r|)$ is an odd function. By Eulers formula $e^{i\varphi} = \cos\varphi + i\sin\varphi$, one quickly finds that the Fourier Transform of an even function includes only (also even) $\cos$ terms and the complex part vanishes, while the FT of an odd function only contains $\sin$ terms and the real part vanishes. The integral in (D.1j) is therefore ony complex, $\int \mathrm{d}r\ rV(|r|)e^{-ipr} \in \mathbb{C} \setminus \mathbb{R}$. But the prefactor makes the final result in (D.1j) completely real again. This can help as a quick check wether the computed result of the integral is correct.

D.2 Analytic continuation of the Heaviside step function

The step function $\Theta : \mathbb{R} \to \mathbb{R}$, as given in

$$\Theta(x) = \begin{cases} 0 & \text{when} \quad x < 0 \\ 1 & \qquad\quad\; x \geq 0 \end{cases}, \tag{3.18 revisited}$$

obvously cannot be simply extended on the complex plane. Anyway, in section 3.5.1, we already formulated *weaker constraints* instead of $\Theta(z) = \Theta(Re\, z)$, namely

- Step function behaviour only on the poles which are laid on the unit ring $|z| = 1$
- Approximate step function behaviour.
- Freedom of poles for $\Theta(z)$, so it does not contribute with poles to $v(z)$.

Freedom of poles means, we cannot have a rational function, so all theta approximations introduced in this thesis leave the stage. Such a theta approximation may be given by

$$\Theta_k(z) = \frac{1}{1 + \exp(-2kz)}, \quad \text{and} \quad \Theta(x) = \lim_{k\to\infty} \Theta_k(x) \quad \text{for } x \in \mathbb{R} \tag{D.4}$$

Inserting $z = e^{i\phi}$ gives...

okay this is not true.

Appendix E

General Relativity formulary

In this section, I use greek lowercase letters ($\alpha\beta\ldots\mu\nu\ldots$) for all indices which may in general be running in 4 or $4+n$ dimensions. Einstein sum convention is used, but summation symbols are given when special emphazise on the summation is intended.

1. Christoffels for Tensor

$$\Gamma^k_{ij} = \frac{g^{kl}}{2}\left(\partial_i g_{jl} + \partial_j g_{il} - \partial_l g_{ij}\right) \tag{E.1}$$

2. Christoffel symmetry:

$$\Gamma^\alpha_{\beta\gamma} = \Gamma^\alpha_{\gamma\beta} \tag{E.2}$$

3. Covariant derivative for covariant vector t:

$$\nabla_a t^\nu = \partial_a t^\nu + \Gamma^\nu_{ac} t^c \tag{E.3}$$

4. Covariant derivative for a $(2,0)$ tensor A:

$$\nabla_\lambda A^{\mu\nu} = \sum_\delta \partial_\lambda A^{\mu\nu} + \Gamma^\mu_{\delta\lambda} A^{\delta\mu} + \Gamma^\nu_{\delta\lambda} A^{\mu\delta} \tag{E.4}$$

5. Covariant derivative for a $(1,1)$ tensor A:

$$\nabla_a T^b_c = \partial_a T^b_c + \Gamma^b_{ad} T^d_c - \Gamma^d_{ac} T^a_d \tag{E.5}$$

6. Energy conservation equation with sums

$$\sum_\mu \nabla_\mu T^{\mu\nu} = \sum_{\mu,\rho} \partial_\mu T^{\mu\nu} + \Gamma^\mu_{\rho\mu} T^{\rho\mu} + \Gamma^\nu_{\rho\mu} T^{\mu\rho} \tag{E.6}$$

7. Lowering and raising indices

$$g_{\beta\gamma} A^{\alpha\gamma} = A^\alpha_\beta \tag{E.7}$$

8. Metric identity
$$g^{\alpha\beta}g_{\beta\gamma} = g_{\gamma\beta}g^{\beta\alpha} = \delta^{\alpha}_{\gamma} \tag{E.8}$$

9. Riemann Tensor
$$R^{\delta}_{\sigma\mu\nu} = \partial_{\mu}\Gamma^{\delta}_{\nu\sigma} - \partial_{\nu}\Gamma^{\delta}_{\mu\sigma} + \Gamma^{\delta}_{\mu\gamma}\Gamma^{\gamma}_{\nu\sigma} - \Gamma^{\delta}_{\nu\gamma}\Gamma^{\gamma}_{\mu\sigma} \tag{E.9}$$

10. Ricci tensor (sign is convention)
$$R_{\mu\nu} = \pm R^{\gamma}_{\mu\gamma\nu} \tag{E.10}$$

11. $(1,1)$-form of Ricci tensor
$$R^{a}_{b} = g^{ca}R_{cb} \tag{E.11}$$

E.1 Christoffel symbols for spherical symmetric spacetimes

The Christoffel symbols for a general d-dimensional spherical symmetric static metric, the parametrization $g_{tt} = -(1 - A(r))$, $g_{rr} = 1/(1 - A(r))$ and the alternative parametrization $g_{tt} = -e^{\nu(r)}$, $g_{rr} = g^{-\nu(r)}$. The index naming convention follows section 3. f' indicates the derivation $\partial_r f(r)$.

$$\Gamma^{t}_{tr} = \Gamma^{t}_{rt} = \frac{1}{2}g^{tt}\partial_r g_{tt} \quad = \frac{1}{2}\frac{A'}{A-1} \qquad = \frac{\nu'}{2} \tag{E.12}$$
$$\Gamma^{r}_{tt} = \frac{1}{2}g^{rr}\partial_r g_{tt} \quad = \frac{1}{2}(A-1)A' \qquad = \frac{1}{2}e^{2\nu}\nu' \tag{E.13}$$
$$\Gamma^{r}_{rr} = \frac{1}{2}g^{rr}\partial_r g_{rr} \quad = \frac{1}{2}\frac{A'}{1-A} \qquad = -\frac{1}{2}\nu' \tag{E.14}$$
$$\Gamma^{i}_{r}i = \Gamma^{i}_{ir} = \frac{1}{2}g^{ii}\partial_r g_{ii} \quad = \frac{1}{r} \tag{E.15}$$
$$\Gamma^{i}_{\phi\phi} = \frac{1}{2}g^{ii}\partial_i g_{ii} \quad = -\cos(\theta_i)\sin(\theta_i) \tag{E.16}$$
$$\Gamma^{\phi}_{r\phi} = \Gamma^{\phi}_{\phi r} = \frac{1}{2}g^{\phi\phi}\partial_r g_{\phi\phi} = \frac{1}{r} \tag{E.17}$$
$$\Gamma^{\phi}_{\phi i} = \Gamma^{\phi}_{i\phi} = \frac{1}{2}g^{\phi\phi}\partial_i g_{\phi\phi} = \frac{1}{\tan(\theta_i)} \tag{E.18}$$

Appendix F

Finales Abstellgleis für Texte

F.0.1 Black holes in particle detectors

Abschnitt ggf. komplett löschen.

Quantum black hole formation in particle detectors is usually assumed by super-Planckian particle collision processes (Hoop conjecture). In such a process with a center of mass energy in the order of the (fundamental) Planck mass and a impact parameter (cross section estimation) in the order of the (fundamental) Planck length, enough matter is compressed to form an event horizon of quantum size. This experimental signature is the main motivation for investigating black holes in large extra dimensions.

For literature about the experimental setup and observation of black holes in particle accelerators like the LHC, see e.g. [10, 11, 18, 39, 40, 45, 56].

F.0.2 Sucht Bleibe: Requirements for self-complete black hole metrics

The following three properties for short-scale improved Black holes were proposed in [59]. They imply the newly developed theory is equipped with a *characteristic length scale* l_0 which is, of course, associated with an energy scale $1/l_0$ of theory validity.

1. A *regular black hole* that has no more curvature (Ricci scalar) singularity at the origin, in terms
$$R(0) < \infty. \tag{F.1}$$
2. *Classical low-energy limit*, that is, Schwarzschild behaviour of the metric for big distances, in terms
$$g_{00}(r) = 1 - \frac{2GM}{r} \quad \text{for} \quad r \gtrsim l_0. \tag{F.2}$$
3. *Self-encoding* of the characteristic minimal length scale l_0 in the radius of the *extremal* configuration r_0, that is,
$$l_0 = r_0. \tag{F.3}$$

This third requirement is crucial: Self-encoding enables l_0 being the only *universal scale*, as the theory requires no new length scale like $\sqrt{\beta}$ from GUP, θ from NCG or ℓ_0 from String Theory.

List of figures and tables

This list helps to find and identify figures; they are labeled by their size and type (illustration or plots) and marked if they were not self-made.

List of figures

List of tables

Bibliography

[1] Adler, Ronald J., Chen, Pisin and Santiago, David I., "The Generalized uncertainty principle and black hole remnants", *Gen.Rel.Grav.*, **33**, 2101–2108 (2001). [DOI], [arXiv:gr-qc/0106080 [gr-qc]]. (Not cited.)

[2] Ansoldi, Stefano, "Spherical black holes with regular center: A Review of existing models including a recent realization with Gaussian sources", *arXiv*, e-print, (2008). [arXiv:0802.0330 [gr-qc]]. (Cited on pages 35, 54, 57, 59, 61, and 83.)

[3] Ashtekar, Abhay and Lewandowski, Jerzy, "Background independent quantum gravity: A Status report", *Class.Quant.Grav.*, **21**, R53 (2004). [DOI], [arXiv:gr-qc/0404018 [gr-qc]]. (Cited on page 69.)

[4] Aurilia, A. and spallucci, E., "Planck's uncertainty principle and the saturation of Lorentz boosts by Planckian black holes", *arXiv*, e-print, (2013). [arXiv:1309.7186 [gr-qc]]. (Not cited.)

[5] Aurilia, Antonio and Spallucci, Euro, "Why the length of a quantum string cannot be Lorentz contracted", *Adv.High Energy Phys.*, **2013**, 531696 (2013). [DOI], [arXiv:1309.7741 [hep-th]]. (Not cited.)

[6] Balasin, Herbert and Nachbagauer, Herbert, "The energy-momentum tensor of a black hole, or what curves the Schwarzschild geometry?", *Class.Quant.Grav.*, **10**, 2271 (1993). [DOI], [arXiv:gr-qc/9305009 [gr-qc]]. (Not cited.)

[7] Barvinsky, A.O., "Nonlocal action for long distance modifications of gravity theory", *Phys.Lett.*, **B572**, 109–116 (2003). [DOI], [arXiv:hep-th/0304229 [hep-th]]. (Cited on page 68.)

[8] Barvinsky, A.O., "Aspects of Nonlocality in Quantum Field Theory, Quantum Gravity and Cosmology", *arXiv*, e-print, (2014). [arXiv:1408.6112 [hep-th]]. (Cited on page 68.)

[9] Bekenstein, Jacob D. and Kamajian, Alfred T., "Information in the Holographic Universe", *Scientific American*, (December 17, 2005), p. ... (Cited on pages 50 and 83.)

[10] Bleicher, Marcus and Nicolini, Piero, "Large Extra Dimensions and Small Black Holes at the LHC", *J.Phys.Conf.Ser.*, **237**, 012008 (2010). [DOI], [arXiv:1001.2211 [hep-ph]]. (Cited on page 80.)

[11] Bleicher, Marcus and Nicolini, Piero, "Mini-review on mini-black holes from the mini-Big Bang", *Astron. Nachr.*, **335**, 605–611 (2014). [DOI], [arXiv:1403.0944 [hep-th]]. (Cited on pages 22 and 80.)

[12] Bonanno, A. and Reuter, M., "Spacetime structure of an evaporating black hole in quantum gravity", *Phys.Rev.*, **D73**, 083005 (2006). [DOI], [arXiv:hep-th/0602159 [hep-th]]. (Cited on page 70.)

[13] Carr, B.J., "The Black Hole Uncertainty Principle Correspondence", *arXiv*, e-print, (2014). [arXiv:1402.1427 [gr-qc]]. (Cited on page 69.)

[14] Carr, Bernard, Modesto, Leonardo and Premont-Schwarz, Isabeau, "Generalized Uncertainty Principle and Self-dual Black Holes", *arXiv*, e-print, (2011). [arXiv:1107.0708 [gr-qc]]. (Cited on page 69.)

[15] Carroll, Sean M., *Spacetime and geometry: An introduction to general relativity*, (Addison Wesley, San Francisco, 2004). (Cited on pages 11 and 12.)

[16] Casadio, R., "What is the Schwarzschild radius of a quantum mechanical particle?", *arXiv*, e-print, (2013). [arXiv:1310.5452 [gr-qc]]. (Not cited.)

[17] Casadio, Roberto, Micu, Octavian and Nicolini, Piero, "Minimum length effects in black hole physics", *arXiv*, e-print, (2014). [arXiv:1405.1692 [hep-th]]. (Not cited.)

[18] Cavaglia, Marco, "Black hole and brane production in TeV gravity: A Review", *Int.J.Mod.Phys.*, **A18**, 1843–1882 (2003). [DOI], [arXiv:hep-ph/0210296 [hep-ph]]. (Cited on pages 20, 21, 80, and 82.)

[19] Dirkes, Alain R. P., Maziashvili, Michael and Silagadze, Zurab K., "Black hole remnants due to Planck-length deformed QFT", *arXiv*, e-print, (2013). [arXiv:1309.7427 [gr-qc]]. (Not cited.)

[20] Dvali, Gia and Gomez, Cesar, "Self-Completeness of Einstein Gravity", *arXiv*, e-print, (2010). [arXiv:1005.3497 [hep-th]]. (Not cited.)

[21] Dvali, Gia and Gomez, Cesar, "Self-Completeness of Einstein Gravity", *arXiv*, e-print, (2010). [arXiv:1005.3497 [hep-th]]. (Not cited.)

[22] Dvali, G. and Gomez, C., "Minimal length and black hole area quantization", *Fortsch.Phys.*, **59**, 579–585 (2011). [DOI]. (Cited on page 50.)

[23] Dvali, Gia and Gomez, Cesar, "Black Hole's Quantum N-Portrait", *Fortsch.Phys.*, **61**, 742–767 (2013). [DOI], [arXiv:1112.3359 [hep-th]]. (Cited on page 50.)

[24] Dymnikova, Irina, "Cosmological term as a source of mass", *Class.Quant.Grav.*, **19**, 725–740 (2002). [DOI], [arXiv:gr-qc/0112052 [gr-qc]]. (Cited on pages 54 and 57.)

[25] Elizalde, Emilio and Hildebrandt, Sergi R., "The Family of regular interiors for nonrotating black holes with T0(0)=T1(1)", *Phys.Rev.*, **D65**, 124024 (2002). [DOI], [arXiv:gr-qc/0202102 [gr-qc]]. (Cited on page 57.)

[26] Emparan, Roberto and Reall, Harvey S., "Black Holes in Higher Dimensions", *Living Rev.Rel.*, **11**, 6 (2008). [arXiv:0801.3471 [hep-th]]. (Cited on page 19.)

[27] Falls, Kevin, Litim, Daniel F. and Raghuraman, Aarti, "Black Holes and Asymptotically Safe Gravity", *Int.J.Mod.Phys.*, **A27**, 1250019 (2012). [DOI], [arXiv:1002.0260 [hep-th]]. (Cited on page 70.)

[28] Fließbach, T., *Allgemeine Relativitätstheorie*, Spektrum Lehrbuch, 5. Auflage, (Spektrum-Akademischer Vlg, Heidelberg, 2006). (Cited on page 11.)

[29] Frolov, V. and Novikov, I.D., *Black Hole Physics: Basic Concepts and New Developments*, Fundamental Theories of Physics, (Springer Netherlands, 1998). (Cited on page 23.)

[30] Giddings, Steven B., "Possible observational windows for quantum effects from black holes", *arXiv*, e-print, (2014). [arXiv:1406.7001 [hep-th]]. (Not cited.)

[31] Gingrich, Douglas M., "Noncommutative geometry inspired black holes in higher dimensions at the LHC", *JHEP*, **1005**, 022 (2010). [DOI], [arXiv:1003.1798 [hep-ph]]. (Not cited.)

[32] Goenner, Hubert F. M., "On the History of Unified Field Theories", *Living Reviews in Relativity*, **7**(2) (2004). [DOI]. URL (accessed September 2014): http://www.livingreviews.org/lrr-2004-2. (Cited on page 66.)

[33] Griffiths, J.B. and Podolskỳ, J., *Exact Space-Times in Einstein's General Relativity*, Cambridge Monographs on Mathematical Physics, (Cambridge University Press, Cambridge, 2009). (Cited on pages 16, 17, 18, and 60.)

[34] Hayward, Sean A., "Formation and evaporation of regular black holes", *Phys.Rev.Lett.*, **96**, 031103 (2006). [DOI], [arXiv:gr-qc/0506126 [gr-qc]]. (Cited on pages 61 and 83.)

[35] Hossenfelder, Sabine, "What black holes can teach us", *arXiv*, e-print, (2004). [arXiv:hep-ph/0412265 [hep-ph]]. (Cited on pages 21, 22, 23, and 82.)

[36] Hossenfelder, Sabine, "Minimal Length Scale Scenarios for Quantum Gravity", *Living Reviews in Relativity*, **16**(2) (2013). [DOI]. URL (accessed September 2014): http://www.livingreviews.org/lrr-2013-2. (Not cited.)

[37] Isi, Maximiliano, Mureika, Jonas and Nicolini, Piero, "Self-Completeness and the Generalized Uncertainty Principle", *JHEP*, **1311**, 139 (2013). [DOI], [arXiv:1310.8153 [hep-th]]. (Cited on pages 28 and 69.)

[38] Isi, Maximiliano, Mureika, Jonas and Nicolini, Piero, "Self-Completeness in Alternative Theories of Gravity", *arXiv*, e-print, (2014). [arXiv:1402.3342 [hep-th]]. (Cited on page 69.)

[39] Kanti, Panagiota, “Black holes in theories with large extra dimensions: A Review”, *Int.J.Mod.Phys.*, **A19**, 4899–4951 (2004). [DOI], [arXiv:hep-ph/0402168 [hep-ph]]. (Cited on pages 20 and 80.)

[40] Kanti, Panagiota and Winstanley, Elizabeth, “Hawking Radiation from Higher-Dimensional Black Holes”, *arXiv*, e-print, (2014). [arXiv:1402.3952 [hep-th]]. (Cited on pages 67 and 80.)

[41] Kempf, Achim, Mangano, Gianpiero and Mann, Robert B., “Hilbert space representation of the minimal length uncertainty relation”, *Phys.Rev.*, **D52**, 1108–1118 (1995). [DOI], [arXiv:hep-th/9412167 [hep-th]]. (Cited on pages 27, 28, and 69.)

[42] Kiefer, Claus, “Quantum gravity: General introduction and recent developments”, *Annalen Phys.*, **15**, 129–148 (2005). [DOI], [arXiv:gr-qc/0508120 [gr-qc]]. (Cited on page 70.)

[43] Kiefer, Claus, *Quantum gravity*, International series of monographs on physics, 136, (Oxford Univ. Press, Oxford [u.a.], 2007), 2. ed. edition. (Cited on page 70.)

[44] Koch, Benjamin, *Black hole production and graviton emission in models with large extra dimensions*, Ph.D. thesis, (Goethe-Universität Frankfurt, Frankfurt, 2007). [ADS]. (Cited on page 11.)

[45] Koch, Benjamin, Bleicher, Marcus and Hossenfelder, Sabine, “Black hole remnants at the LHC”, *JHEP*, **0510**, 053 (2005). [DOI], [arXiv:hep-ph/0507138 [hep-ph]]. (Cited on pages 21, 22, 80, and 82.)

[46] Köppel, Sven, Iso, Maximiliano, Knipfer, Marco, Mureika, Jonas and Nicolini, Piero, “Self-Completeness and the Generalized Uncertainty Principle in Extra Dimensions”, in preparation, (2014). (Cited on pages 40 and 69.)

[47] Maldacena, Juan Martin, “Black holes in string theory”, *arXiv*, e-print, (1996). [arXiv:hep-th/9607235 [hep-th]]. (Cited on page 70.)

[48] Misner, Charles, Thorne, Kip and Wheeler, John, *Gravitation*, (W. H. Freeman, New York, 1973). (Cited on pages 11, 12, 14, 17, 57, and 60.)

[49] Modesto, Leonardo, “Loop quantum black hole”, *Class.Quant.Grav.*, **23**, 5587–5602 (2006). [DOI], [arXiv:gr-qc/0509078 [gr-qc]]. (Cited on page 69.)

[50] Modesto, Leonardo, “Super-renormalizable Quantum Gravity”, *Phys.Rev.*, **D86**, 044005 (2012). [DOI], [arXiv:1107.2403 [hep-th]]. (Cited on page 68.)

[51] Modesto, Leonardo, Moffat, John W. and Nicolini, Piero, “Black holes in an ultraviolet complete quantum gravity”, *Phys.Lett.*, **B695**, 397–400 (2011). [DOI], [arXiv:1010.0680 [gr-qc]]. (Cited on pages 27, 38, 61, and 68.)

[52] Myers, Robert C., "Tall tales from de Sitter space", in Gomberoff, A. and Marolf, D., eds., *Lectures on Quantum Gravity*, Series of the Centro De Estudios Científicos, p. 12345. Springer, (2006). (Cited on page 18.)

[53] Nicolini, Piero, "Noncommutative Black Holes, The Final Appeal To Quantum Gravity: A Review", *Int.J.Mod.Phys.*, **A24**, 1229–1308 (2009). [DOI], [arXiv:0807.1939 [hep-th]]. (Cited on pages 6, 38, and 68.)

[54] Nicolini, Piero, "Entropic force, noncommutative gravity and un-gravity", *Phys.Rev.*, **D82**, 044030 (2010). [DOI], [arXiv:1005.2996 [gr-qc]]. (Cited on page 68.)

[55] Nicolini, Piero, "Nonlocal and generalized uncertainty principle black holes", *arXiv*, e-print, (2012). [arXiv:1202.2102 [hep-th]]. (Cited on pages 27 and 38.)

[56] Nicolini, Piero, Mureika, Jonas, Spallucci, Euro, Winstanley, Elizabeth and Bleicher, Marcus, "Production and evaporation of Planck scale black holes at the LHC", *arXiv*, e-print, (2013). [arXiv:1302.2640 [hep-th]]. (Cited on page 80.)

[57] Nicolini, Piero, Smailagic, Anais and Spallucci, Euro, "Noncommutative geometry inspired Schwarzschild black hole", *Phys.Lett.*, **B632**, 547–551 (2006). [DOI], [arXiv:gr-qc/0510112 [gr-qc]]. (Cited on pages 30 and 68.)

[58] Nicolini, Piero and Spallucci, Euro, "Holographic screens in ultraviolet self-complete quantum gravity", *Adv.High Energy Phys.*, **2014**, 805684 (2014). [DOI], [arXiv:1210.0015 [hep-th]]. (Cited on page 32.)

[59] Nicolini, Piero and Spallucci, Euro, "Holographic screens in ultraviolet self-complete quantum gravity", *Adv.High Energy Phys.*, **2014**, 805684 (2014). [DOI], [arXiv:1210.0015 [hep-th]]. (Cited on pages 41, 42, 43, 50, 55, 65, and 80.)

[60] Nicolini, Piero and Winstanley, Elizabeth, "Hawking emission from quantum gravity black holes", *JHEP*, **1111**, 075 (2011). [DOI], [arXiv:1108.4419 [hep-ph]]. (Cited on page 68.)

[61] Niedermaier, Max and Reuter, Martin, "The Asymptotic Safety Scenario in Quantum Gravity", *Living Reviews in Relativity*, **9**(5) (2006). [DOI]. URL (accessed September 2014): `http://www.livingreviews.org/lrr-2006-5`. (Cited on page 70.)

[62] Penrose, Roger, *The large, the small and the human mind*, (Cambridge Univ. Press, Cambridge, 1997). (Cited on pages 9 and 82.)

[63] Perez, Alejandro, "The Spin-Foam Approach to Quantum Gravity", *Living Reviews in Relativity*, **16**(3) (2013). [DOI]. URL (accessed September 2014): `http://www.livingreviews.org/lrr-2013-3`. (Cited on page 69.)

[64] Reuter, M., "Nonperturbative evolution equation for quantum gravity", *Phys.Rev.*, **D57**, 971–985 (1998). [DOI], [arXiv:hep-th/9605030 [hep-th]]. (Cited on page 70.)

[65] Rizzo, Thomas G., "Noncommutative Inspired Black Holes in Extra Dimensions", *JHEP*, **0609**, 021 (2006). [DOI], [arXiv:hep-ph/0606051 [hep-ph]]. (Cited on pages 29, 30, and 68.)

[66] Rovelli, Carlo, "Loop Quantum Gravity", *Living Reviews in Relativity*, **11**(5), 12345 (2008). [DOI]. URL (accessed September 2014):
http://www.livingreviews.org/lrr-2008-5. (Cited on page 69.)

[67] Scardigli, Fabio and Casadio, Roberto, "Gravitational tests of the Generalized Uncertainty Principle", *arXiv*, e-print, (2014). [arXiv:1407.0113 [hep-th]]. (Not cited.)

[68] Spallucci, Euro and Smailagic, Anais, "Black holes production in self-complete quantum gravity", *Phys.Lett.*, **B709**, 266–269 (2012). [DOI], [arXiv:1202.1686 [hep-th]]. (Not cited.)

[69] Spallucci, Euro and Smailagic, Anais, "Semi-classical approach to quantum black holes", *arXiv*, e-print, (2014). [arXiv:1410.1706 [gr-qc]]. (Not cited.)

[70] Stephani, Hans, Kramer, Dietrich, Maccallum, Malcolm, Hoenselaers, Cornelius and Herlt, Eduard, *Exact Solutions of Einstein's Field Equations*, Cambridge Monographs on Mathematical Physics, (Cambridge University Press, Cambridge, 2003). (Cited on page 16.)

[71] Susskind, Leonard, "Trouble for remnants", *arXiv*, e-print, (1995). [arXiv:hep-th/9501106 [hep-th]]. (Not cited.)

[72] Susskind, Leonard, "Singularities, Firewalls, and Complementarity", *arXiv*, e-print, (2012). [arXiv:1208.3445 [hep-th]]. (Not cited.)

[73] Susskind, Leonard and Uglum, John, "Black hole entropy in canonical quantum gravity and superstring theory", *Phys.Rev.*, **D50**, 2700–2711 (1994). [DOI], [arXiv:hep-th/9401070 [hep-th]]. (Not cited.)

[74] Thiemann, Thomas, "Lectures on loop quantum gravity", *Lect.Notes Phys.*, **631**, 41–135 (2003). [DOI], [arXiv:gr-qc/0210094 [gr-qc]]. (Cited on page 69.)

[75] Thiemann, Thomas, "Loop Quantum Gravity: An Inside View", *Lect.Notes Phys.*, **721**, 185–263 (2007). [DOI], [arXiv:hep-th/0608210 [hep-th]]. (Cited on page 69.)

[76] Wagner, Marc, "Quantum Field Theory II", lecture notes, (2013). (Cited on pages 69 and 73.)

[77] Wald, Robert M., *General Relativity*, (The University of Chicago Press, Chicago and London, 1984). (Cited on pages 11, 12, 17, and 60.)

[78] Wald, Robert M., "Teaching general relativity", *arXiv*, e-print, (2005). [arXiv:gr-qc/0511073 [gr-qc]]. (Cited on page 11.)

[79] Winstanley, Elizabeth, "Hawking radiation from rotating brane black holes", *arXiv*, e-print, (2007). [arXiv:0708.2656 [hep-th]]. (Cited on page 22.)

[80] Witten, Edward, “Anti-de Sitter space, thermal phase transition, and confinement in gauge theories”, *Adv.Theor.Math.Phys.*, **2**, 505–532 (1998). [arXiv:hep-th/9803131 [hep-th]]. (Not cited.)

Acknowledgement

First of I all, I want to thank Piero Nicolini for his patience and availability in the past year. His knowledge in people and papers was a great help to navigate in the Quantum Gravity landscape.

Second, I would like to thank Marcus Bleicher for kind FIAS hospitality and group supervision.

Erklärung

Ich versichere hiermit, die vorliegende Arbeit selbständig verfasst und keine anderen als die angegebenen Quellen und Hilfsmittel vewendet zu haben. Alle Stellen der Arbeit, die wörtlich oder sinngemäß aus Veröffentlichungen oder aus anderen fremden Texten entnommen wurden, sind von mir als solche kenntlich gemacht worden. Ferner erkläre ich, dass die Arbeit nicht – auch nicht auszugsweise – für eine andere Prüfung verwendet wurde.

Frankfurt am Main, im November 2014

Sven Köppel